NASA Contractor Report 4300

Modeling of Thermal Lensing in Side and End-Pumped Finite Solid-State Laser Rods

Vincent G. Brackett

GRANT NAG1-666
JUNE 1990

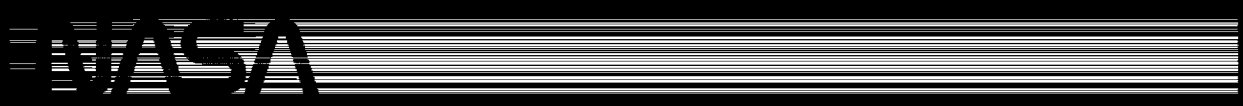

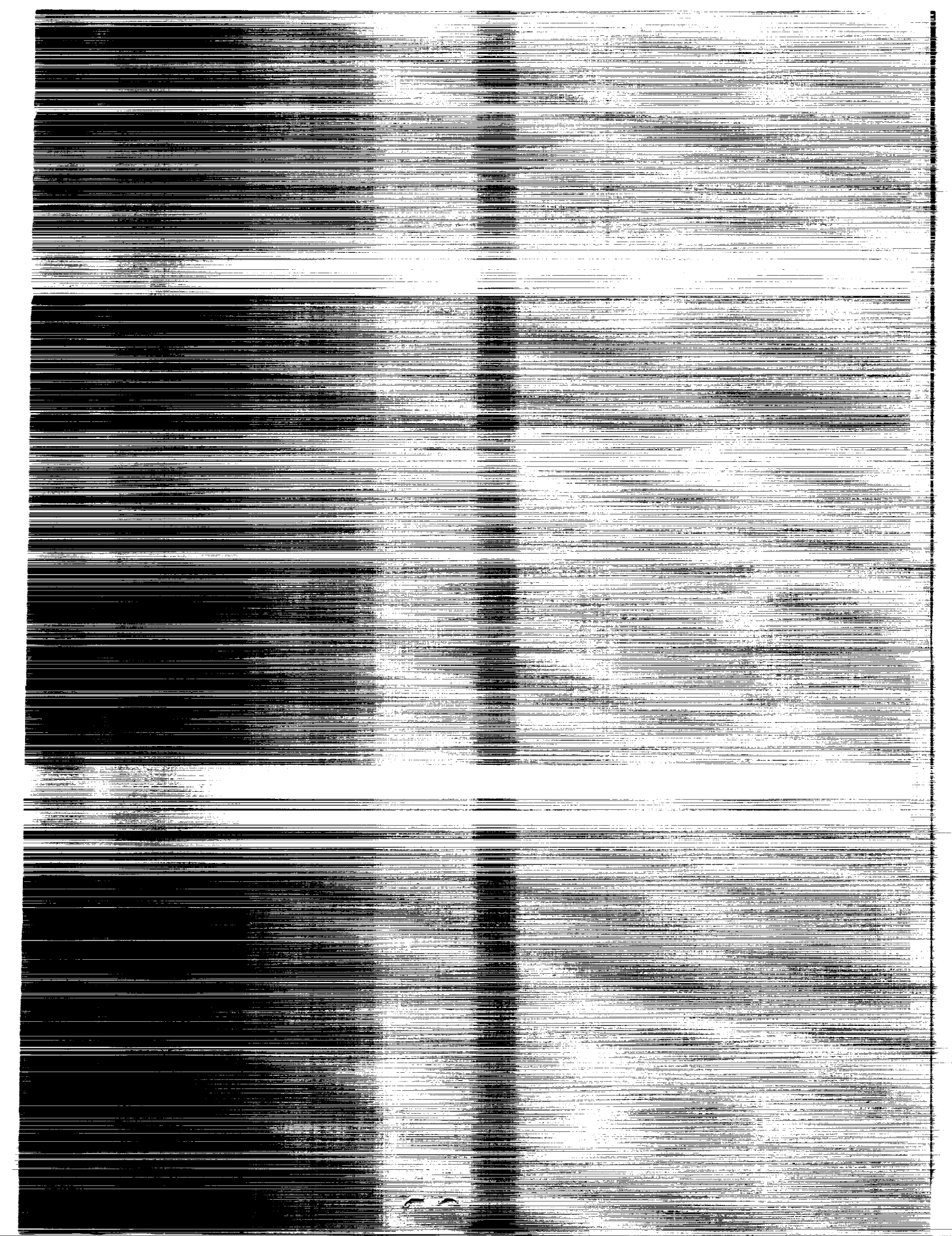

NASA Contractor Report 4300

Modeling of Thermal Lensing in Side and End-Pumped Finite Solid-State Laser Rods

Vincent G. Brackett
Hampton University
Hampton, Virginia

Prepared for
Langley Research Center
under Grant NAG1-666

National Aeronautics and
Space Administration
Office of Management
Scientific and Technical
Information Division

1990

Table of Contents

Table of Contents (cont.)

Tables

Figures

Figures (cont.)

Abstract

Modeling of Thermal Lensing in Side and End-Pumped Finite Solid-State Laser Rods

Student: Vincent G. Brackett Department: Mathematics
Date of Birth: December 17, 1942 Advisor: Dr. U.O.Farrukh

An analytical expression for approximating the time-dependent thermal focal length in finite solid-state laser rods has been derived. The analysis is based on the temperature variation of the material refractive index caused by optical pumping of these rods. Several quantities were found to be relevant to this analysis. These quantities were the specific thermal profiles of the rods, type of optical pumping employed, type of cooling scheme employed (side and end-cooling parameters), and the specific material characteristics of the rods. The Thermal Lensing Model was formulated using the geometric ray tracing approach. The focal lengths are then approximated, by calculating the phase shift in the index of refraction, as the different rays of an incident plane wave are tracked through a lens-like crystal medium. The approach also applies in the case of Gaussian or parabolic pump beams. It is shown that the prediction of thermal focal length is in good quantitative agreement with experimentally obtained data.

CHAPTER 1

Introduction

The next generation of solid-state lasers (to be used for remote sensing of the atmosphere from space platforms), are under development. Various new lasing materials and laser configuations are being investigated. Currently, the solid-state, end-pumped diode lasers are the most promising candidates due to their small size, reliability, performance, low power and cooling requirements, etc. Analyzing thermal lensing effects for these end-pumped configuations, using various cooling schemes are of interest to the designers of laser systems. Theoretical formulation, numerical calculations, and experimental data on thermal lensing does not exist for end-pumped configuations.

The management of thermal energy deposited in a solid-state material is critical in the design of laser systems.[1] Any solid laser material operating in either pulsed or continuous wave (CW) mode of operation dissipates an appreciable amount of heat. The heat arises from non-radiative energy transitions as the pump beam traverses the material. Stated very briefly, when a material is excited to provide more atoms (or molecules) in a higher energy state than in some lower state, the material will be capable of amplifying radiation at the frequency corresponding to the ener-

gy level difference.[2] The acronym **LASER** derives its name from this process: **"Light Amplification by Stimulated Emission of Radiation."**

It's during this process that some fraction of the total energy of the pump beam is absorbed by the lasing material. This absorbed energy is then dissipated as heat. In the cylindrical geometries normally used, the heat is extracted from the surface of the cylinder, thereby generating a radial thermal gradient. Both radial and axial gradients are present in end-pumped lasers. Employment of active cooling to dissipate heat from laser crystals will also affect the thermal gradients. Therefore, the thermal gradients present in laser rods are governed by many factors. These include: geometries of the rod in use, type of laser material, thermal diffusivity of the material, and type of pumping and active cooling schemes employed. A **Temperature Distribution Model** has been developed to model the time dependent temperature distributions of finite solid-state laser rods that include the above factors.[1,3]

The change in temperature, within a laser rod, causes thermal defocusing and distortion of the laser beam. This is due to the temperature variation of the material refractive index. These thermal gradients cause stresses within the laser material. The generated stresses induce birefringence and non-uniform expansion (bulge) in the laser

rod. Collectively, the above factors of temperature variation of the refractive index, induced birefringence, and bulge are called thermal lensing. Thermal lensing is the defocusing and distortion of a laser beam transmitted through a material medium, due to the non-uniform heating of the material.[4]

In this thesis, using the **Temperature Distribution Model**, thermal lensing effects will be analyzed to develop a **Thermal Lensing Model**. The **Thermal Lensing Model** will be employed to predict changes in the focal length and resultant distortions due to the time dependent temperature variations of the refractive index for two common laser materials that are under evaluation. These materials are Neodymium doped Yttrium Aluminum Garnet (YAG) ($Y_3AL_5O_{12}$) and Titanium doped Aluminum Oxide (Sapphire) (AL_2O_3). From this point onward, these two materials will be called Nd:YAG and Ti:AL_2O_3 respectively. They will be evaluated for various pumping (side and end) and cooling schemes. The induced birefringence and bulge caused by stress in the laser material will be discussed. However, these factors will not be implemented in the first version of the **Thermal Lensing Model** as they are minor in nature.

In the next chapter, the **Temperature Distribution Model** will be discussed. It's from this model's output that the time dependent temperature profiles are derived. These profiles serve as input to the **Thermal Lensing Model**.

CHAPTER 2

Temperature Distribution Model

The problem of managing the thermal energy deposited within a solid-state laser material under active pumping has long been of critical importance in the design of laser systems.[1] Koechner's paper on the transient temperature profile in solid-state lasers was the original work in this area.[5] In it, the time dependent temperature distribution of an infinitely long laser rod with a uniform heat source was determined. This configuation was adequate to treat the flashlamp pumping of relatively long laser rods, and rods with little or no end cooling employed. However, this treatment has become inapplicable to other pump configuations. Recently, several new solid-state laser materials have been introduced, each with their own thermal deposition mechanisms.[6] Additionally, several other novel laser techniques such as end-pumping with laser diodes have also been developed. For these systems, the assumptions of a uniform distribution of pump energy and an infinite rod length are no longer valid. The one dimensional approach of Koechner[5] does not apply when the length of the laser rod is comparable to its diameter. Furthermore, the longitudinal symmetry of an infinite rod is broken when it is end-pumped.

It was for these reasons that the Temperature Distribution Model was developed. The time dependent temperature distribution of a cylindrical rod of finite length has been derived by Farrukh et al. in two separate papers.[1,3] Additionally, they studied the evolution of thermal profiles for various pumping and cooling schemes. The general expression of the temperature distribution is given as:[7]

$$T(r,z) = \sum_{n,m=1}^{\infty} C_{nm}\phi_n(r)\,\psi_m(z) * f(t) \qquad (2\text{-}1)$$

where ϕ_n is the radial eigenfunction, ψ_m is the axial eigenfunction, C_{nm} is the pump pulse expansion coefficient, and f(t) is the time dependence function. The time dependence function f(t) for the on and off periods of the pumping pulse is given, respectively as:[7]

$$f(t) = \frac{\tau_{nm}}{K * Lamda} * \left\{ \frac{\left(1 - e^{-\frac{ncycle}{\tau_{nm}}}\right)}{\left(1 - e^{\frac{cycle}{\tau_{nm}}}\right)} * \left(e^{-\frac{t-ncycle + offtime}{\tau_{nm}}}\right) + \left(1 - e^{-\frac{t-ncycle}{\tau_{nm}}}\right) \right\} \qquad (2\text{-}2)$$

$$f(t) = \frac{\tau_{nm}}{K * Lamda} * \left\{ \frac{\left(1 - e^{-\frac{ncycle}{\tau_{nm}}}\right)}{\left(1 - e^{\frac{cycle}{\tau_{nm}}}\right)} * \left(e^{-\frac{t-ncycle + offtime}{\tau_{nm}}}\right) \right\} \qquad (2\text{-}3)$$

where K is the inverse of diffusivity, Lamda is the thermal conductivity, and τ_{nm} is the time constant for specific eigenfunctions.

The expression for temperature distribution is general and applies to various situations such as pulsed or continuous operations of the laser. A variety of different pumping and cooling schemes including end-pumping by a Gaussian beam were also discussed. To gain an appreciation for the capability of this model, we will look at two of the more interesting cases that this model can be used to evaluate. These are end-pumped single and multiple pulse operations for two common solid-state laser materials (Nd:YAG and Ti:AL_2O_3).

A. Single Pulse Operations

If a laser rod is pumped by a single pump pulse, a transient thermal profile will be established. This is the result of a fast pump-introduced heating process followed by a slow recovery of the rod to its ambient temperature. Although this thesis will primarily address long pump pulses, it is appropriate to distinguish the difference between short and long pump pulses. If the duration of the pumping pulse is very short in comparison to the laser rod relaxation time, then the heat energy deposited in the rod is considered to be deposited instantaneously. (The laser rod relaxation time is defined as the time required for the

rod to relax to its ambient temperature.) Rod relaxation times are approximately 3.5 seconds for Nd:YAG and 300ms for Ti:AL_2O_3 for typical rod dimensions. When a pulse is characterized as short or long, this characterization depends on the laser rod material. If the pump pulse duration is less than one percent of the relaxation time of the rod, then the pump pulse is considered to be short. In this case, as previously stated, the heat energy is deposited instantaneously. An example of this will be shown in a later graph. For long pulse operations, the heat energy being deposited builds up and relaxes simultaneously during the pumping pulse.

Figure 2-1 is an illustration of the transient nature of temperature distribution in an optically pumped cylindrical laser rod for a long pumping pulse. During the

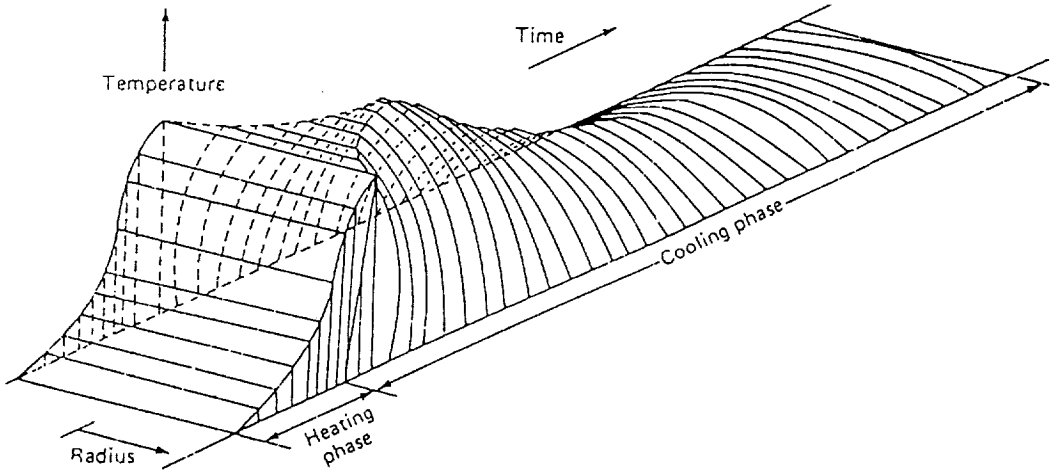

Figure 2-1. Thermal Relaxation of a Single Input Pulse in a Cylindrical Laser Rod[2]

pulse, heat energy is absorbed by the laser crystal. At the end of the pump pulse, the temperature of the rod has increased above the ambient in a spatially non-uniform manner. Since only the surface of the rod is in contact with the coolant, a radial and axial heat flow develops during and at the end of the pump pulse. The initial non-uniform spatial temperature distribution changes to a nearly parabolic temperature profile which then decays at a rate determined by the rod specific relaxation time constant. Since lasing action occurs during or at the end of the pump pulse, the optical distortion in single pulsed lasers arises from the thermal gradients established during the pumped cycle.

Figure 2-2 and 2-3 are examples of the **Temperature Distribution Model** output for the time dependent heat propagation in end-pumped Nd:YAG and Ti:AL_2O_3 laser rods for a pump beam with spatially circular and Gaussian profiles respectively, with moderate side cooling. In both of these figures, the energy absorbed as heat, is $1J/cm^3$ at the front end of the rod for the circular pump and at the center of the front end for the Gaussian pump. Figure 2-2 was chosen as an example because it shows the impact of side cooling in generating radial gradients in a Nd:YAG rod after only 20ms into its thermal relaxation cycle. Also in Figure 2-2, the temperature at the center of rod has not

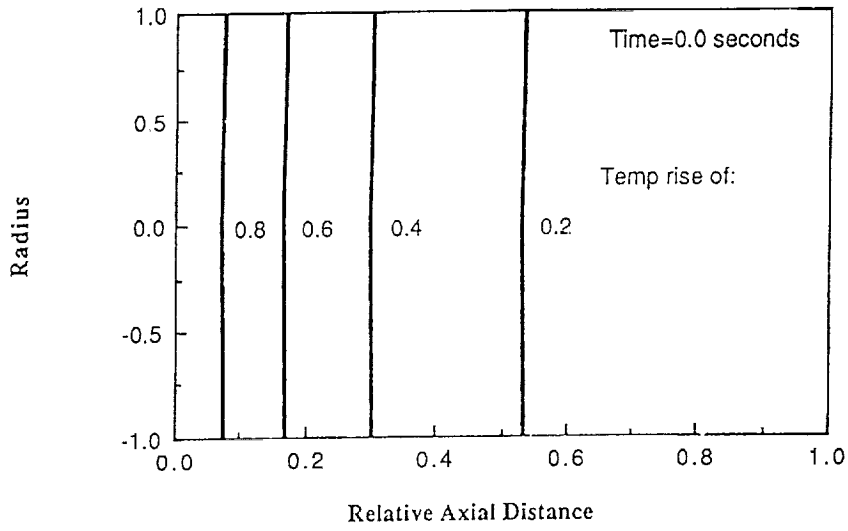

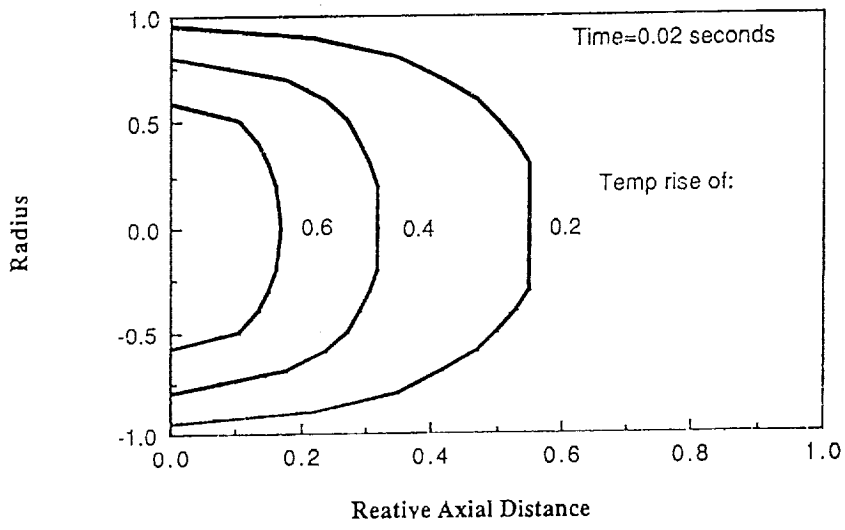

Figure 2-2. Heat Propagation in Nd:YAG Laser Rod (End-Pumped, Single Pulse with a Uniform Cross Section Pumping Beam)

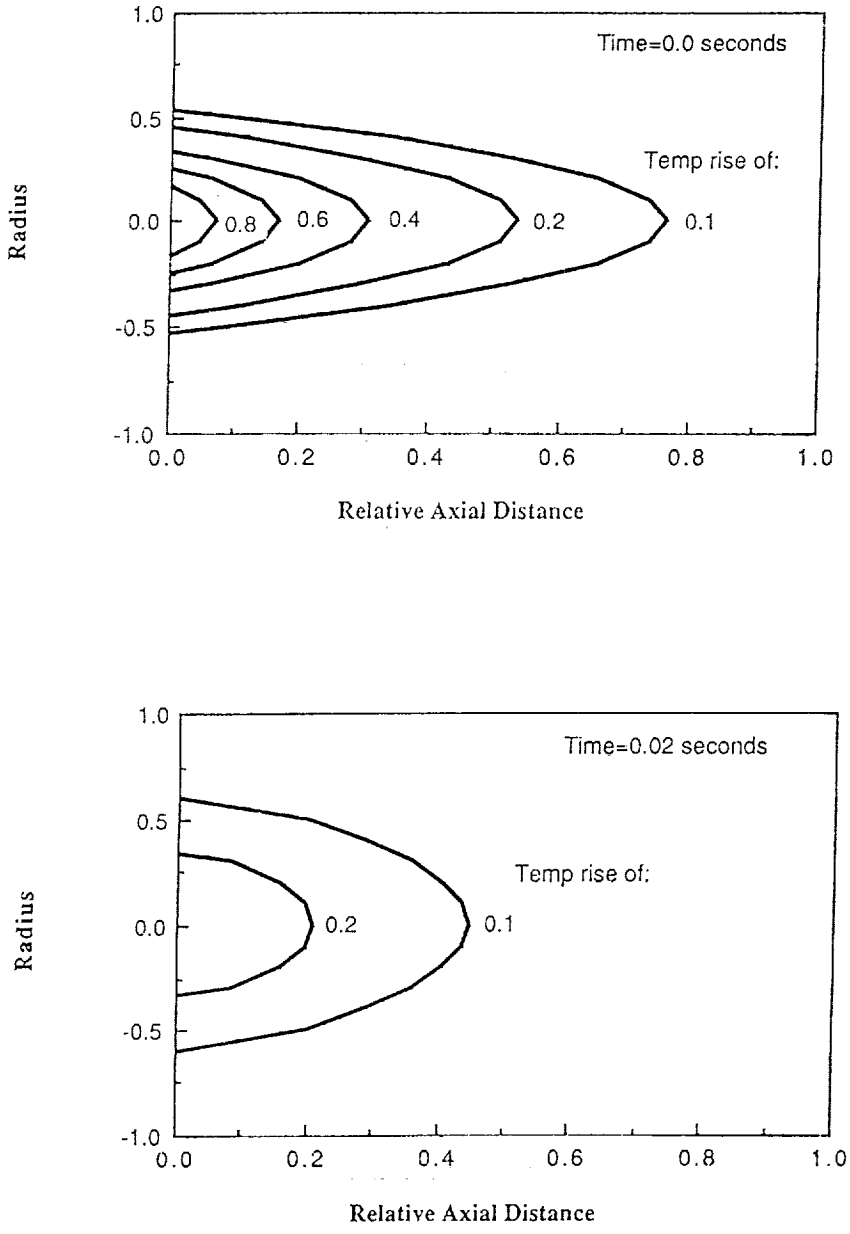

Figure 2-3. Heat Propagation in Ti:AL_2O_3 Laser Rod (End-Pumped, Single Pulse with a Gaussian Cross Section Pumping Beam)

appreciably relaxed toward the ambient temperature at the 20ms point in time. Figure 2-3 was chosen as an example to illustrate the difference between a circular and Gaussian pumping beam. This figure also shows that after only 20ms into the thermal relaxation cycle, the Ti:AL_2O_3 laser rod has significantly relaxed toward its ambient temperature. However, the thermal energy content in the Gaussian pump case is only about 1/8 of that of the circular pump case.

Figure 2-4 is an example of the model output of the temperature rise above ambient for five different pulse durations for a Nd:YAG laser rod with one pulse of 50mJ of absorbed energy. The Nd:YAG laser was end-pumped with a Gaussian beam and subjected to moderate side cooling. The rod ends were not cooled. The 1ms pulse in this figure is an example of a short pulse where the heat energy is deposited instantaneously. The remaining pulses in this figure are examples of relatively long pulses. In Figure 2-4, the rod has essentially relaxed to the ambient temperature approximately 3.5 seconds after completion of the pumping pulse.

Figure 2-5 is an example of the model output of the temperature rise above ambient for five different pulse durations for a Ti:AL_2O_3 laser rod using 50mJ of absorbed energy per pulse. The Ti:AL_2O_3 laser rod was end-pumped with a Gaussian beam and subjected to moderate side-

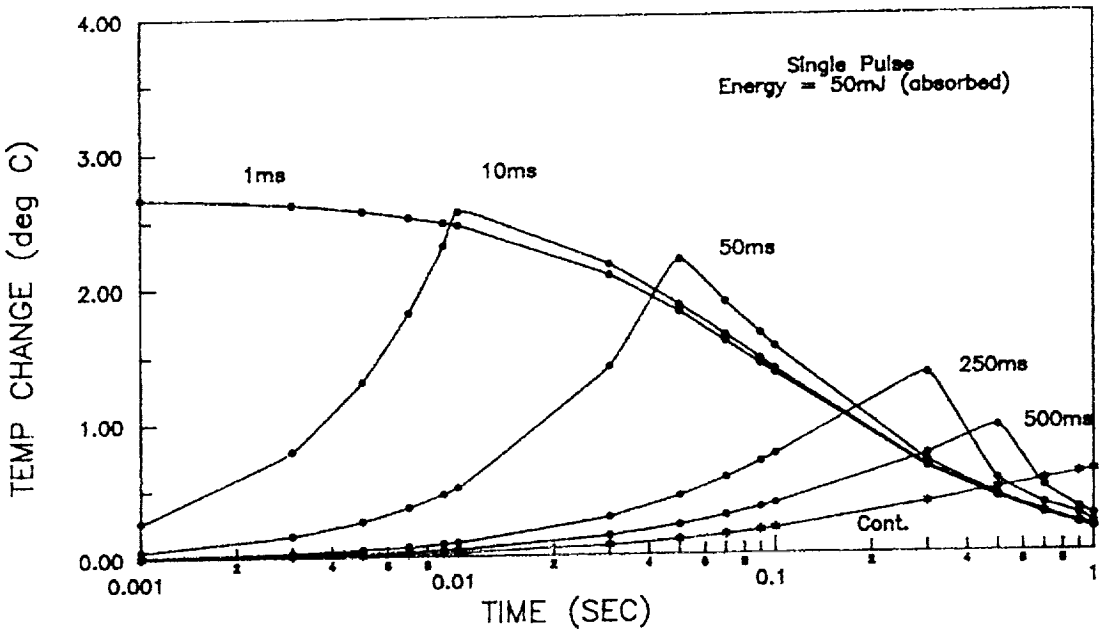

Figure 2-4. Temperature Profiles for Various Durations of a Single Pump Pulse for Nd:YAG (At Center of Pump-End Face)

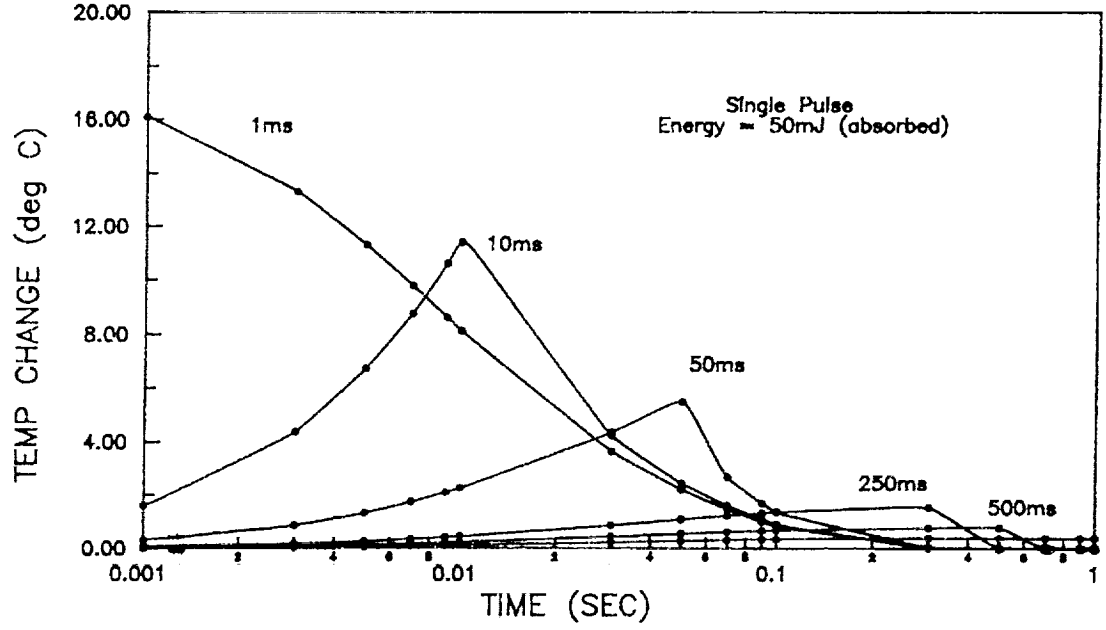

Figure 2-5. Temperature Profiles for Various Durations of a Single Pump Pulse for Ti:AL_2O_3 (At Center of Pump-End Face)

cooling. The rod ends were not cooled. The 1ms pulse in this figure is an example of a short pulse where the heat energy is deposited instantaneously. The remaining pulses in this figure are examples of relatively long pulses. In Figure 2-5, the rod has essentially relaxed to thermal equilibrium approximately 300ms after completion of the pumping pulse.

Comparison of Figures 2-4 and 2-5 also shows that the Ti:AL_2O_3 rod has a greater temperature rise than the Nd:YAG rod under the same conditions of absorbed energy, pulse duration, and cooling scheme. These results are not unexpected as the thermal conductivity of Ti:AL_2O_3 is higher than Nd:YAG.

B. Multiple Pulse Operations

In the previous section, we discussed pump induced thermal profiles that occur for single-pulse operations. The pulse input intervals are long with respect to the thermal relaxation times of the laser rod. Additionally, the rod has returned to the ambient temperature before the onset of the next pumping pulse. If the laser is operated at a repetition rate at which there exists a residual temperature distribution from the previous pulse, a temperature buildup in the rod will occur. The temperature at specific points will increase until a steady-state condition is reached. Figure 2-6 is an illustration of the tem-

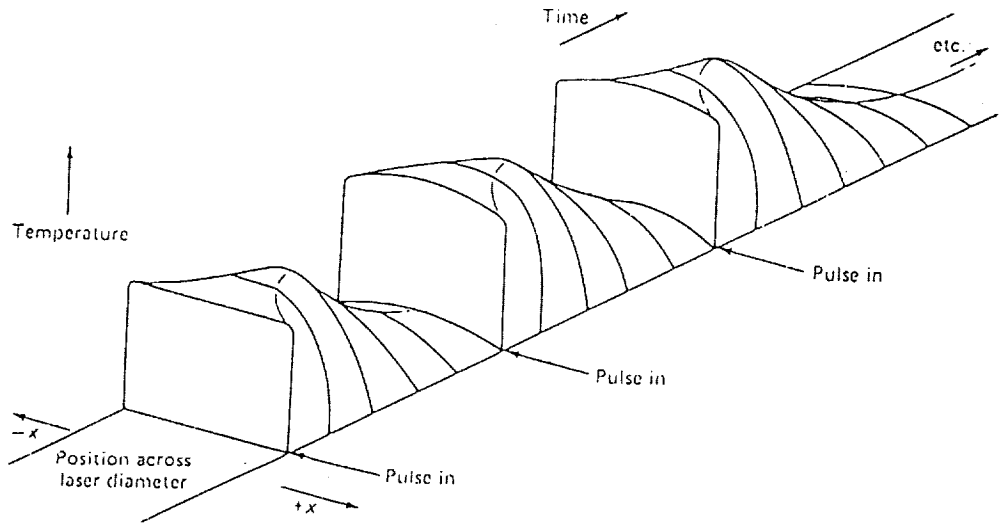

Figure 2-6. Thermal Relaxation in a Solid Cylinder with Pulse Input Intervals near the Thermal Relaxation Times[2]

perature profile of a laser operated at a low repetition rate.

Figure 2-7 is an illustration of thermal buildup at a pulse interval smaller than the thermal relaxation time. Under these conditions, the laser will soon establish a steady-state operating condition where the radial and axial rate of flow of heat out of the rod will equal the rate of heat deposition. During the transition period, the rod radial and axial thermal profiles will continue to change until the steady-state equilibrium temperature is reached. In the extreme case, when the interval between pulses be-

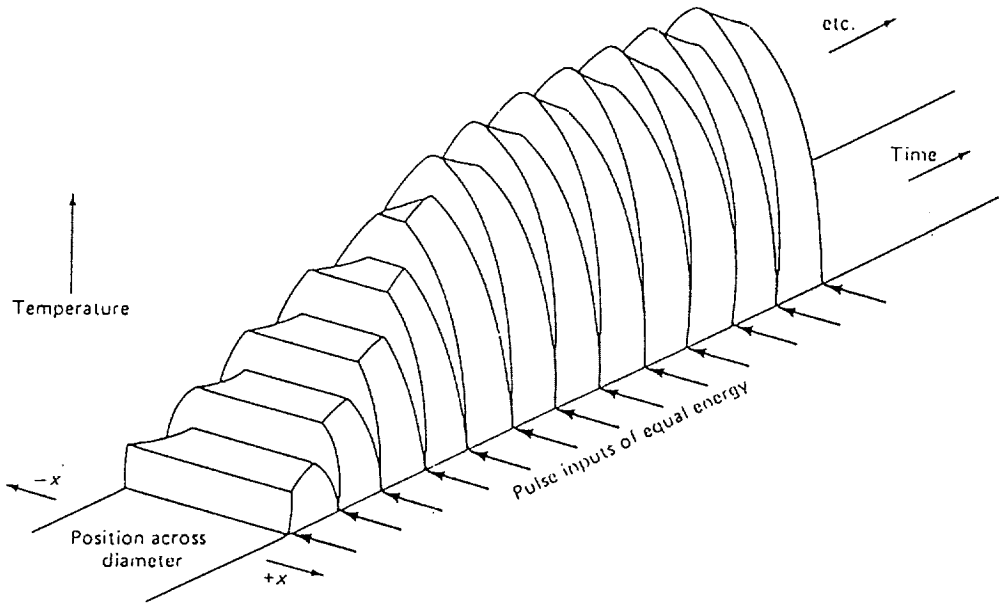

Figure 2-7. Thermal Buildup when Pulse Interval is Small Compared to Thermal Relaxation Time[2]

comes negligibly small compared to the thermal relaxation time, the thermal profile of the laser rod will approach the profiles of continuously pumped rods with the same total power deposition. The transient temperature distributions, as the rod approaches thermal equilibrium, has a large effect on the laser energy output and beam divergence of the laser[2]. These transient periods will be discussed in the next chapter on thermal lensing.

Figures 2-8 and 2-9 are examples of a Gaussian end-pumped Nd:YAG laser being operated at a high pulse repetition rate. Figure 2-8 depicts the detailed buildup of tem-

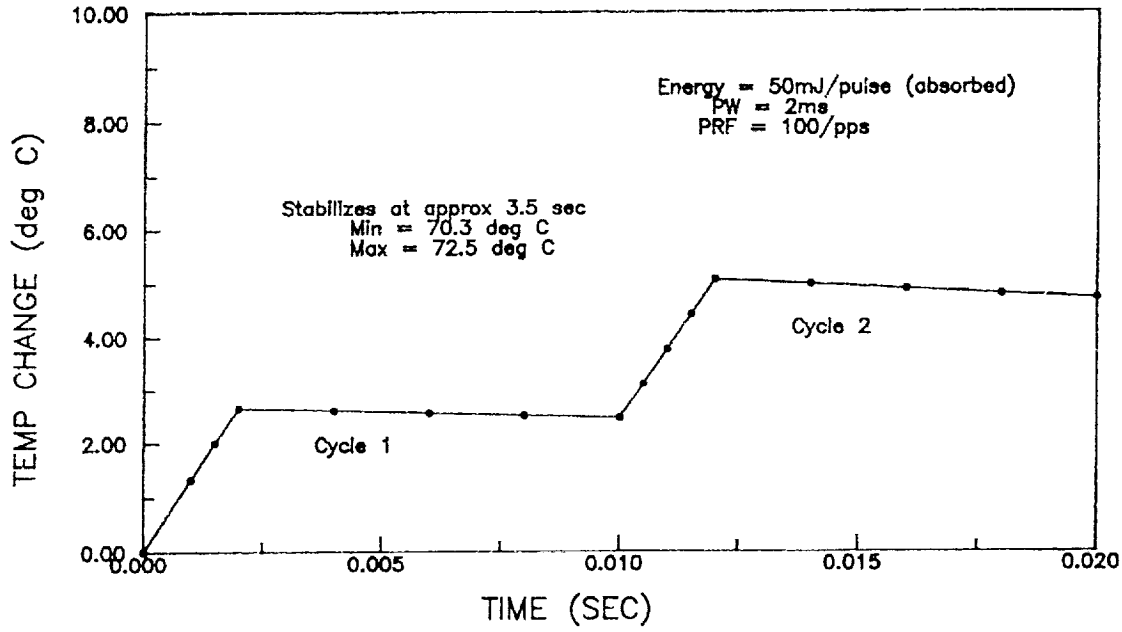

Figure 2-8. Variation of Temperature for Nd:YAG (At Center of Pump-End Face)

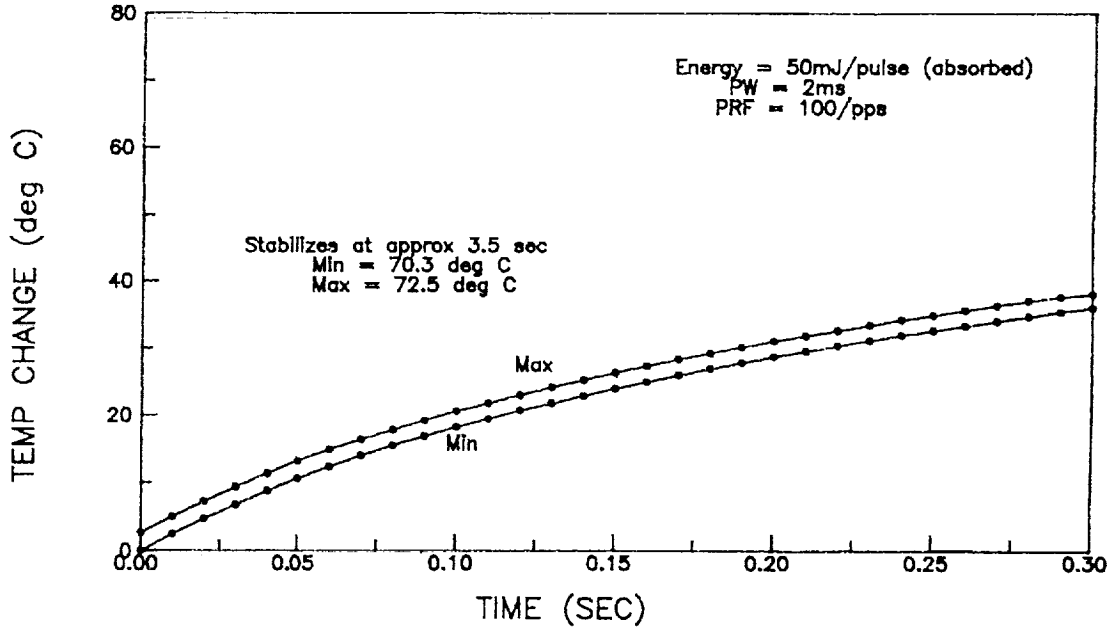

Figure 2-9. Extreme Temperature for Nd:YAG (At Center of Pump-End Face)

perature for two pump cycles. Figure 2-9 shows the maximum and minimum temperatures within each pulse cycle. These graphs show that the Nd:YAG laser will reach a steady-state temperature in approximately 3.0 seconds. The estimated maximum temperature of the Nd:YAG rod is approximately 72.5°C above the ambient at the center of the rod pump-end face.

This knowledge of the maximum temperature is critical to laser design. For example, if the temperature exceeds the stress fracture limit of the rod, the laser crystal will fracture. The stress fracture temperature limit for Nd:YAG is approximately 115°C.[2]

Figure 2-10 and 2-11 are examples of the output from

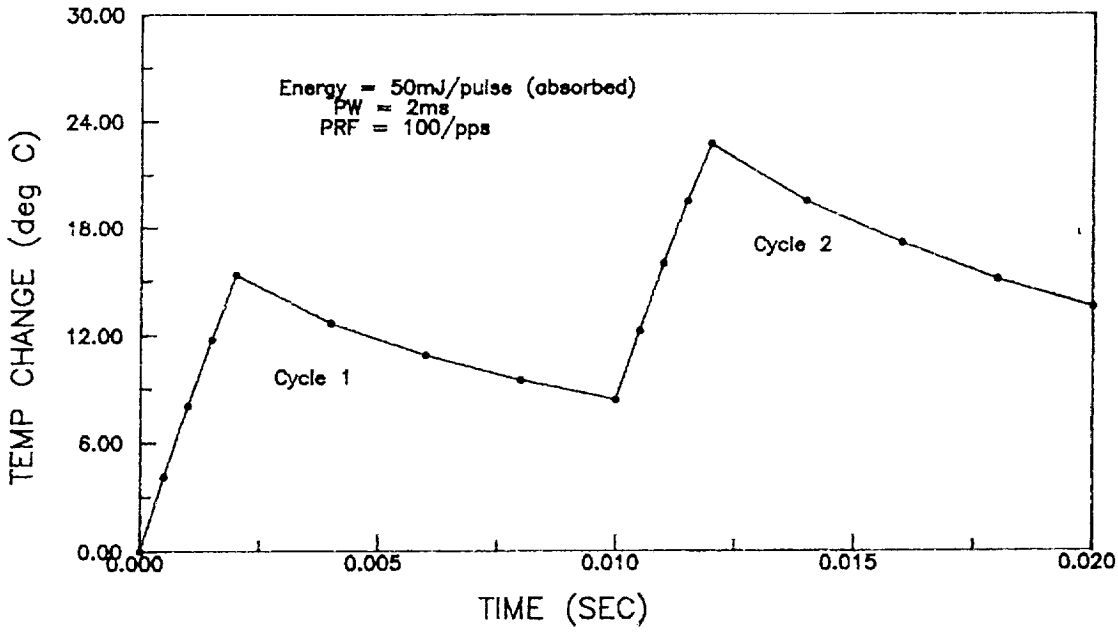

Figure 2-10. Variation of Temperature for Ti:AL_2O_3 (At Center of Pump-End Face)

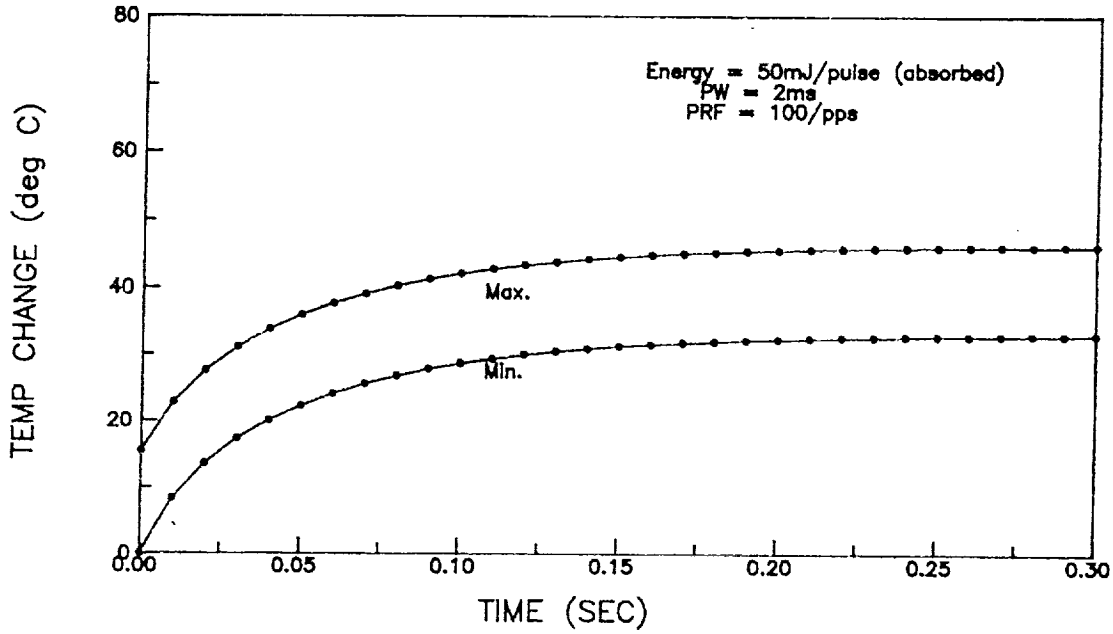

Figure 2-11. Extreme Temperature for Ti:AL_2O_3 (At Center of Pump-End Face)

the Temperature Distribution Model of the temperature rise due to accumulation effects of multipulse operations for Gaussian end-pumped Ti:AL_2O_3 rods. As can be seen, the rod reaches a steady-state temperature in approximately 300ms and has a maximum temperature of approximately 42°C at the center of the pump-end face.

The above presented example profiles from the Temperature Distribution Model are just a few of the many profiles that can be generated. Other profiles, such as radial and axial temperature profiles versus time, can also be generated for a variety of pumping and cooling schemes.

C. Summary of the Temperature Distribution Model

The general theory describing the transient thermal profiles in CW and pulse-pumped lasers for a large variety of operating parameters are presented in Koechner[2,5] and Farrukh et al.[1,3,7] These general theories were implemented by Farrukh into a general analytical model. The model then generates thermal profiles for a large variety of finite solid-state lasers, with user specified operating parameters. Examples of typical profiles were presented throughout this section to give the reader a feel for the capabilities of this model.

These time-dependent derived thermal profiles are critical in determining thermal lensing effects which depend upon the spatial distribution of temperature and its gradients.[8]

In the next chapter, the theory of thermal lensing and formulation of the **Thermal Lensing Model** will be discussed. The model takes as its input, the time-dependent temperature profiles from the **Temperature Distribution Model** outlined above. The **Thermal Lensing Model** is then used to estimate the focal lengths and distortions present in finite solid-state Nd:YAG and Ti:AL_2O_3 laser rods.

CHAPTER 3

Thermal Lensing

A. Introduction to Thermal Lensing.

Thermal lensing is the distortion and defocusing of a laser beam transmitted through material medium, due to the non-uniform heating of the material.[4] Any solid-state laser material operating in either the steady-state, pulsed, or CW mode of operation must dissipate an appreciable amount of heat. This is the result of a fast pump-introduced heating process (where some fraction of the total pump energy is deposited in the laser rod as heat), followed by a slow recovery of the rod to its ambient temperature. In the cylindrical rod geometries normally used, the heat is removed on the surface of the rod. This process generates radial and axial thermal gradients in the rod.

The change in temperature, within a laser rod, causes thermal defocusing and distortion of the laser beam. This is due to the temperature variation of the material refractive index. Additionally, these thermal gradients cause stresses within the laser material. The generated stresses induce birefringence and non-uniform elongation of the rod and bulging of the ends. Collectively, these above factors of temperature variation of the refractive index, birefringence, and bulge are referred to as thermal lensing. From

Koechner[9], the temperature dependent variation of the refractive index constitutes the major contribution to thermal lensing. The stress dependent variation of the refractive index (birefringence) modifies the focal length about 20 percent.[9] The effects of end-face curvature, caused by an elongation of the rod on thermal lensing is less than six percent.[9]

The resulting distortion and defocusing of laser beams have been observed in a variety of experiments. Several theoretical treatments of thermal lensing have been given. These include geometrical-optics[10], wave-optics[11], and the vector Kirchhoff diffraction formulation of thermal lensing[4,11] to account for thermally-induced birefringence.

In the general theory for the formulation of the **Thermal Lensing Model**, various effects of thermal lensing will be discussed. However, in the model, only thermal lensing due to the temperature variation of the material refractive index using ray-trace methodology will be implemented. The ray-trace method was chosen as the simplest approach to obtain a working model. This method makes maximum use of the temperature profiles generated by the **Temperature Distribution Model** previously discussed. This approach also accounts for 75-80 percent of the thermal lensing effects present in side and end-pumped laser rods. In general, the model will give the user a first approximation of the

thermal focal length and the degree of distortion expected for rods of specific dimensions and specified operating parameters. The input to this approach will be the temperature profiles generated by the **Temperature Distribution Model**.

In the next section, a detailed one dimensional theory of thermal lensing from Koechner[2,9] will be presented. The presented theory will outline the effects of temperature, birefringence, and bulge that contribute to thermal lensing for a side-pumped Nd:YAG laser rod.

B. One Dimensional Theory of Thermal Lensing.

The one dimensional theory of thermal lensing is looked at because the basic underlying theory and mathematical formulation can be modified and applied to the problem of developing the **Thermal Lensing Model**.

Consider the case of the CW side-pumped Nd:YAG rod where the heat generated within the laser rod, due to the optical pumping, are removed by a coolant flowing along the cylindrical rod surface. As a result of the assumption of uniform internal heat generation and uniform cooling along the cylindrical surface of an infinitely long rod, the temperature profiles will be strictly radial. The end effects and small variation of coolant temperature in the axial direction are neglected here. The radial temperature distribution in a very long cylindrical rod is obtained from the

one dimensional heat conduction equation:[13]

$$\frac{d^2T}{dr^2} + \frac{dT}{rdr} + \frac{Q}{K} = 0 \qquad [3\text{-}1]$$

where K is the material thermal conductivity and Q is the rate at which heat is generated per unit volume. The solution to equation (3-1) gives the temperature at any point along a radius of length r. With the boundary condition $T(r_o)$ for $r=r_o$, where $T(r_o)$ is the temperature at the rod surface and r_o is the radius of the rod, then:

$$T(r) = T(r_o) + \frac{Q}{4K}(r_o^2 - r^2) \qquad [3\text{-}2]$$

This temperature profile is parabolic, with the highest temperature being at the center of the rod. The heat generated per unit volume, for uniform heat absorbtion, can be expressed as:

$$Q = \frac{P_a}{\pi r_o^2 L} \qquad [3\text{-}3]$$

where P_a is the total power absorbed by the rod; r_o is the rod radius; and L is the length of the rod. The temperature difference between the rod surface and the center is given by:

$$T(0) - T(r_o) = \frac{P_a}{4\pi KL} \qquad [3\text{-}4]$$

The transfer of heat between the rod and the coolant

creates a temperature difference between the rod surface and the coolant. A steady-state equilibrium temperature will be reached when the rate of the total internal generation (P_a) of heat is equal to the rate at which heat is removed from the rod by the coolant. For a typical Nd:YAG rod, the equilibrium temperature is reached about 3 1/2 seconds after laser turn-on. Figure 3-1 depicts an example of the radial temperature profile of a 20 pulse per second, side-pumped, Nd:YAG laser at thermal equilibrium.

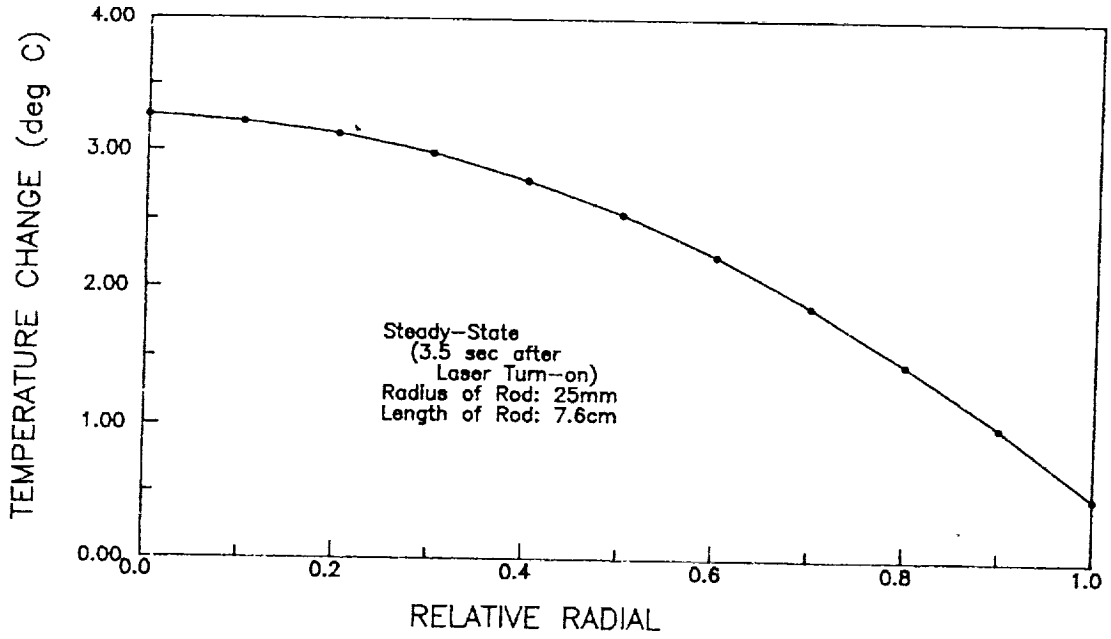

Figure 3-1. Radial Temperature Distribution for a Nd:YAG Crystal

The heat is generated at the rate of 0.3 Joules per pulse and negligible cooling was assumed at the ends of the rod. With these conditions, axial thermal gradients do not exist

in this rod.

These temperature gradients generate mechanical radial, tangential, and axial stresses in the laser rod, since the hotter inside area of the rod is constrained from expansion by the cooler rod surface. Normally, these stresses are calculated when one needs to find the birefringence and the stress fracture limit of the crystal. For Nd:YAG rods, Koechner[2,9] has provided a sample of these calculations. For example, if the approximate temperature differential between the center and the surface of the rod is 115°C, then the crystal may fracture. The equations for these calculations are derived by Timoshenko and Goodier.[15]

Having discussed the basic theory of one dimensional temperature distribution and the mechanical stresses caused by the thermal gradients, our attention can now be turned to the photoelastic effects (birefringence). The mechanical stresses generate thermal strains in the rod, which in turn produce refractive index variations via the photoelastic effect. The refractive index of a medium is specified by the indicatrix. In its most general case, the indicatrix is in the shape of an ellipsoid. A change of refractive index due to strain is given by a small change in the shape, size, and orientation of the indicatrix.[16] Since Nd:YAG is a cubic crystal, the indicatrix is a

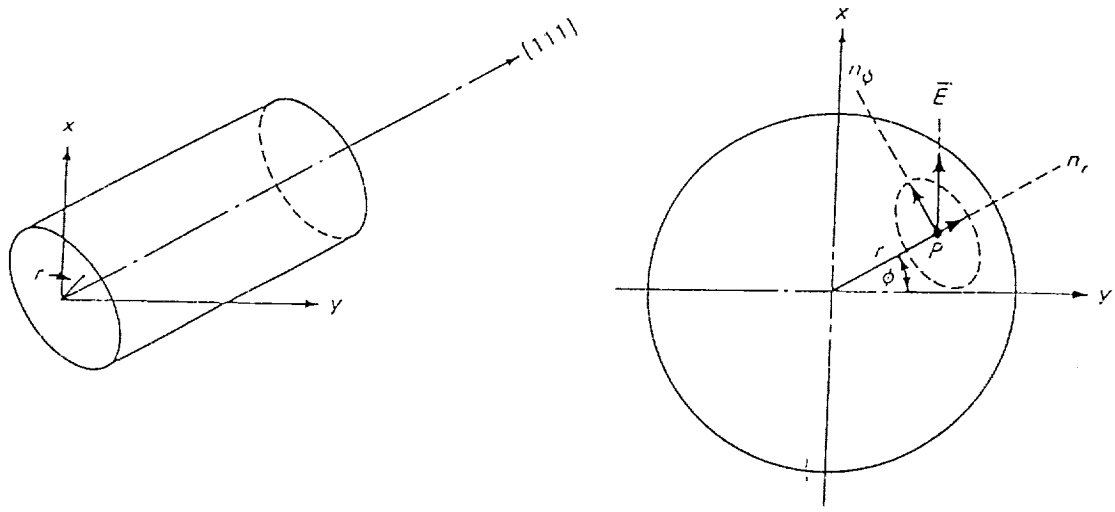

Figure 3-2. Crystal Orientation for a Nd:YAG Rod (left) and Orientation of Indicatrix of a Thermally Stressed Rod in a Plane Perpendicular to the Rod Axis (right)[2]

sphere. Under stress, the indicatrix becomes an ellipsoid. Nd:YAG rods are grown with the cylindrical axes along the [111] direction. An illustration of this is depicted in Figure 3-2. The light propagates in this direction, and thus the change of the refractive index along the [111] axis is of interest.

Since the transverse stresses are in the radial and tangential direction (see Figure 3-2), the local indicatrix also orients its axis in those directions. In a cylindrical coordinate system, the photoelastic changes in the refractive index for the radial and tangential polarizations are only obtained after a considerable amount of tensor

analysis. This is normally done using the vector Kirchhoff diffraction formulation approach. Various treatments of these involved birefringence calculations for Nd:YAG are covered in detail in references 4, 8, 12, and 17. The expressions for the radial and tangential refractive index changes for Nd:YAG are given by[8,17] as:

$$\Delta n_r = -\frac{1}{2} n_o^3 \frac{\alpha Q}{K} C_r r^2 \qquad (3\text{-}5)$$

$$\Delta n_\phi = -\frac{1}{2} n_o^3 \frac{\alpha Q}{K} C_\phi r^2 \qquad (3\text{-}6)$$

where Δn_r and Δn_ϕ are the radial and tangential stress dependent changes of the refractive index, respectively; n_o is the refractive index of the rod at its ambient temperature; α is the thermal coefficient of expansion for Nd:YAG; Q is the heat generated per unit volume; and K is the thermal conductivity of Nd:YAG. The coefficients C_r and C_ϕ are functions of the electrooptical coefficients that were determined from tensor analysis for Nd:YAG. Both coefficients were calculated by Koechner[2] for Nd:YAG. Their values are listed as $C_r = 0.017$ and $C_\phi = -0.0025$ respectively.

Having explored the temperature and stresses in a Nd:YAG rod, the optical distortions which are a result of both the thermal gradients and the stresses can now be discussed. The change in the refractive index can be separated into a temperature and a stress-dependent contribu-

tion.[2] Therefore:

$$n(r) = n_o + \Delta n(r)_T + \Delta n(r)_S \qquad (3\text{-}7)$$

where n(r) is the radial variation of the refractive index; n_o is the refractive index of the material at ambient temperature; $\Delta n(r)_T$ and $\Delta n(r)_S$ are the temperature and stress-dependent changes of the refractive index, respectively.

The temperature dependent change of the refractive index can be expressed as:[2]

$$\Delta n(r)_T = [T(r) - T(0)]\frac{dn}{dT} \qquad (3\text{-}8)$$

where T(r) and T(0) are the temperature at the radius r and center of the rod, respectively. With the aid of equations (3-2 through 3-4) and equation (3-8), we obtain:[2]

$$\Delta n(r)_T = -\frac{Q}{4K}\frac{dn}{dT}r^2 \qquad (3\text{-}9)$$

Comparing equations (3-5, 3-6, and 3-9), we see that the refractive index in a laser rod shows a quadratic variation with radius. An optical beam propagating along the rod axis also develops a quadratic spatial phase variation. This perturbation is equivalent to the effect of a spherical lens[14]. The focal length of a lens-like medium whose index of refraction is assumed to vary according to:[2]

$$n(r) = n_o\left(1 - \frac{2r^2}{b^2}\right) \qquad (3\text{-}10)$$

where b measures the degree of variation of the index of refraction is given by:[14]

$$f = \frac{r^2}{4n_o L} \qquad [3\text{-}11]$$

The total variation of the refractive index is obtained by introducing equations (3-5, 3-6, and 3-9) into (3-7). This gives us:[2]

$$n(r) = n_o\left\{1 - \frac{Q}{2K}\left(\frac{1}{2n_o}\frac{dn}{dT} + n_o^2\alpha C_{r,\phi}\right)r^2\right\} \qquad [3\text{-}12]$$

As was previously discussed, the change in the refractive index, due to thermal strain, is dependent on the radial (r) and tangential (ø) stresses where C_r= 0.017 and C_ϕ= -0.0025. Therefore, the expression for n(r) in (3-12) yeilds two values. Comparing equations (3-10) and (3-12) yields the focal length (f') equation:[2]

$$f' = \frac{K}{QL}\left(\frac{dn}{2dT} + \alpha C_{r,\phi} n_o^3\right)^{-1} \qquad [3\text{-}13]$$

The first term in the parentheses is the temperature dependent variation of the refractive index. The second term contains the stress dependent variations of the refractive index. Because of the birefringence, Nd:YAG has two effective focal lengths. One is due to the radial electrooptic

(C_r) coefficient and the second is due to the tangential (C_ϕ) coefficient.

In our final expression for the focal length of a Nd:YAG rod, we must also include the effect of rod end distortion (bulge). The stresses, that cause bulging, are found to occur within a region of approximately one radius from the ends for Nd:YAG.[18] This deviation from flatness of the rod ends is obtained from:[2]

$$L[r] = \alpha L_o[T[r] - T[0]] \qquad [3\text{-}14]$$

where α is the thermal coefficient of expansion for Nd:YAG and L_o is the length of the end section of the rod where expansion occurs. With $L_o = r_o$ and equation (3-2), we obtain:[2]

$$L[r] = -\alpha r_o \frac{Qr^2}{4K} \qquad [3\text{-}15]$$

The contribution to the focal length of the rod caused by end-face curvature is given by the thick-lens formula of geometric optics[16] as:

$$f'' = \frac{R}{2(n_o - 1)} \qquad [3\text{-}16]$$

where the radius of end-face curvature is defined as $R = -(d^2L/dr^2)^{-1}$. From the expressions (3-14, 3-15, and 3-16) follows the focal (f") length of the rod caused by bulge:[2]

$$f'' = K[\alpha Q r_o (n_o - 1)]^{-1} \qquad (3\text{-}17)$$

Inserting equation (3-17) into (3-13) gives us the final expression for the focal length of a Nd:YAG rod:[2]

$$f = \frac{KA}{P_a}\left(\frac{dn}{2dT} + \alpha C_{r,\phi}\, n_o^3 + \frac{\alpha r_o (n_o - 1)}{L} \right)^{-1} \qquad (3\text{-}18)$$

where A is the rod cross-sectional area and P_a is the power absorbed.

This expression accounts for the temperature, stress-dependent variation of the refractive index, and end-face curvature. If one introduces the appropriate material parameters for Nd:YAG into equation (3-18), then one finds that the temperature dependent variation of the refractive index constitutes the major contribution to thermal lensing.[2] The stress dependent variation of the refractive index and end-face curvature modifies the focal length by approximately 20 percent and less than 6 percent, respectively.[2]

Figure 3-3 depicts the graph of the approximation of the focal lengths, using equation (3-18), for a side-pumped Nd:YAG rod. The focal lengths were calculated using the following parameters: length and radius of the rod was 7.6cm and 25mm, respectively; dn/dt, the material variation of the refractive index was 8.9×10^{-6}; index of refraction

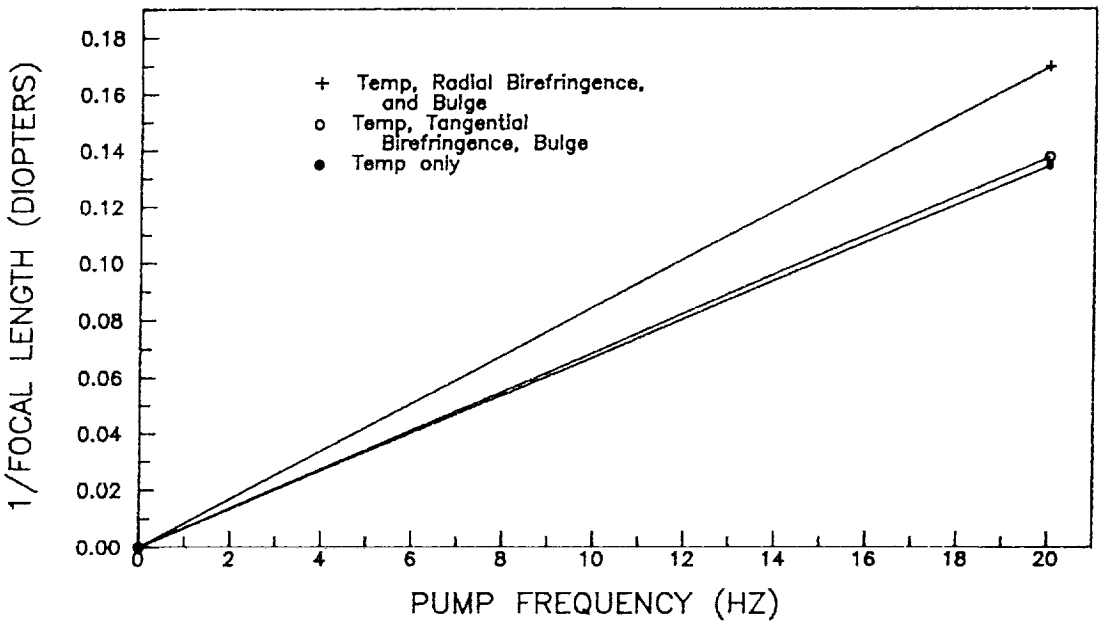

Figure 3-3. Predicted Thermal Focusing Effects in Nd:YAG

(n_o) was 1.825; thermal conductivity (K) was 0.103; α, the thermal coefficient for expansion was 7.9×10^{-6}; the radial (C_r) and tangential (C_ϕ) variation of the refractive index were 0.017 and -0.0025, respectively; and, the power absorbed (P_a) by the rod (as heat), was $6.119 w/cm^3$.

This completes the one dimensional theory of thermal lensing for a Nd:YAG rod. The same analysis holds for Ti:AL_2O_3 and other laser materials. As was previously stated, the temperature dependent variation of the refractive index will be the only aspect implemented in the Thermal Lensing Model. The implementation of birefringence and bulge effects will be left as future enhancements to the

model. In the next section, the formulation of the Thermal Lensing Model is developed.

C. Two Dimensional Model Formulation.

Formulation of the thermal lensing ray-trace model requires basic understanding of various optical theories. These include the theories of ray tracing[16], wave optics in crystals[11,19], Fresnel diffraction theory of waves in lens-like mediums[14], geometrical-optics[10], etc. It was not the purpose of this thesis to become trapped into the finer details of the referenced optic theories. Nor do we intend to repeat the derivations of the referenced theories. If more detailed information is desired, then we refer the reader to the attached list of references and other literature on the subject.

The basic task of this research is to formulate a computer ray-trace model that allows for a first approximation of focal length. The model is to be based on the temperature variation of the refractive index. The approximations of focal length are then obtained on specific crystals operated with specified parameters. This will be done by modifying the focal length expression (3-11) for a thin lens. The focal lengths are then approximated, by calculating the phase shift in the index of refraction, as the different rays of a plane wave front are tracked through a lens-like crystal medium. The localized change in the ray

direction as it transverses a lens-like medium is assumed to obey Snell's law which is given by:[19]

$$n_i \sin\theta_o = n_2 \sin\theta_i \qquad [3\text{-}19]$$

where n_1 and n_2 are the index of refractions of two adjacent mediums, respectively; and θ_i and θ_o are the input and output angles of the ray at the boundary between the adjacent mediums.

To assist in the formulation of the model, it is appropriate to introduce, and explain, two tables and a figure before proceeding. Table 3-1 depicts an illustration of the output block of radial and axial temperature profiles, provided by the Temperature Distribution Model. This output is based on a 20pps, side-pumped, Nd:YAG laser. The laser was operated with moderate side cooling and rod

Table 3-1. Block of Radial and Axial Temperature Profiles for a Nd:YAG Crystal

Temperature Distribution Radial Diffusivity..... 26.95 Radius of Rod (cm)..... 0.25 Length of Rod (cm)..... 7.6 Time (sec)..... 3.5			
R\L	0.00 ...	0.50 ...	1.00
0.00	2.9139	2.9139	2.9139
0.20	2.8020	2.8020	2.8020
0.40	2.4660	2.4660	2.4660
0.60	1.9047	1.9047	1.9047
0.80	1.1276	1.1276	1.1276
1.00	0.2248	0.2248	0.2248

ends were not cooled. In the vertical direction, are the radial temperatures starting from the center of the rod (top) and increments outward to the surface of the rod (bottom). In the horizontal direction, are the axial temperatures starting from the front face (left) of the rod and increments to the back end (right) of the rod. In this particular example, a set of 10 equally spaced increments was chosen to represent the 25mm x 7.6cm rod in both the axial and radial directions. Additionally, in Table 3-1, the temperatures are observed only to vary in the radial direction. The displayed block of temperatures in Table 3-1 is an example of a side-pumped Nd:YAG rod at thermal equilibrium, when rod ends aren't cooled.

Table 3-2 displays a block of radial and axial index of refractions for the temperatures presented in Table 3-1.

Table 3-2. Block of Radial and Axial Index of Refraction for the Temperatures in Table 3-1

Index of Refractions			
R\L	0.00 ...	0.50 ...	1.00
0.00	1.825026	1.825026	1.825026
0.20	1.825025	1.825025	1.825025
0.40	1.825022	1.825022	1.825022
0.60	1.825017	1.825017	1.825017
0.80	1.825010	1.825010	1.825010
1.00	1.825002	1.825002	1.825002

The block of temperature variations of the Index of Refractions were calculated from the expression:

$$n(r,z) = n_o + \alpha T(r,z) \qquad (3\text{-}20)$$

where n_o is the index of refraction for the rod at its ambient temperature and α is the dn/dt specified for the rod.

Table 3-2, shows that the index of refraction is only changing in the radial direction which was expected for a side-pumped Nd:YAG rod with no end cooling employed. For end-pumped rods, the index of refraction would change in both the radial and axial direction. The incremental partition of the index of refractions in Table 3-2 are the same as the partitions of temperatures displayed in Table 3-1.

The user specified partition, selected for use in the **Temperature Distribution Model**, governs the partition of the **Thermal Lensing Model**. The partition of 10 equally spaced increments are normally chosen because it is more than adequate for first approximations. Increasing the number of partitions does increase the accuracy of the approximation. However, the time required to run the **Temperature Distribution Model** increases linearly as the number of partitions increases. Comparison of the temperature outputs for a partition of 10 and 20 equally spaced increments showed a mere 0.4 percent difference in the approxi-

mated temperatures.

Figure 3-4 illustrates the three types of pumping beam profiles used to pump a laser rod. All three types of pumping profiles can be used to end pump a rod. (Normally, only the circular and parabolic beam profiles are used to describe the distribution of heat deposition in side-pumped operations.)

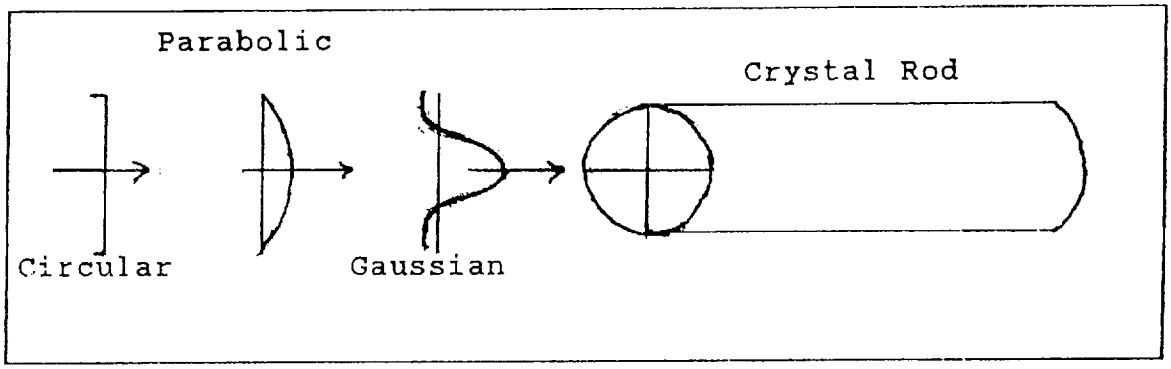

Figure 3-4. Types of Pump Beam Profiles

The above mentioned types of pump beam profiles have been implemented in the Temperature Distribution Model. In the thermal lensing ray-trace model, the focal length of the rod irrespective of the type of pumping beam used can be approximated. However, only the circular pump beam has been implemented for distortion calculations. Implementation of distortion calculations for parabolic and Gaussian beam profiles have been left as a future model enhancement. Table 3-1 represents a matrix of temperatures for a specif-

ic rod operating with user specified parameters. It serves as one of the primary inputs to the **Thermal Lensing Model.**

A radially dependent phase delay is experienced by a wave front propagating through a medium with a varying index of refraction n. Thus, a thin slab of the crystal medium can be approximated as a thin lens. The lensing model traces wave fronts propagating through the rod starting from several radial positions at the rod front face. As the ray propagates through the rod, a series of thin lenses are setup and the temperature dependence of the index of refraction is calculated at specified locations. Using these calculations, a focal length associated with each tracing ray can be estimated. An average focal length for the rod is obtained by taking the mean of the focal lengths of the individual tracing rays. The specified axial increment of the temperature matrix determines the number of equivalent thin lens placed in series that the tracing ray must pass through. For example, with an axial incremental spacing of 0.1, as depicted in Table 3-1, 20 equivalent thin lens are placed in series from the front to the back of the rod.

A plane wave propagating through a lens-like medium acts as a spherical thin lens and diverges. Using this fact, the thin lens focal expression (3-11) was changed to:

$$f_r = - \frac{(rr_o)^2}{\Delta z L \sum [n_r(r,z) - n_o(0,z)]} \qquad (3\text{-}21)$$

where r_o and r are the exiting relative radius of the ray and the radius of the rod in cm, respectively; z is the specified axial increment of the rod (dimensionless); L is the length of the rod in cm; and $n_r(r,z)$, $n_o(0,z)$ are the temperature dependent index of refraction for the radial point of interest and for the center of the rod, respectively. The focal length expression (3-21) can be applied upon determination of the quantities r_o, $n_r(r,z)$, and $n_o(0,z)$. Calculating these scalar quantities are the essence of the thermal lensing ray-trace model.

The radial variation in temperature, as confirmed by use of curve fitting algorithms, is quadratic in nature. This fact allowed the selection and development of a binomial interpolation algorithm to obtain values of temperature at points other than the selected matrix points. The binomial interpolation algorithm is based on the approximation:

$$ax^2 + bx + c = T \qquad (3\text{-}22)$$

where a,b,and c are constant coefficients, x is either the radial (r) or axial (z) coordinate, and T is the temperature. By invoking this algorithm using a set of three collinear temperature (input) values along with their coordinate specifications, we can obtain a value for the temperature at any other point not specified in the temperature matrix.

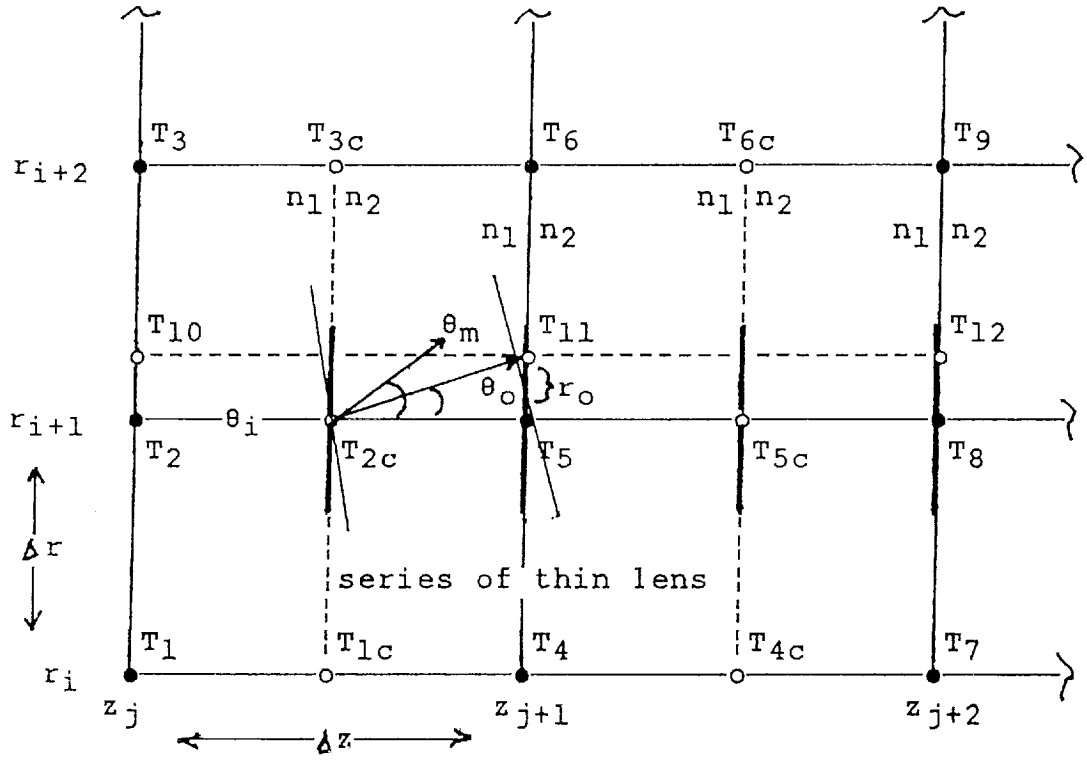

Figure 3-5. Partial Illustration of the Thermal Lensing Matrix With a Series of Thin Lens Overlaid

The temperature matrix (obtained from the input file) is illustrated in Figure 3-5. A wave front ray will be traced starting at the r_{i+1} radial input position through a series of equally spaced ($\Delta z/2$) thin lenses. The r_{i+1} ray was selected to illustrate the definition of the input and output angles that occur as the ray passes through a thin lens. These angles are necessary to calculate the exiting radius of the ray (r_o) for use in the focal length expression (3-21) and distortion calculations.

The r_1 ray (center of the rod) is also traced to ob-

tain a summation of the temperature variation of the index of refraction at the center of the rod, $n_o(0,z)$. As illustrated in Figure 3-5, temperatures T_1 through T_9 are obtained from the temperature matrix provided as input. Invoking the binomial interpolation algorithm allowed the calculation of the intermediate temperatures T_{1c} through T_{6c} for use in the thermal lensing scheme. This completes the basic setup of the thermal lensing scheme and provides the framework to proceed with the ray-tracing of specific input rays.

A collimated plane wave entering the rod will have an input angle (θ_i) equal to zero. As it passes through the first lens, the angle (θ_m) between the normal to the surface of constant temperature and the rod axis will be calculated at $\Delta z/2$. To calculate θ_m, we determine first the surface of constant temperature by obtaining the r and z derivatives of expression (3-22). The derivatives are given by:

$$\frac{dT(r)}{dr} = 2ar_i + b \qquad (3\text{-}23)$$

$$\frac{dT(z)}{dz} = 2a\left(\frac{\Delta z}{2}\right) + b \qquad (3\text{-}24)$$

where r_i is the input radius, Δz is the axial incremental spacing, and a,b are the calculated coefficients using the appropriate radial and axial temperature points in the in-

terpolation algorithm. The angle θ_m at $\Delta z/2$ is then calculated using the trigonometric expression:

$$\theta_m = \tan^{-1}\left(\frac{dr}{dz}\right) \qquad [3\text{-}25]$$

On finding the angle θ_m, the next step is to determine the specific values of the index of refraction on each side of the imagined lens. Due to the fact that the temperature dependent index of refraction changes very little between adjacent points (<< 1), it was decided to compute the index of refraction on each side of θ_m according to the following expressions:

$$n_1 = n_o + \alpha\left(\frac{T_2 + T_m}{2}\right) \qquad [3\text{-}26]$$

$$n_2 = n_o + \alpha\left(\frac{T_m + T_5}{2}\right) \qquad [3\text{-}27]$$

where n_o is the index of refraction of the rod at its ambient temperature; α is the specified dn/dT of the rod; and T_2, T_5, and T_M (same as T_{2c} in the first stage of tracing) are the specific temperature points before, at, and after the position of the imagined lens.

By invoking Snell's law, the output angle (θ_o) of the ray passing through the thin lens can be obtained by substitution in the expression:

$$\theta_o = \theta_m - \sin^{-1}\left[\frac{n_2}{n_1}\sin(\theta_m - \theta_i)\right] \qquad (3\text{-}28)$$

After finding the output angle, the change in output radius (r_o) can be calculated from the trigonometric expression:

$$r_o = \frac{\Delta z}{2}\tan\theta_o + r_m \qquad (3\text{-}29)$$

where r_m is the midpoint radial position of the ray (same as r_{i+1} for initial entry of the ray into the rod). The output angle (θ_o) and output radius (r_o) are then sent to a recursive numerical algorithm to refine the output values at Δz to meet operator specified accuracy criteria for θ_o.

The phase shift in the temperature variation of the index of refraction can be calculated, for the initial entry of the ray into the rod, and is proportional to the expression:

$$n_r(r,z) = n_1 + n_2\sqrt{1 + \frac{(r_o - r_m)r}{\left(\frac{\Delta z}{2}L\right)^2}} \qquad (3\text{-}30)$$

and for later increments of the rod to:

$$n_r(r,z) = n_1\sqrt{1 + \frac{(r_m - r_i)r}{\left(\frac{\Delta z}{2}L\right)^2}} + n_2\sqrt{1 + \frac{(r_o - r_m)r}{\left(\frac{\Delta z}{2}L\right)^2}} \qquad (3\text{-}31)$$

The individual calculations from each lens, as the ray propagates through the rod, are retained and summed to determine the value for $n_r(r,z)$ which is then used in the focal length expression (3-21).

One-to one distortion mapping of a ray propagating through a lens-like medium is a straight forward calculation when dealing with side and end-pumped circular beams. The input irradiance (I) of the collimated plane wave is constant as it enters the crystal medium. The incremental change in irradiance is then calculated at the output end of the rod from the expression:

$$\Delta I = \frac{r_i^2[i+1] - r_i^2(i)}{r_o^2(i+1] - r_o^2(i)} \qquad [3\text{-}32]$$

where r_o, r_i are the output and input radius of the ray being traced, respectively. The percentage of total distortion (D), for each ray, is then calculated from the expression:

$$D = 100 - \left(\frac{r_o^2[i+1] - r_i^2[i+1]}{r_i^2[i+1]} \right) \qquad [3\text{-}33]$$

This completes the formulation of the thermal lensing ray-trace model. Now, it's just a formality of computer record keeping to invoke the binomial interpolation algorithm, using r_o, to calculate T_{10}, T_{11}, and T_{12}, reset

the output radius (r_o) of the previous rod segment equal to the input radius (r_i) of the next rod segment, reset the output angle (θ_o) equal to the input angle (θ_i), and increment forward to the next imagined thin lens. The calculations are repeated until the ray exits the rod. When the ray exits the rod, the focal length and distortion associated with the ray are calculated and retained. Then, the ray-trace program increments upward in the matrix of temperatures to trace the next input ray. Upon completion of the ray tracing for a block of temperatures, the mean of the individual focal lengths and distortion present for that block of temperatures are then calculated. The model then increments forward to the next block of input temperatures (at a later time) and repeats the process until the input file of temperatures are exhausted and a time dependent average focal length are obtained.

The **Thermal Lensing Model** program code is contained in Appendix A. An example of the lensing model inputs and output are enclosed in Appendix B and C, respectively.

CHAPTER 4

Analysis and Discussion of Thermal Lensing

The next generation of solid-state lasers (used for remote sensing of the atmosphere from space platforms), are under development. Various new lasing materials and laser configuations are being investigated. Currently, the solid-state, end-pumped diode lasers are the most promising candidates due to their small size, reliability, performance, low power and cooling requirements, etc. Analyzing thermal lensing effects for these end-pumped configuations, using various cooling schemes are of interest to the designers of laser systems. Theoretical formulations, numerical calculations and experimental data do not exist for end-pumped configuations.

Before proceeding with the analysis of thermal lensing in end-pumped Nd:YAG and Ti:AL_2O_3 laser rods, an assessment of the validity of the **Thermal Lensing Model** was conducted. The validation was based on the comparison of model results with the experimental data for a repetitively pulsed side-pumped Nd:YAG laser. This case was interesting from two points. It was the only laser found, with actual experimental data on thermal focal length. The second point of interest is that the laser was side-pumped. The later point allowed for the extrapolation of Koechner's predic-

tion which are based on a CW side-pumped Nd:YAG laser. Thus, the model results were compared to both the experimental results and Koechner's theoretical formulation for a long continuously side-pumped rod.

A. Model Validation.

Research of the literature shows that theoretical formulation and experimental data on thermal lensing effects do not exist for repetitive pulsed end-pumped lasers due to their recent development. In fact, very little data exist on repetitively pulsed side-pumped lasers. The vast majority of data published such as theoretical formulations, theoretical calculations, experimental results, etc. are based on CW side-pumped lasers dating back to the early 1970's. Most of these early analyses were conducted by Koechner[5,9] and are still being referenced to as the authoritative source on the subject today.

A recent experiment, depicting the results of thermal focusing for a repetitive pulsed side-pumped Nd:YAG laser has been completed.[20] The laser rod used in the experiment had a length of 7.6cm, a radius of 25mm, was side-pumped uniformly, and cooled along its length (ends were not cooled). Each pump pulse had a duration of 130μs and an energy level of 10 Joules. Experimental calculations indicated that approximately 3.5 percent of the pump energy was absorbed into the rod as heat.

Both, the Temperature Distribution Model and Thermal Lensing Model were executed using the Nd:YAG material characteristics and the laser configuation of the experimental setup. The modeling and experimental results, along with Koechner's prediction of focal length from equation (3-18) are shown in Figure 4-1. (It should be noted that Koechner's prediction, used in Figure 4-1, did not include birefringence and bulge effects.)

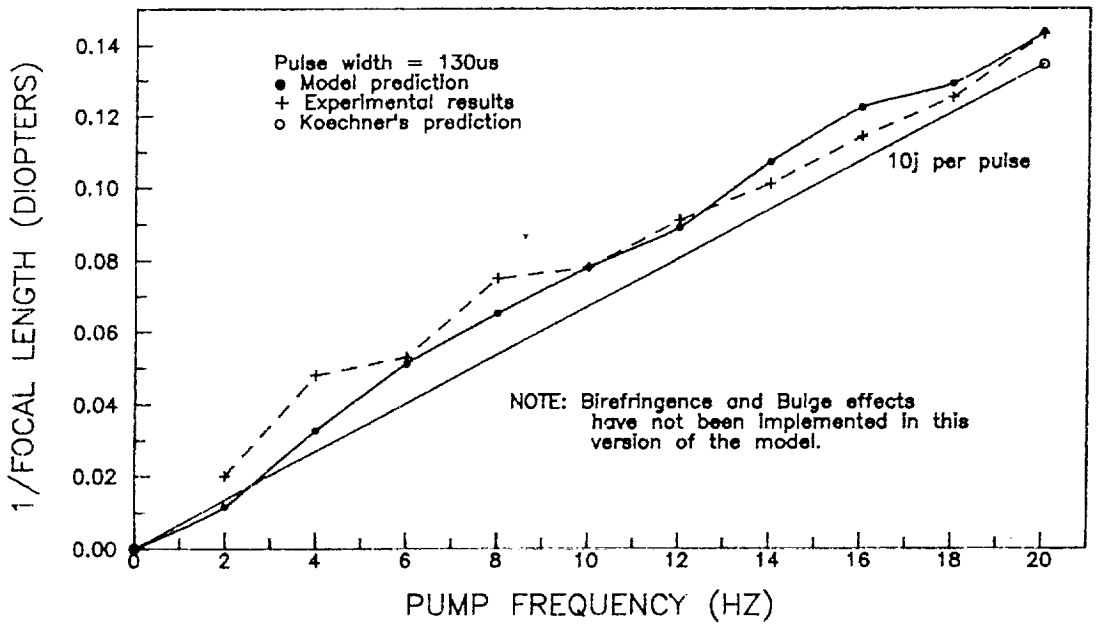

Figure 4-1. Thermal Focusing in Nd:YAG Rod

Figure 4-1 shows that the model's prediction of the thermal focal length are in good agreement with the experimental results and Koechner's theoretical prediction of focal length for an equivalent power problem. Thus, the ray-

trace model, based on the thermal gradients provided by the Temperature Distribution Model, will give a fairly accurate first order approximation.

Transient thermal focal length calculations of a side-pumped Nd:YAG rod do indicate an appreciable deviation from the standard steady-state power calculations using Koechner's prediction equation (3-18). Starting from an inactive condition, the Nd:YAG rod thermal focal length did stabilize at about 3.5 seconds. However, the steady-state calculations from the model at the end of each pump pulse indicates a higher focusing power of about 15-25 percent at frequencies of 4-20 hertz over the results as predicted by Koechner. This was not unexpected as the model was executed in an repetitive pulsed mode. Where as, Koechner's prediction are based on a thermally stabilized CW pulsed (same power) rod.

The transient side-pumped thermal focal length varies from 28 meters at 100ms to 6.97 meters at the steady-state equilibrium condition. The time dependent focal length, as shown in Figure 4-2, was computed at the end of each pump pulse for the above described laser rod. The rod was pumped by a 20 Hz, 10 Joule per pulse flash lamp. The horizontal line was obtained by using Koechner's formula for a thermally stabilized CW pulsed (same power) rod whose surface temperature was kept at a fixed value.

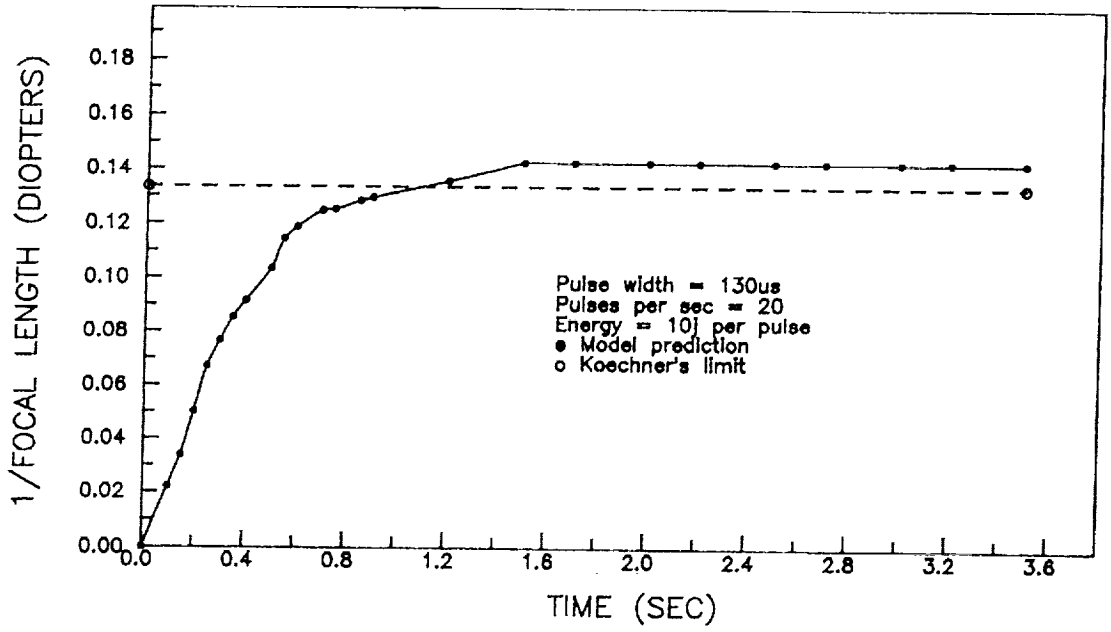

Figure 4-2. Transient Thermal Focal Length for a Side-Pumped Nd:YAG Rod

Thermally induced focusing varies significantly in the time interval between pulses. Even at a 10Hz repetition frequency, the variation in the Nd:YAG thermally induced focal length was approximately 10 percent.

The model was also used to estimate the impact of surface cooling on the focal length. Focal length was found to be very sensitive in the low end of the surface cooling parameter. Figure 4-3 displays the results of focal length versus cooling in side-pumped Nd:YAG rods. The cooling parameter is a dimensionless quantity obtained by multiplying the length of the rod by the surface heat transfer

coefficient and dividing by the bulk thermal conductivity of the rod material. Koechner's formulation, by comparison, is for a fixed surface temperature.

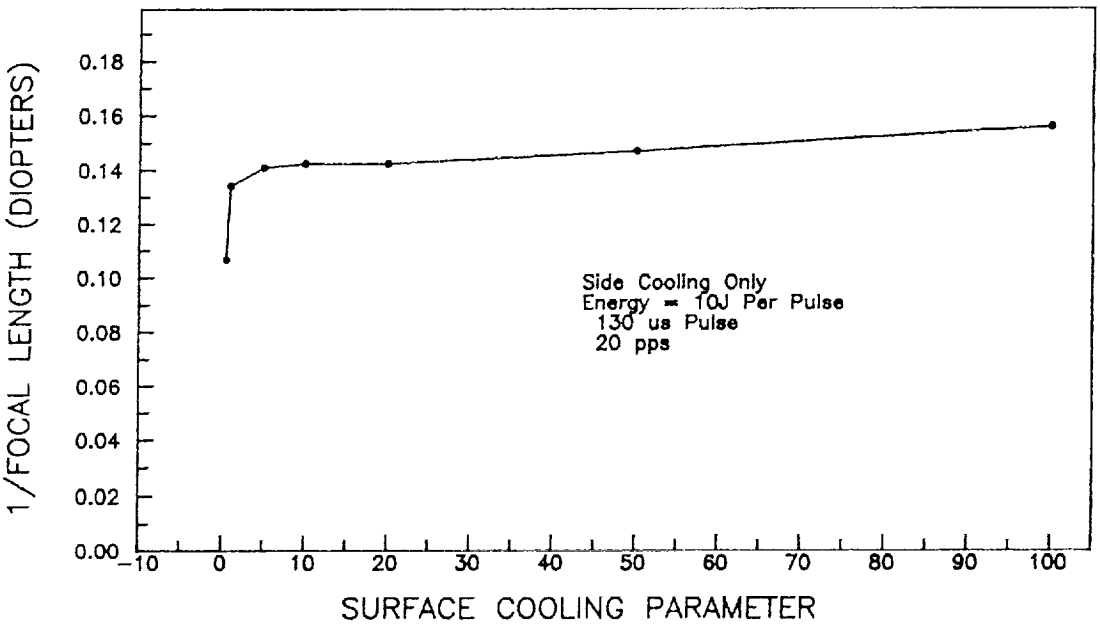

Figure 4-3. Focal Length vs Cooling in Side-Pumped Nd:YAG Rod

Figure 4-3 is also important to system designs. It shows that above a certain point, very little is gained from additional cooling. Therefore, the most efficient cooling for the laser is critical for spaced based applications. Power consumption in space platforms are one of the most critical design parameters. Additional unneeded cooling may strain the limited power resources available in space.

One-to-one mapping of intensity in the repetitive pulsed side-pumped Nd:YAG laser showed distortion to be negligible during the rod transient period. This result was expected due to the presence of only radial thermal gradients (no axial gradients) as a result of the uniform pumping of the rod and the absence of end-cooling.

B. Analysis of Thermal Lensing in End-Pumped Nd:YAG and Ti:AL_2O_3 Laser Rods.

Thermal lensing calculations have been obtained for the two end-pumped laser rod configuations depicted in Table 4-1 below. Both of these laser crystals are currently undergoing feasibility experiments in the laboratory at NASA Langley Research Center. It should be noted here that the comparison is not between crystals of different dimensions, but between cyystals of practical dimensions. Both

Table 4-1. End-Pumped Laser Rod Characteristics

Parameters	Nd:YAG	Ti:AL_2O_3
Rod Length (cm)	1.0	0.6
Rod Radius (cm)	0.4	0.2
Thermal Diffusivity (cm^2/s)	26.947	8.87
Thermal Conductivity (W/cm ^oK)	0.103	0.330
Material dn/dt	$8.9x10^{-6}$	$1.28x10^{-5}$
Index of Refraction	1.825	1.7654
Optical Attenuation	3.0	3.0
Pump Wavelength (microns)	1.15	0.6438
Pump Energy Absorbed (J/cm^3)	0.050	0.050
Pump Pulse Duration (seconds)	0.010	0.010

crystals were end-pumped by a Gaussian beam where the ratio

of the beamwidth to the rod radius is 0.5. With the exception of the rod material characteristics, all other parameters such as side and end cooling, energy absorbed, pump pulse duration, etc. were the same for both rods. Both, the Temperature Distribution Model and the Thermal Lensing Model were executed using the appropriate material characteristics of the rod and the laser configuation depicted in Table 4-1.

Figures 4-4 and 4-5 presents the single pulse transient behavior of thermal focal length for Nd:YAG and $Ti:AL_2O_3$ crystals, respectively. Both rods were end-pumped

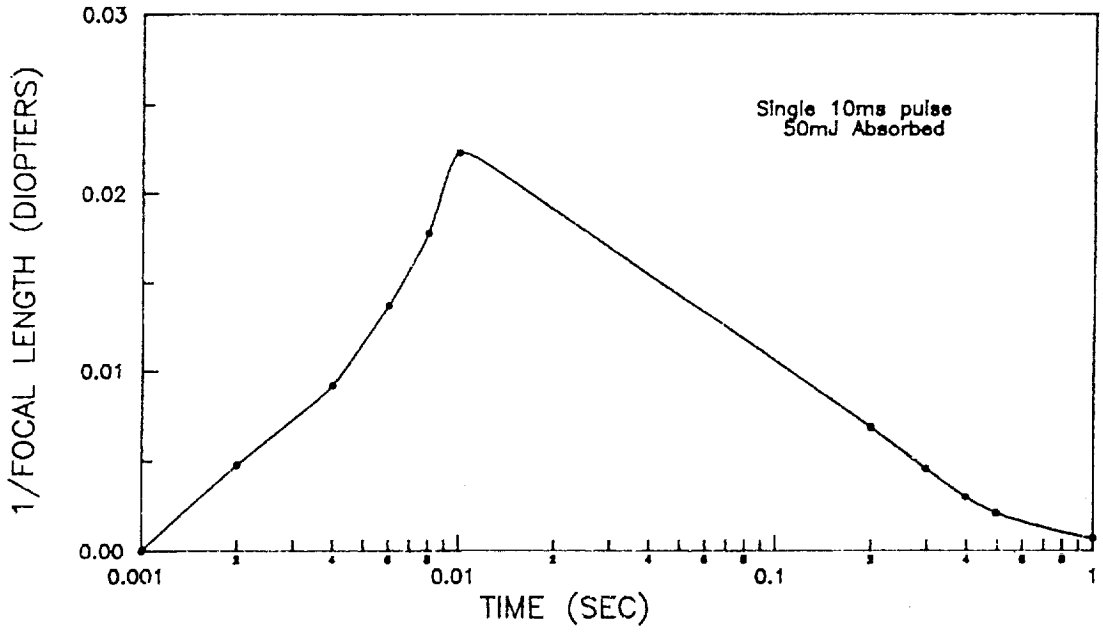

Figure 4-4. Single Pulse Transient of Thermal Focal Length in Nd:YAG Crystal

with a single pulse of 10ms duration. The energy absorbed

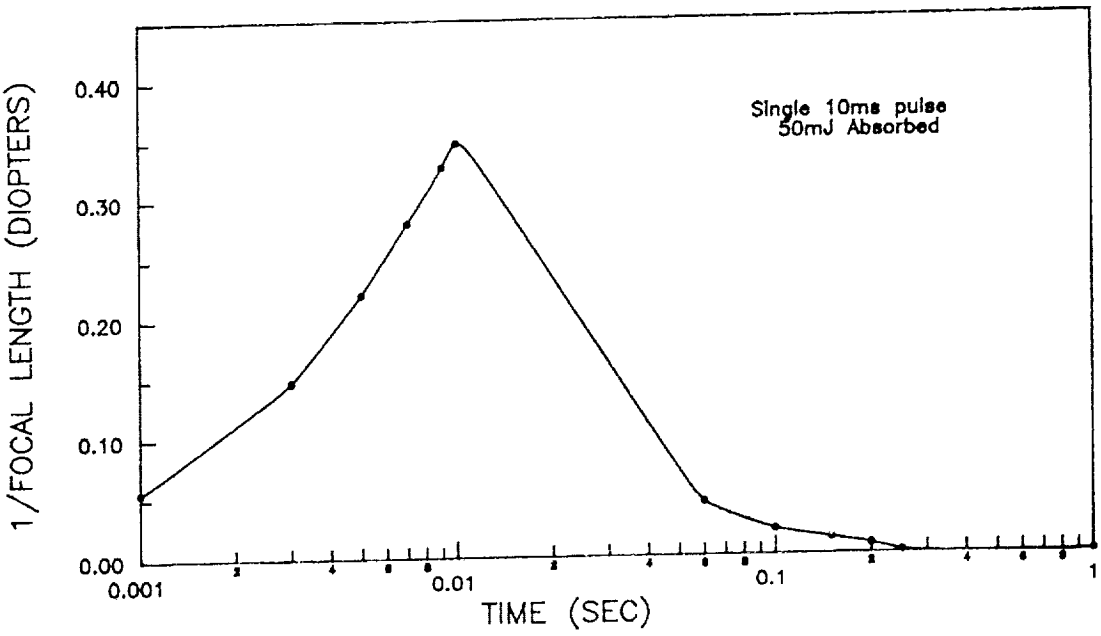

Figure 4-5. Single Pulse Transient of Thermal Focal Length in Ti:AL_2O_3 Crystal

into the rod as heat was assumed to be 50mJ per pulse. Moderate side cooling parameter of 20 was employed. Ends were not cooled. (The cooling parameter is a dimensionless quantity obtained by multiplying the length of the rod by the surface heat transfer coefficient and dividing by the bulk thermal conductivity of the rod material.) Starting from an inactive condition, the thermal focal length for Nd:YAG ranged from 205 meters at 2ms to the minimum of 44.8 meters at 10ms when the pump pulse was turned off. For Ti:AL_2O_3, the thermal focal length ranged from 18 meters at 1ms to 2.87 meters at 10ms. Although some residual heat still exist in the rods, as the rods relaxes to its ambient

condition, the thermal focal lengths are no longer measurable 1.30 seconds and 250ms after pump shutdown for Nd:YAG and Ti:AL_2O_3 rods, respectively. For all practical purposes, as far as focal length is concerned, the rods have returned to their ambient state at this point.

The transient thermal focal length profiles for Nd:YAG and Ti:AL_2O_3 during multiple pulse operations are shown in Figures 4-6 and 4-7. As seen in Figure 4-6, the Nd:YAG rod

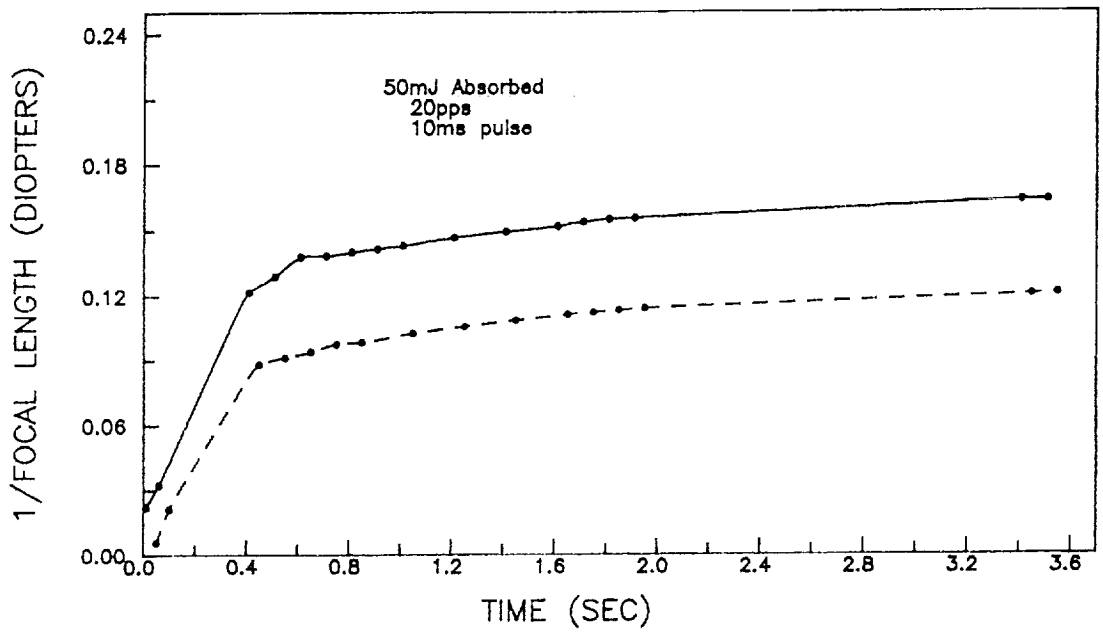

Figure 4-6. Transient Thermal Focal Length for a Multiple Pulsed, End-Pump Nd:YAG Rod

thermal focal length stabilized at about 3.5 seconds. For Ti:AL_2O_3, the rod thermal focal length stabilized at about 300ms. In both rods, it was found that the thermal focal lengths stabilized at the same time the temperatures became

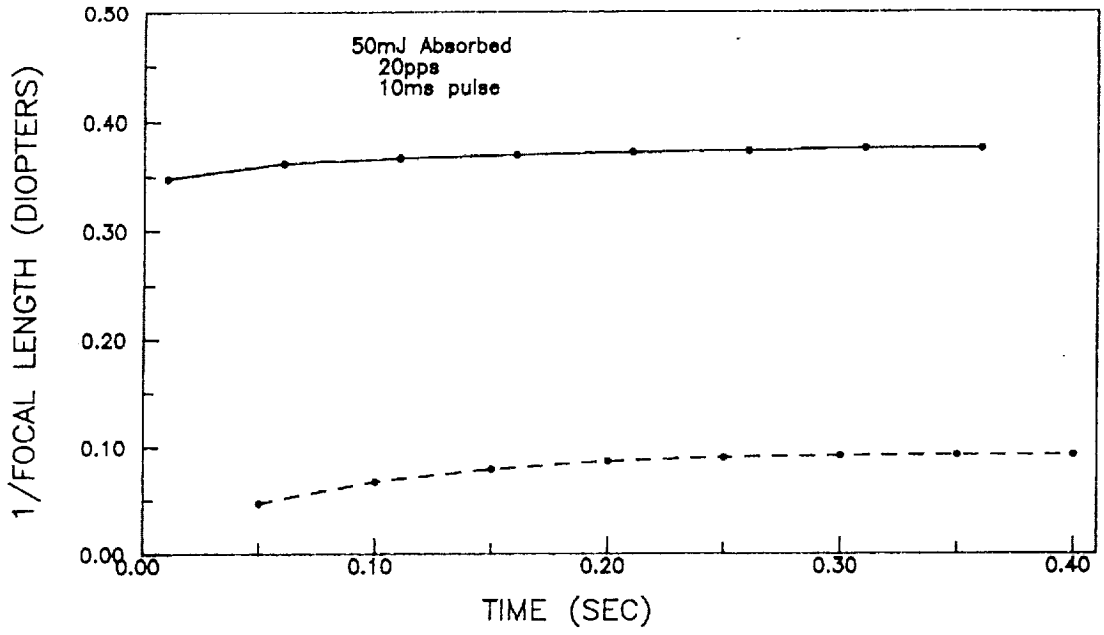

Figure 4-7. Transient Thermal Focal length for a Multiple Pulsed, End-pumped Ti:AL_2O_3 Rod

stabilized which was expected. The Nd:YAG transient end-pumped thermal focal length varied from 44 meters at 10ms to 6.11 meters at the steady-state equilibrium condition. For Ti:AL_2O_3, the thermal focal length varied from 2.87 meters at 10ms to 2.66 meters at steady-state equilibrium. These time dependent focal lengths, shown in the solid lines, in Figures 4-6 and 4-7 were computed at the end of each pump pulse for the described laser rods. Both rods were pumped at a 20 Hz rate. Energy absorbed into the rods as heat was assumed to be 50 mJ per pulse.

Thermally induced focusing varied significantly in the

time interval between pulses as shown by the dashed lines in Figures 4-6 and 4-7. The variation was approximately 26 and 75 percent for Nd:YAG and Ti:AL_2O_3, respectively. The time dependent focal length between pulses were computed at the start of each pump pulse for the above rods. Not accounting for the temporal variation of the thermally induced focal length during the pulse relaxation period, may lead to significant errors during design.

The next factor looked at was thermal focusing versus pump frequency and the impact of side and end cooling on thermal focal lengths. Figures 4-8 and 4-9 depict the results for Nd:YAG and Ti:AL_2O_3, respectively. Pump frequen-

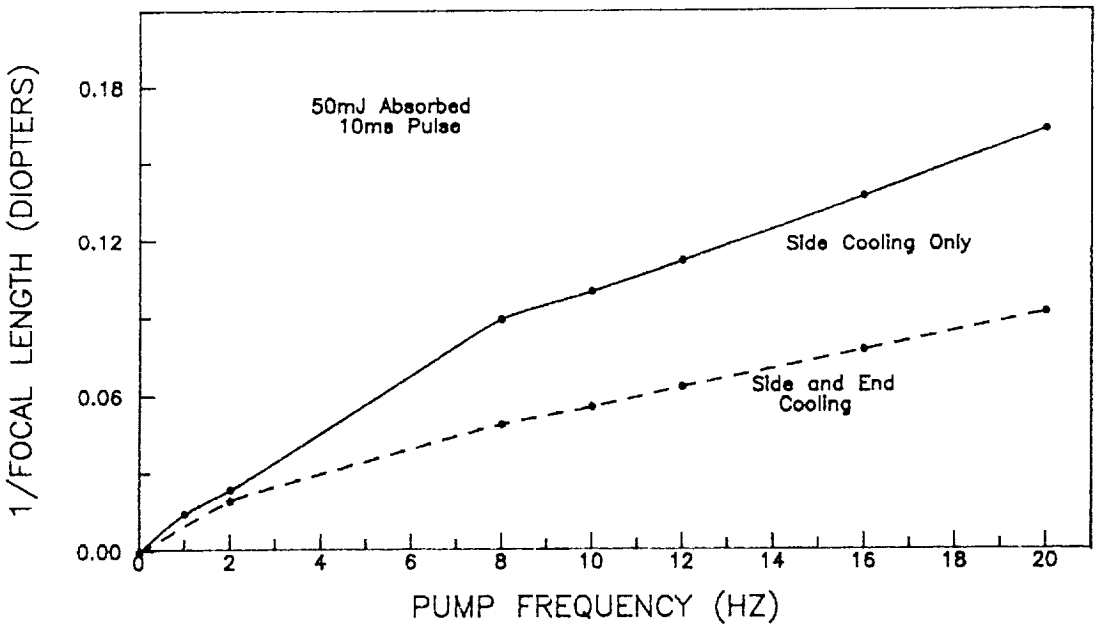

Figure 4-8. Thermal Focusing in End-Pumped Nd:YAG Rod

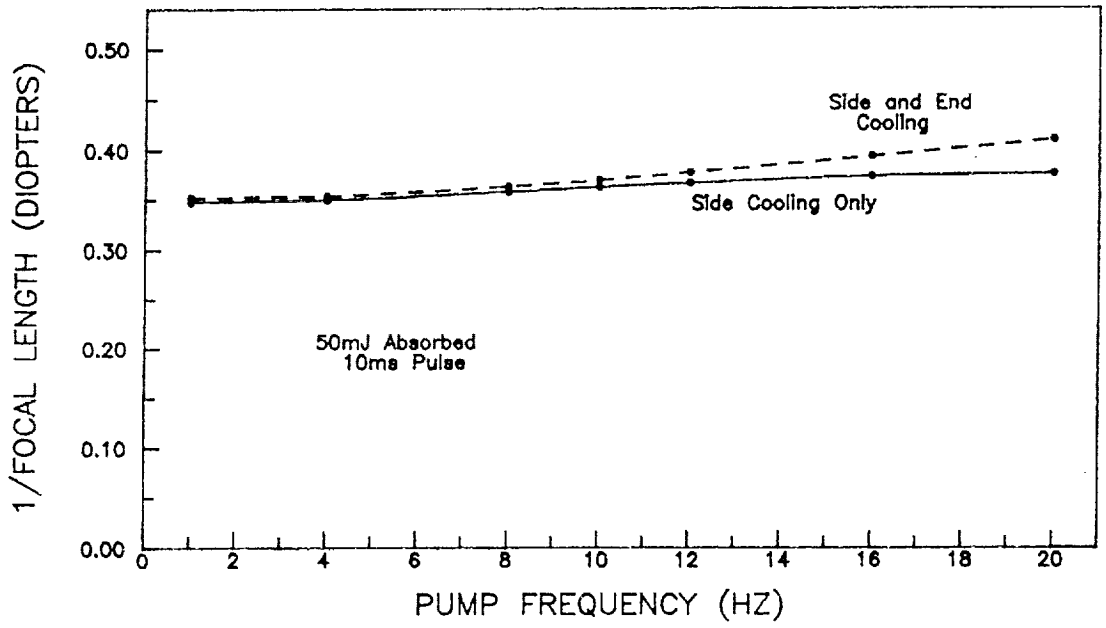

Figure 4-9. Thermal Focusing in End-Pumped Ti:AL_2O_3 Rod

cy was varied between 1 and 20 HZ. For each frequency, the rod was allowed to stabilize (3.5s for Nd:YAG and 300ms for Ti:AL_2O_3) before calculations were made. In both figures, moderate side cooling parameter of 20 was employed. For calculations involving both side and end cooling, end cooling was set equal to the side cooling. As shown in Figure 4-8, the impact of end cooling caused a significant decrease in the Nd:YAG thermal focal length above 2 Hz. This result was expected as the radial and axial temperature gradients near the rod ends become smoother due to end cooling.

For $Ti:AL_2O_3$, very little impact from end cooling was experienced until the 12 HZ pump frequency was reached. However, in comparison to Nd:YAG where the thermal focal length was significantly decreased, the opposite effect was obtained for $Ti:AL_2O_3$. End cooling of $Ti:AL_2O_3$ crystals causes small increases in the thermal focal length as the pump frequency is increased. This result was not expected. However, upon further analysis of the temperature profiles for $Ti:AL_2O_3$, it was apparent that the radial and axial temperature gradients near the ends were greater due to end cooling.

Finally, the model was used to estimate the impact of surface cooling on the induced thermal focal lengths for end-pumped Nd:YAG and $Ti:AL_2O_3$ laser crystals. The rods were pumped at a 20 HZ rate and energy absorbed into the rod as heat was assumed at 50mJ per pulse. Figures 4-10 and 4-11 presents the results of focal length versus side cooling for these configuations. The focal length was found to be very sensitive only on the low end of the surface cooling parameter for both rods. Therefore, sizing end-pumped lasers for correct cooling is critical for spaced based applications as previously explained.

Distortion calculations were not performed on these end-pumped lasers as the function for mapping of Gaussian beams has not been implemented in the model (left as a fu-

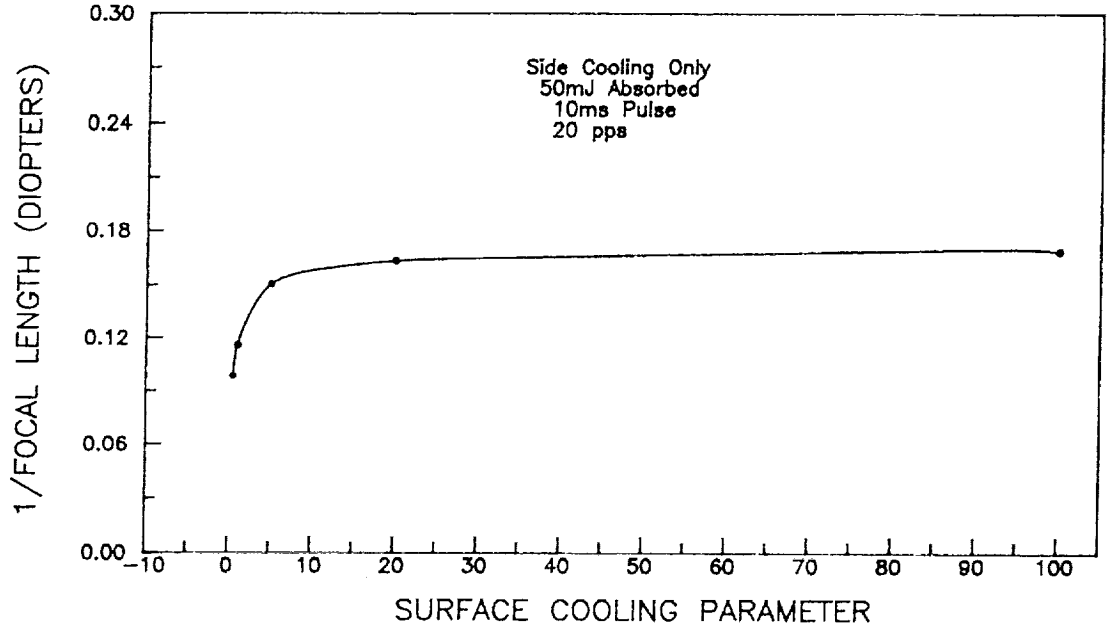

Figure 4-10. Focal Length vs Side Cooling in End-Pumped Nd:YAG Rod

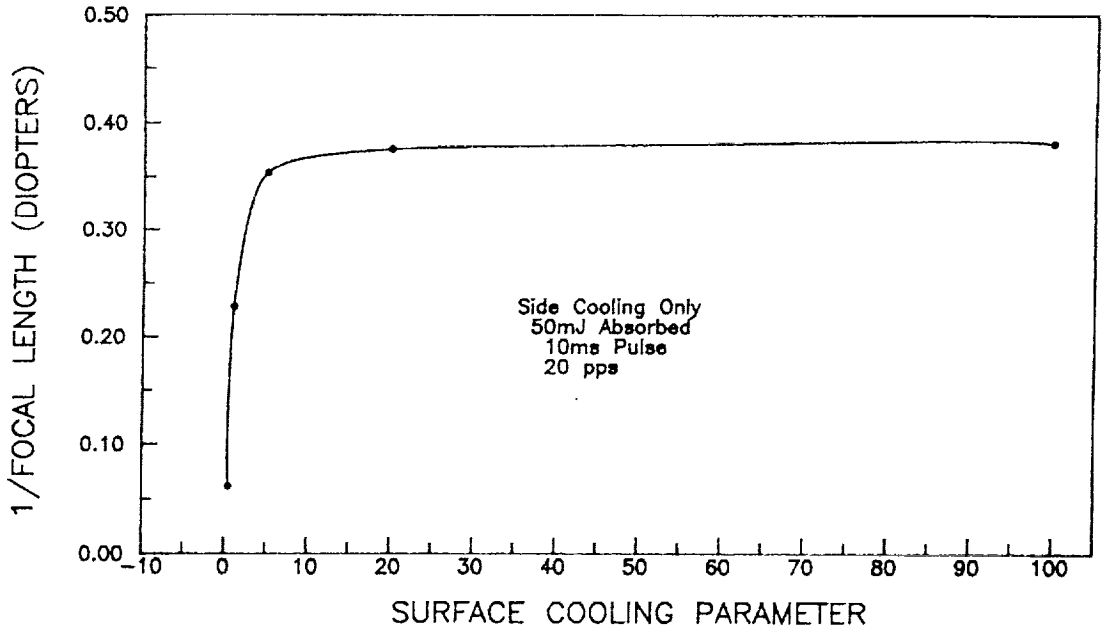

Figure 4-11. Focal Length vs Side Cooling in End-Pumped Ti:AL_2O_3 Rod

ture model enhancement). Unlike the side-pumped configuation, previously discussed, where distortion was non-existent at thermal equilibrium, preliminary indications are that distortion in the end-pumped configuations will be on the order of 3-5 percent at thermal equilibrium.

CHAPTER 5

Summary and Conclusions

An analytic expression for approximating the time-dependent thermal focal length in finite solid-state laser rods has been derived. The analysis is based on the temperature variation of the material refractive index caused by optical pumping of these rods. This analysis is also applicable to situations where the laser rod is side or end-pumped by circular, parabolic, or Guassian beam profiles. Short or long pulse, continuous wave (CW), or repetitive pulsed operations are also applicable. The repetitive pulsed, end-pumped solid-state diode laser configuations are of current research interest as the next generation of lasers will come from this category.

Several quantities were found to be relevant to this analysis. These quantities were the specific thermal profiles of the rods, type of optical pumping employed, type of cooling scheme employed (side and end-cooling parameters), and the specific material characteristics of the rods.

The Thermal Lensing Model was formulated using geometric ray tracing based on the focal length expression for a thin lens. The focal lengths are then approximated, by calculating the phase shift in the index of refraction, as

the plane wave is tracked through a lens-like crystal medium.

Thermally induced temperature profiles, for end-pumped laser rods operating with specified parameters, are approximated by the **Temperature Distribution Model**. These thermal profiles are then inputted to the developed **Thermal Lensing Model**. The **Thermal Lensing Model** is then used to approximate the transient thermal focal length and estimate the final rise in thermal focal length for the laser rod under evaluation. Various pumping and cooling schemes can be evaluated for their effect on the induced thermal focal length. For circular pump beam profiles, distortion calculations are also approximated by the model.

The numerical examples for end-pumped, repetitively pulsed Nd:YAG and Ti:AL_2O_3 laser rods showed the following major results.

a. The minimum induced thermal focal length is achieved at the time of pump pulse turn off for both rods operating under single long pulse conditions.

b. For multiple pulse operations, the minimum induced thermal focal length was achieved when the rod reached its thermal equilibrium condition (3.5 seconds for Nd:YAG and 300ms for Ti:AL_2O_3).

c. Thermally induced focusing varied significantly in the time interval between pulses (26 percent for Nd:YAG and 75 percent for Ti:-AL_2O_3).

d. Employment of end-cooling significantly decreased thermal focusing in Nd:YAG above the 2 Hz pump frequency. For Ti:AL_2O_3, the opposite effect was found. Small increases were noticed in the thermal focal length for pump frequencies above 12 Hz.

e. Under conditions when only the side cooling was varied, the induced thermal focal length was found to be very sensitive at the low end of the scale for both rods.

The model was validated against experimental data and theoretical calculations of thermal focal length for a repetitive pulsed, side-pumped Nd:YAG laser. It is seen that the prediction of thermal focal length is in good quantitative agreement with experimentally observed behavior. Thus, the **Thermal Lensing Model**, based on the thermal profiles provided by the **Temperature Distribution Model**, will give a fairly accurate first order approximation of the thermal focal length.

Appendix A

Computer Program Listing

1. Functional Description

The Thermal Lensing Model (**THERLENS.FOR**) is not a standalone computer program. Its primary input is dependent on the output of a previously developed theoretical model titled: **Temperature Distribution Model** for finite optically pumped laser rods. The output of the **Temperature Distribution Model** (blocks of temperature data versus time), along with other thermal lensing constants (see Appendix B), are inputted to the lensing model. The model then calculates the finite changes in focal length and distortion effects due to the temperature gradients within the laser rod. Appendix C depicts the **Thermal Lensing Model** output.

Currently, the lensing model can calculate the thermal lensing effects for side and end-pump configurations and distortion approximations for circular pump beams only. (Note: Distortion calculations for parabolic and Gaussian pump beams will be implemented in the future.) The optical axis of the laser rod is assumed to be along the axis of the rod.

2. Environmental Characteristics

This program was written in the Fortran language. It was compiled and linked using the Microsoft Fortran 77 Optimizing Compiler Version 4.10. The Thermal Lensing Model can be executed on any IBM/IBM compatible 286/386AT micro-computer with a 287/387 Math Coprocessor. This version can also be executed on the VAX 750 mini-computer. The source program size on the AT-machine is 46,527 bytes and the executable program is 69,621 bytes. The enclosed program code contains all changes through March 1, 1990.

3. Thermal Lensing Program Listing

(Program listing starts on next page)

03-01-90
18:42:07

Source Line Microsoft FORTRAN Optimizing Compiler Version 4.10

```
 1  $DEBUG
 2  C
 3  C   A COMPUTER PROGRAM SIMULATION MODEL TO COMPUTE THERMAL LENSING FROM
 4  C   TEMPERATURE DISTRIBUTION PROFILES IN OPTICALLY PUMPED LASER CRYSTAL
 5  C   RODS. (YY.FOR)
 6  C
 7  C   ************************************************************************
 8  C
 9  C       THERLENS.FOR:    Version 1.0
10  C                 Language:    Microsoft Fortran77 Version 4.10
11  C
12  C         Written by:    Vincent G. Brackett
13  C                                Graduate Student Applied Mathematics
14  C                                Hampton University
15  C                                Hampton, Va. 23668
16  C
17  C     Thesis Advisor:    Dr. Usamah O. Farrukh
18  C                                Department of Engineering
19  C                                Hampton University
20  C
21  C                        For:    NASA Langley Research Center
22  C                                Hampton, Va.  23666
23  C
24  C                     GRANT:    NAG 1-666
25  C                   Monitor:    Philip Brockman
26  C
27  C                       Date:    Last Revised: March 1, 1990
28  C
29  C   ************************************************************************
30  C
31  C
32  C   THIS PROGRAM USES THE TEMPERATURE OUTPUT PROFILES OF A PREVIOUSLY
33  C   DEVELOPED COMPUTER SIMULATION MODEL (THAT MODEL PREDICTS THE
34  C   NORMALIZED TEMPERATURE DISTRIBUTIONS VERSUS TIME IN FINITE SIDE AND
35  C   END-PUMPED LASER CRYSTAL RODS) TO PREDICT THERMAL LENSING (FINITE
36  C   CHANGE IN FOCAL LENGTHS) CAUSED BY THE RESULTANT TEMP GRADIENTS IN
37  C   THOSE RODS. THERMAL DISTORTION OF THE PUMP BEAM ARE CALC AND AVG
38  C   VALUES OF THE FOCAL LENGTHS AND DISTORTION ARE PRESENTED.
39  C
40  C   CAUTION: The matrix mesh of the Temperature Distribution Model and
41  C                 this model must be the same size. To change matrix mesh
42  C                 size, only the parameter statement needs to be changed.
43  C
```

```
      PARAMETER(N=11,M=11)
C
      DIMENSION TEMP(N,M),INDEX(N,M),RAD(M),LON(N),DISTOR(M)
      DIMENSION ANGI(M),ANGM(M),ANGO(M),REND(M),FOCAL(M)
C
      REAL LAMBDA,LAMBDL,K,LRMIN,LRMAX,LR,LENG,LON,IOR,INDEX,N1,N2,LONI
C
      DOUBLE PRECISION PI,SUMIOR,SUMINT,SIOR0,SIORJ,SINTJ,ANGIJ,ANGOJ
      DOUBLE PRECISION RI,RM,RO,Z,A,B,C
C
      CHARACTER*1 XX(140)
C
      COMMON /BLOCK1/IOR,DT,ACC,N1,N2,ZI,RI,RM,TM,LONI,I
      COMMON /BLOCK2/R1,R2,R3,Z1,Z2,Z3
      COMMON /BLOCK3/T1,T2,T3,T4,T5,T6,T7,T8,T9
      COMMON /BLOCK4/T1C,T2C,T3C,T4C,T5C,T6C,T10,T11,T12
C
      OPEN(4,FILE='THERLEN1.INP',STATUS='OLD')
      OPEN(5,FILE='THERLEN2.INP',STATUS='OLD')
      OPEN(6,FILE='THERLENS.OUT',STATUS='UNKNOWN')
C
C                          ...(PROCESSING OF INPUT FILE ONE)...
C
      WRITE(6,*)'  '
      WRITE(6,*)'   ......THERMAL LENSING OUTPUT FILE......'
      WRITE(6,*)'   '
      WRITE(6,*)'    .........INPUT FILE #1.........'
      WRITE(6,*)'   '
      READ(4,'(80A1)') (XX(I),I=1,80)
      WRITE(6,*) (XX(I),I=1,80)
      READ(4,'(80A1)') (XX(I),I=1,80)
      WRITE(6,*) (XX(I),I=1,80)
      READ(4,*) WL
      WRITE(6,*) '..WAVELENGTH OF INTEREST IN UM..(WL).: ',WL
      READ(4,*)TOI
      WRITE(6,*)'..TEMPERATURE OF INTEREST IN DEG C..(TOI).: ',TOI
      READ(4,*) IOR
      WRITE(6,*) '..INDEX OF REFRACTION..(IOR).: ',IOR
      READ(4,*) DT
      WRITE(6,*) '..ALPHA (dn/dt)..(DT).: ',DT
      READ(4,*) TNF
      WRITE(6,*) '..TEMP NORMALIZATION FACTOR..(TNF).: ',TNF
      READ(4,*) TINF
      WRITE(6,*) '..TIME NORMALIZATION FACTOR..(TINF).: ',TINF
      READ(4,*) IDATA
      WRITE(6,*) '..0=RELATIVE TEMP; 1=ACTUAL TEMP..(IDATA).: ',IDATA
      READ(4,*) ZI
      WRITE(6,*) '..AXIAL INCREMENT FACTOR..(ZI).: ',ZI
      READ(4,*) POWER
      WRITE(6,*) '..POWER MULTIPLICATION FACTOR..(POWER).: ',POWER
      READ(4,*) ACC
```

```
      WRITE(6,*)'..OUTPUT ANGLE ACCURACY CRITERIA..(ACC).:',ACC
      READ(4,*) TPUMP
      WRITE(6,*) '..TYPE OF PUMPING (0=side, 1=end)..:',TPUMP
      WRITE(6,*) '-------------------------------------------------'
      WRITE(6,*) '-------------------------------------------------'
C
C                        ...(PROCESSING OF INPUT FILE TWO)...
C
      WRITE(6,*)'   '
      WRITE(6,*)'     .......INPUT FILE #2......'
      WRITE(6,*)'   '
      JJ=0
    5 CONTINUE
      IF((JJ/3)*3.NE.JJ) GOTO 10
      READ(5,100,ERR=86) (XX(I),I=1,132)
      WRITE(6,100) (XX(I),I=1,132)
   10 CONTINUE
C
      IF(JJ.NE.0) GO TO 20
      IF(TPUMP.EQ.0) THEN
      DO 15 J=1,80
      READ(5,100,ERR=87) (XX(I),I=1,132)
      WRITE(6,100) (XX(I),I=1,132)
   15 CONTINUE
      ELSEIF(TPUMP.EQ.1) THEN
      DO 16 J=1,81
      READ(5,100,ERR=87) (XX(1),I=1,132)
      WRITE(6,100) (XX(I),I=1,132)
   16 CONTINUE
      ENDIF
C
   20 JJ=JJ+1
      P=P+1
      READ(5,100,ERR=88) (XX(I),I=1,132)
      WRITE(6,*)'   BLOCK OF TEMPERATURE PROFILES FROM INPUT FILE  #2'
      READ(5,100) (XX(I),I=1,132)
      WRITE(6,100) (XX(I),I=1,132)
      READ(5,100) (XX(I),I=1,132)
      WRITE(6,100)  (XX(I),I=1,132)
      READ(5,105) (XX(I),I=1,50),DIFF
      WRITE(6,105) (XX(I),I=1,50),DIFF
      READ(5,105) (XX(I),I=1,50),RADI
      WRITE(6,105) (XX(I),I=1,50),RADI
      READ(5,105) (XX(I),I=1,50),LENG
      WRITE(6,105) (XX(I),I=1,50),LENG
      READ(5,105) (XX(I),I=1,50),SEC
      WRITE(6,105) (XX(I),I=1,50),SEC
C
      DO 25 J=1,2
      READ(5,100) (XX(I),I=1,132)
```

```
      WRITE(6,100) (XX(I),I=1,132)
   25 CONTINUE

      READ(5,115) (XX(I),I=1,7),(LON(I),I=1,N)
      WRITE(6,115) (XX(I),I=1,7),(LON(I),I=1,N)
C
      DO 30 J=1,M
      READ(5,125) (XX(I),I=1,2),RAD(J),(TEMP(I,J),I=1,N)
      WRITE(6,125) (XX(I),I=1,2),RAD(J),(TEMP(I,J),I=1,N)
   30 CONTINUE
      DO 40 J=1,M
      DO 35 I=1,N
      TEMP(I,J)=TEMP(I,J)*POWER
      IF(IDATA.EQ.0) TEMP(I,J)=TEMP(I,J)*TNF
   35 CONTINUE
   40 CONTINUE
      WRITE(6,*)'      '
      WRITE(6,*)'                              THERMAL LENSING PROGRAM OUTPUT DATA'
      WRITE(6,*)'      '
      WRITE(6,*)'                                    INDEX OF REFRACTION MATRIX '
      WRITE(6,*)'      '
      DO 50 J=1,M
      DO 45 I=1,N
      INDEX(I,J)=IOR+(DT*TEMP(I,J))
   45 CONTINUE
     WRITE(6,125) (XX(I),I=1,2),RAD(J),(INDEX(I,J),I=1,N)
   50 CONTINUE
C
C                        ...(CALC OF LENSING AND DISTORTION)...
C
      PI=3.141592653589793D00
      AREA=PI*ZI**2
      SIOR0=0
      DO 60 J=1,M-1
      ANGIJ=0.0D00
      SIORJ=0.0D00
      SINTJ=0.0D00
      DO 55 I=1,N-1
      IF(I.EQ.10) GOTO 65
      IF(J.EQ.1) R1=-RAD(J+1)
      IF(J.GT.1) R1=RAD(J-1)
      R2=RAD(J)
      R3=RAD(J+1)
      IF(J.EQ.1) T1=TEMP(I,J+1)
      IF(J.GT.1) T1=TEMP(I,J-1)
      IF(J.EQ.1) T4=TEMP(I+1,J+1)
      IF(J.GT.1) T4=TEMP(I+1,J-1)
      IF(J.EQ.1) T7=TEMP(I+2,J+1)
      IF(J.GT.1) T7=TEMP(I+2,J-1)
      T2=TEMP(I,J)
```

```
      T5=TEMP(I+1,J)
      T8=TEMP(I+2,J)
      T3=TEMP(I,J+1)
      T6=TEMP(I+1,J+1)
      T9=TEMP(I+2,J+1)
      Z1=LON(I)
      Z2=LON(I+1)
      Z3=LON(I+2)
      Z=LON(I)+(ZI/2)
      CALL INTERP(Z,Z1,Z2,Z3,T,T1,T4,T7,A,B,C)
      T1C=T
      CALL INTERP(Z,Z1,Z2,Z3,T,T2,T5,T8,A,B,C)
      T2C=T
      CALL INTERP(Z,Z1,Z2,Z3,T,T3,T6,T9,A,B,C)
      T3C=T
      Z=LON(I+1)+(ZI/2)
      CALL INTERP(Z,Z1,Z2,Z3,T,T1,T4,T7,A,B,C)
      T4C=T
      CALL INTERP(Z,Z1,Z2,Z3,T,T2,T5,T8,A,B,C)
      T5C=T
      CALL INTERP(Z,Z1,Z2,Z3,T,T3,T6,T9,A,B,C)
      T6C=T
   65 CONTINUE
      LONI=LON(I)
      IF(I.EQ.1)THEN
              CALL INITIAL(RO,ANGOJ)
              SUMIOR=N1+N2*SQRT(1+((((RO-RM)*RADI)/(ZI/2*LENG))**2))
              SIORJ=SIORJ+SUMIOR
              IF(J.EQ.1) SIOR0=SIORJ
              CALL MIDPT(RO,ANGOJ)
      ELSEIF(I.LT.N-1) THEN
              CALL FINAL(RO,ANGOJ)
              SUMIOR=N1*SQRT(1+((((RM-RI)*RADI)/(ZI/2*LENG))**2)) +
     1              N2*SQRT(1+((((RO-RM)*RADI)/(ZI/2*LENG))**2))
              SIORJ=SIORJ+SUMIOR
              IF(J.EQ.1) SIOR0=SIORJ
              CALL MIDPT(RO,ANGOJ)
      ELSEIF(I.EQ.N-1) THEN
              CALL FINAL(RO,ANGOJ)
              REND(J)=RO
              SUMIOR=N1*SQRT(1+((((RM-RI)*RADI)/(ZI/2*LENG))**2)) +
     1              N2*SQRT(1+((((RO-RM)*RADI)/(ZI/2*LENG))**2))
              SIORJ=SIORJ+SUMIOR
              N1=N2
              IF(J.EQ.1) THEN
                  DISTOR(J)=0
              ELSEIF(J.GT.1) THEN
                  DISTOR(J)=100*((RO**2-R2**2)/R2**2)
              ANGO(J)=ASIN(N1*SIN(ANGOJ))
              ENDIF
```

```
245               IF(J.EQ.1) SIOR0=SIORJ
246               IF(SIORJ-SIOR0.EQ.0) THEN
247                   FOCAL(J)=0
248               ELSEIF(SIORJ-SIOR0.NE.0) THEN
249                   FOCAL(J)=-(RO*RADI)**2/(ZI*LENG*(SIORJ-SIOR0))
250               ENDIF
251           ENDIF
252        55 CONTINUE
253        60 CONTINUE
254           WRITE(6,*)'    '
255           WRITE(6,*)'    '
256           WRITE(6,135) WL,TOI,SEC
257           WRITE(6,*)'    '
258           WRITE(6,*)'         RAY    ANGLE OUT       RADIUS          FOCAL '
259          1               '       DISTORTION  '
260           WRITE(6,*)'        (no.)   (radians)        (cm)        LENG(cm)'
261          1               '                (%)'
262           WRITE(6,*)'         ---    ----------      ------       --------'
263          1               '       ----------'
264           DO 70 J=1,M
265           WRITE(6,130) RAD(J),ANGO(J),REND(J),FOCAL(J),DISTOR(J)
266        70 CONTINUE
267           WRITE(6,*)'    '
268           AFOCAL=0
269           DO 75 J=1,M
270           AFOCAL=AFOCAL+FOCAL(J)
271        75 CONTINUE
272           IF(AFOCAL.EQ.0) GOTO 76
273           AFOCAL=AFOCAL/(M-2)
274        76 CONTINUE
275           ADISTOR=0
276           DO 80 J=1,M
277           IF(DISTOR(J).GT.ADISTOR) ADISTOR=DISTOR(J)
278        80 CONTINUE
279           WRITE(6,140) AFOCAL/100
280           WRITE(6,145) ADISTOR
281           WRITE(6,*)'    '
282           WRITE(6,*)'                    .. END THERMAL LENSING OUTPUT..'
283           WRITE(6,*)'.....................................................
284           WRITE(6,*)'  '
285           IF(AFOCAL.EQ.0) THEN
286                 IF(P.GT.1) THEN
287                    WRITE(6,*)'...PROGRAM TERMINATED. LASER ROD HAS ESSENTIALY',
288          1                   ' RELAXED TO STATIC CONDITIONS.'
289                    GOTO 90
290                 ENDIF
291           ENDIF
292           GOTO 5
293        86 CONTINUE
294           WRITE(6,*) '   ERROR ON LINE 109'
295           GOTO 90
```

```
296      87 CONTINUE
297         WRITE(6,*) '   ERROR ON LINE 116/121'
298         GOTO 90
299      88 CONTINUE
300         WRITE(6,*) '   ERROR ON LINE 127'
301   C
302     100 FORMAT(132A1)
303     105 FORMAT(50A1,E11.6)
304     115 FORMAT(7A1,14F12.2)
305     125 FORMAT(2A1,F5.2,14E12.5)
306     130 FORMAT(7X,F5.2,17E15.7)
307     135 FORMAT(//,22X,'THERMAL LENSING CALCUATIONS',
308        1        /,15X,'WAVELENGTH OF INTEREST(um)......  ',E12.6,
309        1        /,15X,'TEMPERATURE OF INTEREST(deg C)..  ',E12.6,
310        1        /,15X,'TIME (sec)......................  ',E12.6)
311     140 FORMAT(7X,'AVERAGE OF THE FOCAL LENGTHS (meters) =',E15.6)
312     145 FORMAT(7X,'INCREMENTAL DISTORTION (%) RANGES FROM 0.0 TO ',E10.3)
313   C
314      90 CONTINUE
315         END
316   C
317   C
318         SUBROUTINE INITIAL(RO,ANGOJ)
319   C
320   C
321   C     This subroutine calculates the initial entry into the temperature
322   C     gradient matix and perdicts the initial angle and radius out for
323   C     the first axial increment of the laser rod.
324   C
325         REAL IOR,LONI,N1,N2
326   C
327         DOUBLE PRECISION ANGMJ,ANGIJ,ANGOJ,A1,A2,A3,RI,RM,RO,Z,A,B,C
328   C
329         COMMON /BLOCK1/IOR,DT,ACC,N1,N2,ZI,RI,RM,TM,LONI,I
330         COMMON /BLOCK2/R1,R2,R3,Z1,Z2,Z3
331         COMMON /BLOCK3/T1,T2,T3,T4,T5,T6,T7,T8,T9
332         COMMON /BLOCK4/T1C,T2C,T3C,T4C,T5C,T6C,T10,T11,T12
333   C
334         RI=R2
335         CALL INTERP(RI,R1,R2,R3,T,T1C,T2C,T3C,A,B,C)
336         DTR=(2*A*RI)+B
337         Z=LONI+ZI/2
338         CALL INTERP(Z,Z1,Z2,Z3,T,T2,T5,T8,A,B,C)
339         DTZ=(2*A*Z)+B
340         IF(DTR.EQ.0) THEN
341               ANGMJ=0.0D00
342         ELSEIF(DTR.NE.0) THEN
343               ANGMJ=ASIN(1.0)
344         ENDIF
345         IF(DTZ.GE.1.0E-30) ANGMJ=ATAN(DTR/DTZ)
```

```
      RM=R2
      TM=T2C
      N1=IOR+DT*((TM+T2)/2)
      N2=IOR+DT*((TM+T5)/2)
      A1=SIN(ANGMJ-ANGIJ)
      A2=(N2/N1)*A1
      A3=ASIN(A2)
      ANGOJ=ANGMJ-A3
C     ANGOJ=ANGMJ-ASIN((N2/N1)*SIN(ANGMJ-ANGIJ))
      RO=(ZI/2)*TAN(ANGOJ)+RM
      CALL REFINE(RO,ANGIJ,ANGMJ,ANGOJ,T4,T5,T6)
C
      RETURN
      END
C
C
      SUBROUTINE MIDPT(RO,ANGOJ)
C
C     This subroutine calculates the intermediate angles and predicts
C     the mid-point position of the next axial increment prior to
C     entry into the next increment of the temperature gradient matrix.
C
      REAL IOR,LONI,N1,N2
C
      DOUBLE PRECISION ANGMJ,ANGIJ,ANGOJ,A1,A2,A3,RI,RM,RO,Z,A,B,C
C
      COMMON /BLOCK1/IOR,DT,ACC,N1,N2,ZI,RI,RM,TM,LONI,I
      COMMON /BLOCK2/R1,R2,R3,Z1,Z2,Z3
      COMMON /BLOCK3/T1,T2,T3,T4,T5,T6,T7,T8,T9
      COMMON /BLOCK4/T1C,T2C,T3C,T4C,T5C,T6C,T10,T11,T12
C
      RM=RO
      ANGIJ=ANGOJ
      CALL INTERP(RM,R1,R2,R3,T,T1,T2,T3,A,B,C)
      T10=T
      CALL INTERP(RM,R1,R2,R3,T,T4,T5,T6,A,B,C)
      T11=T
      DTR=(2*A*RM)+B
      CALL INTERP(RM,R1,R2,R3,T,T7,T8,T9,A,B,C)
      T12=T
      Z=LONI+ZI
      CALL INTERP(Z,Z1,Z2,Z3,T,T10,T11,T12,A,B,C)
      DTZ=(2*A*Z)+B
      TM=T
      IF(DTR.EQ.0) THEN
            ANGMJ=0.0D00
      ELSEIF(DTR.NE.0) THEN
            ANGMJ=ASIN(1.0)
      ENDIF
```

```
      IF(DTZ.GE.1.0E-30) ANGMJ=ATAN(DTR/DTZ)
      CALL INTERP(RM,R1,R2,R3,T,T4C,T5C,T6C,A,B,C)
      N1=N2
      N2=IOR+DT*((TM+T)/2)
      A1=SIN(ANGMJ-ANGIJ)
      A2=(N2/N1)*A1
      A3=ASIN(A2)
      ANGOJ=ANGMJ-A3
C     ANGOJ=ANGMJ-ASIN((N2/N1)*SIN(ANGMJ-ANGIJ))
      RO=(ZI/2)*TAN(ANGOJ)+RM
      CALL REFINE(RO,ANGIJ,ANGMJ,ANGOJ,T4C,T5C,T6C)
C
      RETURN
      END
C
C
      SUBROUTINE FINAL(RO,ANGOJ)
C
C     This subroutine calculates the final angle and radius out for
C     all subsequent axial increments of the laser rod.
C
      REAL IOR,LONI,N1,N2
C
      DOUBLE PRECISION ANGMJ,ANGIJ,ANGOJ,A1,A2,A3,RI,RM,RO,Z,A,B,C
C
      COMMON /BLOCK1/IOR,DT,ACC,N1,N2,ZI,RI,RM,TM,LONI,I
      COMMON /BLOCK2/R1,R2,R3,Z1,Z2,Z3
      COMMON /BLOCK3/T1,T2,T3,T4,T5,T6,T7,T8,T9
      COMMON /BLOCK4/T1C,T2C,T3C,T4C,T5C,T6C,T10,T11,T12
C


      RI=RM
      RM=RO
      ANGIJ=ANGOJ
      IF(I.LT.10) CALL INTERP(RM,R1,R2,R3,T,T1C,T2C,T3C,A,B,C)
      IF(I.EQ.10) CALL INTERP(RM R1,R2,R3,T,T4C,T5C,T6C,A,B,C)
      DTR=(2*A*RM)+B
      CALL INTERP(RM,R1,R2,R3,T,T1,T2,T3,A,B,C)
      T10=T
      CALL INTERP(RM,R1,R2,R3,T,T4,T5,T6,A,B,C)
      T11=T
      CALL INTERP(RM,R1,R2,R3,T,T7,T8,T9,A,B,C)
      T12=T
      IF(I.LT.10) Z=LONI+ZI/2
      IF(I.EQ.10) Z=LONI+ZI/2
      CALL INTERP(Z,Z1,Z2,Z3,T,T10,T11,T12,A,B,C)
      DTZ=(2*A*Z)+B
      IF(DTR.EQ.0) THEN
            ANGMJ=0.0D00
      ELSEIF(DTR.NE.0) THEN
```

```
446               ANGMJ=ASIN(1.0)
447         ENDIF
448         IF(DTZ.GE.1.0E-30) ANGMJ=ATAN(DTR/DTZ)
449         TM=T
450         N1=N2
451         IF(I.LT.10) N2=IOR+DT*((TM+T11)/2)
452         IF(I.EQ.10) N2=IOR+DT*((TM+T12)/2)
453         A1=SIN(ANGMJ-ANGIJ)
454         A2=(N2/N1)*A1
455         A3=ASIN(A2)
456         ANGOJ=ANGMJ-A3
457  C      ANGOJ=ANGMJ-ASIN((N2/N1)*SIN(ANGMJ-ANGIJ))
458         RO=(ZI/2)*TAN(ANGOJ)+RM
459         IF(I.LT.10) CALL REFINE(RO,ANGIJ,ANGMJ,ANGOJ,T4,T5,T6)
460         IF(I.EQ.10) CALL REFINE(RO,ANGIJ,ANGMJ,ANGOJ,T7,T8,T9)
461  C
462         RETURN
463         END
464  C
465  C
466         SUBROUTINE INTERP(R,R1,R2,R3,T,T1,T2,T3,A,B,C)
467  C
468  C
469  C      The subroutine INTERP is a binomial interpolation routine using
470  C      any three points in the R (radial) or Z (axial) direction to find
471  C      the coefficents of A,B, and C of the equation AX**2 + BX + C = T
472  C      so that a temperature T can be determined for any X (R or Z)
473  C      within the non-linear temperature matrix.
474  C
475         DOUBLE PRECISION R,A,B,C
476  C
477         A=((T1-T2)*(R1-R3)-(T1-T3)*(R1-R2))/((R1-R3)*(R1**2-R2**2)-
478        1 (R1-R2)*(R1**2-R3**2))
479         B=((T1-T3)*(R1**2-R2**2)-(T1-T2)*(R1**2-R3**2))/((R1-R3)*
480        1 (R1**2-R2**2)-(R1-R2)*(R1**2-R3**2))
481         C=T1-A*R1**2-B*R1
482         T=A*R**2+B*R+C
483  C
484         RETURN
485         END
486  C
487  C
488         SUBROUTINE REFINE(RO,ANGIJ,ANGMJ,ANGOJ,T1,T2,T3)
489  C
490  C
491  C      The subroutine REFINE is a continous numerical iteration routine
492  C      used to recalculate the final thermal lensing output angle for
493  C      each specified axial increment within each ray until the user
494  C      specified accuracy criteria for the output angle are met.
495  C
```

```
      C
            REAL IOR,LONI,N1,N2
      C
            DOUBLE PRECISION ANGMJ,ANGIJ,ANGOJ,A1,A2,A3,RI,RM,RO
            DOUBLE PRECISION ROO,D,A,B,C
      C
            COMMON /BLOCK1/IOR,DT,ACC,N1,N2,ZI,RI,RM,TM,LONI,I
            COMMON /BLOCK2/R1,R2,R3,Z1,Z2,Z3
      C
            L=0
          5 CONTINUE
            L=L+1
            CALL INTERP(RO,R1,R2,R3,T,T1,T2,T3,A,B,C)
            N2=IOR+DT*((TM+T)/2)
            A1=SIN(ANGMJ-ANGIJ)
            A2=(N2/N1)*A1
            A3=ASIN(A2)
            ANGOJ=ANGMJ-A3
      C     ANGOJ=ANGMJ-ASIN((N2/N1)*SIN(ANGMJ-ANGIJ))
            ROO=(ZI/2)*TAN(ANGOJ)+RM
            D=RO
            RO=ROO
            IF(ABS(D-ROO).GT.ACC) GOTO 5
      C
            RETURN
            END
No errors detected
```

Appendix B

Program Input Files

1. Thermal Lensing Model Input File #1

This file (THERLEN1.INP) contains thermal lensing material characteristics and other constants required to control the Thermal Lensing Model. The example data depicted below are for a pulsed side-pumped Nd:YAG rod.

Input File #1

```
THERMAL LENSING INPUT DATA FOR Nd:YAG ROD

1.15          ; WAVELENGTH OF INTEREST (MICRONS)
37.5          ; TEMPERATURE OF INTEREST (24-42 DEGREES C)
1.825         ; INDEX OF REFRACTION
8.90E-06      ; ALPHA (DN/DT)
0.33          ; TEMPERATURE NORMALIZATION FACTOR
0.05          ; TIME NORMALIZATION FACTOR
1             ; 0 - RELATIVE VALUES IN INPUT FILE; 1 - ACTUAL VALUES
0.10          ; AXIAL INCREMENT
1.0           ; POWER MULTICATION FACTOR
1.0E-06       ; OUTPUT ANGLE ACCURACY CRITERIA
0             ; TYPE OF PUMPING (0=side, 1=end)
```

2. Thermal Lensing Model Input File #2

This file (THERLEN2.INP) is the output file from the model titled: Temperature Distribution Model for finite optically pumped laser rods. It contains that model's control criteria and output temperature data blocks versus time.

Those data blocks of temperatures contained within

this input file are used in the Thermal Lensing Model to calculate the thermal lensing and pump beam distortion effects. The example data depicted below are for a pulsed side-pumped Nd:YAG laser at its steady-state equilibrium temperature. Blocks of temperature data are shown from 3.4-3.6 seconds.

Input File #2

```
 Input Nd:YAG  Side-Pump..MP(20)..GA=20..GL=None..Run=001 03/01/90

..... MIN., MAX. AND INCREMENT OF RADIUS OF ROD     2.500000E-01
  2.500000E-01    2.500000E-01
..... MIN , MAX AND INCR. OF ASPECT RATIO (L/A)          30.400000
     30.400000       50.000000
..... INVERSE OF RADIAL THERMAL DIFFUSIVITY         26.947000
..... THERMAL CONDUCTIVITY    1.030000E-01    1.030000E-01
..... MIN. RADIAL COOLING PARAMETER         20.000000
..... MAX. RADIAL COOLING PARAMETER         20.000000
TYPE OF SCALE 1(LOG) OR 0(LINEAR)                1
  AND INCREMENT (SET TO 1. IF LOG)          1.000000
........ MIN. AND MAX. FRONT COOLING RATIO OR VALUES     6.500000E-04
  6.500000E-04
TYPE OF SCALE 1(LOG) OR 0(LINEAR)                1
  AND INCREMENT (SET TO 1 IF LOG)           1.000000
........ MIN. AND MAX. BACK  COOLING RATIO OR VALUES     6.500000E-04
  6.500000E-04
TYPE OF SCALE 1(LOG) OR 0(LINEAR)                1
  AND INCREMENT (SET TO 1 IF LOG)           1.000000
........ TYPE OF DATA RATIO=0 ACTUAL=1
                    PARAM=2
.............  PROPORTIONAL TO L/A=3              2
....... VARIATION OF END DATA SEPERATE=0
.............................. TOGETHER=1          1
..... MAXIMUM NUMBER OF ROOTS ... RADIAL         17
..... MAXIMUM NUMBER OF ROOTS ... LONGIT         17
      NUMBER OF ORTHOGONAL CHECKS  RADIAL         2
      NUMBER OF ORTHOGONAL CHECKS  LONGIT         3
      BESSEL ROOTS SCHEME ... 1  COMPUTED
                              2  GIVEN
                              3  ALL (GIVEN <21)
                                 (COMPUTED GE 21)
```

```
      ROOTS SCHEME IS                          2
RADIAL AND LONG. INTEGRATION DIVISIONS        1000          100
      TYPE OF PUMP BEAM .....
   RADIAL    EIGENFUNCTION                   -ORDER
             SQUARE PULSE                    +0
             GAUSSIAN                        +1
             PARABOLIC                       +2
   LONGIT    EIGNFUNCTION                    -ORDER
             CONSTANT                        +0
             CONSTANT & ATTENUATED           +1
             FOCUSED(DEFOCUSED)              +2
             FOCUSED & ATTENUATED            +3
     NOTE  NO DIFFRACTION EFFECTS ALLOWED
         GAUSSIAN ENVELOPE ASSUMED
PUMP BEAM CODE                0              0
..... ATTENUATION DATA..0=ATTEN..1=ATTEN*L                  1
.....OPTICAL DATA          3.000000
..... NUMBER OF RADIAL PROFILES ...                  11
..... NUMBER OF LONGIT PROFILES ...                  11
........ CONTINUOUS PUMPPING     ... 0
........ SINGLE PULSE            ... 1
      OR MULTI-PULSED            ... 2                    2
..... MIN. REL. TIME OF INTEREST          3.400000
..... MAX. REL. TIME OF INTEREST          3.600000
TYPE OF SCALE 1(LOG) OR 0(LINEAR)              1
  AND INCREMENT (SET TO 1 IF LOG)          1.000000
........ MULTIPLE PULSES         ... 2            2
........ ONTIME  PER PULSE    1.300000E-04
........ OFFTIME PER PULSE    4.987000E-02
........ ONTIME  SAMPLING RATE                   1
........ OFFTIME SAMPLING RATE                   1
..... ABSORBED ENERGY PER PULSE J/CM3       1574.280000
   .......... DEBUG DESIRED      ... 1
   ............NOT DESIRED       ... 0, NDEBUG=                1
..MIN, MAX, RADIAL CALCULATION RANGE..   0.000000E+00          1.000000
..MIN, MAX LONGITUDINAL CALCULATION RANGE..   0.000000E+00          1.000000
..RADIAL REFERENCE POINTS...          0    0.000000E+00
..AXIAL REFERENCE POINTS...           0    0.000000E+00
 ----------------------------------------
ROD ASPECT RATIO (L/A) ..... =        30.400000
 ----------------------------------------
****************************************
PARAMETER GA IS          20.000000
****************************************
PARAMETER GL OF FRONT     6.500000E-04
PARAMETER GL OF BACK      6.500000E-04
****************************************
```

TEMPERATURE DISTRIBUTION

RADIAL DIFFUSIVITY .....269470E+02
RADIUS OF ROD ..... .250000
LENGTH OF ROD 7.600000
TIME IN SECONDS .....345013E+01

L/R	.00	.10	.20	.30	.40	.50	.60	.70	.80	.90	1.00
.00	.72382E+00	.72383E+00	.72383E+00	.72383E+00	.72383E+00	.72383E+00	.72383E+00	.72383E+00	.72383E+00	.72383E+00	.72382E+00
.10	.71330E+00	.71331E+00	.71331E+00	.71331E+00	.71331E+00	.71331E+00	.71331E+00	.71331E+00	.71331E+00	.71331E+00	.71330E+00
.20	.69403E+00	.69404E+00	.69404E+00	.69404E+00	.69404E+00	.69404E+00	.69404E+00	.69404E+00	.69404E+00	.69404E+00	.69403E+00
.30	.66320E+00	.66320E+00	.66320E+00	.66320E+00	.66320E+00	.66320E+00	.66320E+00	.66320E+00	.66320E+00	.66320E+00	.66320E+00
.40	.62046E+00	.62046E+00	.62046E+00	.62046E+00	.62046E+00	.62047E+00	.62046E+00	.62046E+00	.62046E+00	.62046E+00	.62046E+00
.50	.56521E+00	.56522E+00	.56522E+00	.56522E+00	.56522E+00	.56522E+00	.56522E+00	.56522E+00	.56522E+00	.56522E+00	.56521E+00
.60	.49688E+00	.49689E+00	.49689E+00	.49689E+00	.49689E+00	.49689E+00	.49689E+00	.49689E+00	.49689E+00	.49689E+00	.49688E+00
.70	.41552E+00	.41552E+00	.41552E+00	.41552E+00	.41552E+00	.41552E+00	.41552E+00	.41552E+00	.41552E+00	.41552E+00	.41552E+00
.80	.32288E+00	.32288E+00	.32288E+00	.32288E+00	.32288E+00	.32288E+00	.32288E+00	.32288E+00	.32288E+00	.32288E+00	.32288E+00
.90	.22190E+00	.22190E+00	.22190E+00	.22190E+00	.22190E+00	.22190E+00	.22190E+00	.22190E+00	.22190E+00	.22190E+00	.22190E+00
1.00	.10556E+00	.10556E+00	.10556E+00	.10556E+00	.10556E+00	.10556E+00	.10556E+00	.10556E+00	.10556E+00	.10556E+00	.10556E+00

TEMPERATURE DISTRIBUTION

RADIAL DIFFUSIVITY .....269470E+02
RADIUS OF ROD ..... .250000
LENGTH OF ROD 7.600000
TIME IN SECONDS .....350000E+01

L/R	.00	.10	.20	.30	.40	.50	.60	.70	.80	.90	1.00
.00	.64627E+00	.64627E+00	.64627E+00	.64627E+00	.64627E+00	.64627E+00	.64627E+00	.64627E+00	.64627E+00	.64627E+00	.64627E+00
.10	.64006E+00	.64007E+00	.64007E+00	.64007E+00	.64007E+00	.64007E+00	.64007E+00	.64007E+00	.64007E+00	.64007E+00	.64006E+00
.20	.62144E+00	.62145E+00	.62145E+00	.62145E+00	.62145E+00	.62145E+00	.62145E+00	.62145E+00	.62145E+00	.62145E+00	.62144E+00
.30	.59041E+00	.59041E+00	.59041E+00	.59041E+00	.59041E+00	.59041E+00	.59041E+00	.59041E+00	.59041E+00	.59041E+00	.59041E+00
.40	.54693E+00	.54694E+00	.54694E+00	.54694E+00	.54694E+00	.54694E+00	.54694E+00	.54694E+00	.54694E+00	.54694E+00	.54693E+00
.50	.49096E+00	.49096E+00	.49096E+00	.49096E+00	.49096E+00	.49096E+00	.49096E+00	.49096E+00	.49096E+00	.49096E+00	.49096E+00
.60	.42244E+00	.42244E+00	.42244E+00	.42244E+00	.42244E+00	.42244E+00	.42244E+00	.42244E+00	.42244E+00	.42244E+00	.42244E+00
.70	.34169E+00	.34169E+00	.34169E+00	.34169E+00	.34169E+00	.34169E+00	.34169E+00	.34169E+00	.34169E+00	.34169E+00	.34169E+00
.80	.25008E+00	.25008E+00	.25008E+00	.25008E+00	.25008E+00	.25008E+00	.25008E+00	.25008E+00	.25008E+00	.25008E+00	.25008E+00
.90	.15093E+00	.15093E+00	.15093E+00	.15093E+00	.15093E+00	.15093E+00	.15093E+00	.15093E+00	.15093E+00	.15093E+00	.15093E+00
1.00	.49856E-01	.49856E-01	.49856E-01	.49857E-01	.49857E-01	.49857E-01	.49857E-01	.49857E-01	.49856E-01	.49856E-01	.49856E-01

TEMPERATURE DISTRIBUTION

RADIAL DIFFUSIVITY .....269470E+02
RADIUS OF ROD ..... .250000
LENGTH OF ROD 7.600000
TIME IN SECONDS .....350013E+01

L/R	.00	.10	.20	.30	.40	.50	.60	.70	.80	.90	1.00
.00	.72382E+00	.72383E+00	.72383E+00	.72383E+00	.72383E+00	.72383E+00	.72383E+00	.72383E+00	.72383E+00	.72383E+00	.72382E+00
.10	.71330E+00	.71331E+00	.71331E+00	.71331E+00	.71331E+00	.71331E+00	.71331E+00	.71331E+00	.71331E+00	.71331E+00	.71330E+00
.20	.69403E+00	.69404E+00	.69404E+00	.69404E+00	.69404E+00	.69404E+00	.69404E+00	.69404E+00	.69404E+00	.69404E+00	.69403E+00
.30	.66320E+00	.66321E+00	.66321E+00	.66321E+00	.66321E+00	.66321E+00	.66321E+00	.66321E+00	.66321E+00	.66321E+00	.66320E+00
.40	.62046E+00	.62047E+00	.62047E+00	.62047E+00	.62047E+00	.62047E+00	.62047E+00	.62047E+00	.62047E+00	.62047E+00	.62046E+00
.50	.56521E+00	.56522E+00	.56522E+00	.56522E+00	.56522E+00	.56522E+00	.56522E+00	.56522E+00	.56522E+00	.56522E+00	.56521E+00
.60	.49688E+00	.49689E+00	.49689E+00	.49689E+00	.49689E+00	.49689E+00	.49689E+00	.49689E+00	.49689E+00	.49689E+00	.49688E+00
.70	.41552E+00	.41552E+00	.41552E+00	.41552E+00	.41552E+00	.41552E+00	.41552E+00	.41552E+00	.41552E+00	.41552E+00	.41552E+00
.80	.32288E+00	.32288E+00	.32288E+00	.32288E+00	.32288E+00	.32288E+00	.32288E+00	.32288E+00	.32288E+00	.32288E+00	.32288E+00
.90	.22190E+00	.22190E+00	.22190E+00	.22190E+00	.22190E+00	.22190E+00	.22190E+00	.22190E+00	.22190E+00	.22190E+00	.22190E+00
1.00	.10556E+00	.10556E+00	.10556E+00	.10556E+00	.10556E+00	.10556E+00	.10556E+00	.10556E+00	.10556E+00	.10556E+00	.10556E+00

TEMPERATURE DISTRIBUTION

RADIAL DIFFUSIVITY .....269470E+02
RADIUS OF ROD ..... .250000
LENGTH OF ROD 7.600000
TIME IN SECONDS .....355000E+01

L/R	.00	.10	.20	.30	.40	.50	.60	.70	.80	.90	1.00
.00	.64627E+00	.64627E+00	.64627E+00	.64627E+00	.64628E+00	.64628E+00	.64628E+00	.64627E+00	.64627E+00	.64627E+00	.64627E+00
.10	.64006E+00	.64007E+00	.64007E+00	.64007E+00	.64007E+00	.64007E+00	.64007E+00	.64007E+00	.64007E+00	.64007E+00	.64006E+00
.20	.62144E+00	.62145E+00	.62145E+00	.62145E+00	.62145E+00	.62145E+00	.62145E+00	.62145E+00	.62145E+00	.62145E+00	.62144E+00
.30	.59041E+00	.59041E+00	.59041E+00	.59041E+00	.59042E+00	.59042E+00	.59042E+00	.59041E+00	.59041E+00	.59041E+00	.59041E+00
.40	.54694E+00	.54694E+00	.54694E+00	.54694E+00	.54694E+00	.54694E+00	.54694E+00	.54694E+00	.54694E+00	.54694E+00	.54694E+00
.50	.49096E+00	.49097E+00	.49097E+00	.49097E+00	.49097E+00	.49097E+00	.49097E+00	.49097E+00	.49097E+00	.49097E+00	.49096E+00
.60	.42244E+00	.42244E+00	.42244E+00	.42244E+00	.42244E+00	.42244E+00	.42244E+00	.42244E+00	.42244E+00	.42244E+00	.42244E+00
.70	.34169E+00	.34169E+00	.34169E+00	.34169E+00	.34169E+00	.34169E+00	.34169E+00	.34169E+00	.34169E+00	.34169E+00	.34169E+00
.80	.25008E+00	.25008E+00	.25008E+00	.25008E+00	.25008E+00	.25008E+00	.25008E+00	.25008E+00	.25008E+00	.25008E+00	.25008E+00
.90	.15093E+00	.15093E+00	.15093E+00	.15093E+00	.15093E+00	.15093E+00	.15093E+00	.15093E+00	.15093E+00	.15093E+00	.15093E+00
1.00	.49856E-01	.49857E-01	.49857E-01	.49857E-01	.49857E-01	.49857E-01	.49857E-01	.49857E-01	.49857E-01	.49857E-01	.49856E-01

TEMPERATURE DISTRIBUTION

RADIAL DIFFUSIVITY .....269470E+02
RADIUS OF ROD ..... .250000
LENGTH OF ROD 7.600000
TIME IN SECONDS .....355013E+01

L/R	.00	.10	.20	.30	.40	.50	.60	.70	.80	.90	1.00
.00	.72382E+00	.72383E+00	.72383E+00	.72383E+00	.72383E+00	.72383E+00	.72383E+00	.72383E+00	.72383E+00	.72383E+00	.72382E+00
.10	.71331E+00	.71331E+00	.71331E+00	.71331E+00	.71331E+00	.71331E+00	.71331E+00	.71331E+00	.71331E+00	.71331E+00	.71331E+00
.20	.69403E+00	.69404E+00	.69404E+00	.69404E+00	.69404E+00	.69404E+00	.69404E+00	.69404E+00	.69404E+00	.69404E+00	.69403E+00
.30	.66320E+00	.66321E+00	.66321E+00	.66321E+00	.66321E+00	.66321E+00	.66321E+00	.66321E+00	.66321E+00	.66321E+00	.66320E+00
.40	.62046E+00	.62047E+00	.62047E+00	.62047E+00	.62047E+00	.62047E+00	.62047E+00	.62047E+00	.62047E+00	.62047E+00	.62046E+00
.50	.56521E+00	.56522E+00	.56522E+00	.56522E+00	.56522E+00	.56522E+00	.56522E+00	.56522E+00	.56522E+00	.56522E+00	.56521E+00
.60	.49688E+00	.49689E+00	.49689E+00	.49689E+00	.49689E+00	.49689E+00	.49689E+00	.49689E+00	.49689E+00	.49689E+00	.49689E+00
.70	.41552E+00	.41552E+00	.41552E+00	.41552E+00	.41552E+00	.41552E+00	.41552E+00	.41552E+00	.41552E+00	.41552E+00	.41552E+00
.80	.32288E+00	.32288E+00	.32288E+00	.32288E+00	.32288E+00	.32288E+00	.32288E+00	.32288E+00	.32288E+00	.32288E+00	.32288E+00
.90	.22190E+00	.22190E+00	.22190E+00	.22190E+00	.22190E+00	.22190E+00	.22190E+00	.22190E+00	.22190E+00	.22190E+00	.22190E+00
1.00	.10556E+00	.10556E+00	.10556E+00	.10556E+00	.10556E+00	.10556E+00	.10556E+00	.10556E+00	.10556E+00	.10556E+00	.10556E+00

TEMPERATURE DISTRIBUTION

RADIAL DIFFUSIVITY .....269470E+02
RADIUS OF ROD ..... .250000
LENGTH OF ROD 7.600000
TIME IN SECONDS .....360000E+01

L/R	.00	.10	.20	.30	.40	.50	.60	.70	.80	.90	1.00
.00	.64613E+00	.64613E+00	.64613E+00	.64613E+00	.64613E+00	.64613E+00	.64613E+00	.64613E+00	.64613E+00	.64613E+00	.64613E+00
.10	.63993E+00	.63993E+00	.63994E+00	.63994E+00	.63994E+00	.63994E+00	.63994E+00	.63994E+00	.63994E+00	.63994E+00	.63993E+00
.20	.62131E+00	.62132E+00	.62132E+00	.62132E+00	.62132E+00	.62132E+00	.62132E+00	.62132E+00	.62132E+00	.62132E+00	.62131E+00
.30	.59028E+00	.59028E+00	.59028E+00	.59028E+00	.59028E+00	.59028E+00	.59028E+00	.59028E+00	.59028E+00	.59028E+00	.59028E+00
.40	.54680E+00	.54681E+00	.54681E+00	.54681E+00	.54681E+00	.54681E+00	.54681E+00	.54681E+00	.54681E+00	.54681E+00	.54680E+00
.50	.49082E+00	.49083E+00	.49083E+00	.49083E+00	.49083E+00	.49083E+00	.49083E+00	.49083E+00	.49083E+00	.49083E+00	.49082E+00
.60	.42230E+00	.42231E+00	.42231E+00	.42231E+00	.42231E+00	.42231E+00	.42231E+00	.42231E+00	.42231E+00	.42231E+00	.42230E+00
.70	.34155E+00	.34156E+00	.34156E+00	.34156E+00	.34156E+00	.34156E+00	.34156E+00	.34156E+00	.34156E+00	.34156E+00	.34155E+00
.80	.24995E+00	.24995E+00	.24995E+00	.24995E+00	.24995E+00	.24995E+00	.24995E+00	.24995E+00	.24995E+00	.24995E+00	.24995E+00
.90	.15080E+00	.15080E+00	.15080E+00	.15080E+00	.15080E+00	.15080E+00	.15080E+00	.15080E+00	.15080E+00	.15080E+00	.15080E+00
1.00	.49752E-01	.49753E-01	.49753E-01	.49753E-01	.49753E-01	.49753E-01	.49753E-01	.49753E-01	.49753E-01	.49753E-01	.49752E-01

Appendix C

Program Output File

Thermal Lensing Model Output File

The Thermal Lensing Model output file (**THERLENS.OUT**) rewrites the data from each of the input files. It then calculates thermal lensing and pump beam distortion effects for each block of temperature data obtained from the Temperature Distribution Model. Currently, the lensing model is programmed to calculate 10 equally spaced rays transiting through the laser material. The output data from the Thermal Lensing Model depicted below are for a pulsed side-pumped Nd:YAG laser using the input files in Appendix B.

Thermal Lensing Model Output File

```
.........INPUT FILE #1.........
THERMAL LENSING INPUT DATA FOR Nd:YAG ROD


..WAVELENGTH OF INTEREST IN UM..(WL).:          1.150000
..TEMPERATURE OF INTEREST IN DEG C..(TOI).:        37.500000
..INDEX OF REFRACTION..(IOR).:          1.825000
..ALPHA (dn/dt)..(DT).:     8.900000E-06
..TEMP NORMALIZATION FACTOR..(TNF).:     3.300000E-01
..TIME NORMALIZATION FACTOR..(TINF).:     5.000000E-02
..0=RELATIVE TEMP; 1=ACTUAL TEMP..(IDATA).:              1
..AXIAL INCREMENT FACTOR..(ZI).:     1.000000E-01
..POWER MULTIPLICATION FACTOR..(POWER).:          1.000000
..OUTPUT ANGLE ACCURACY CRITERIA..(ACC).:    1.000000E-06
..TYPE OF PUMPING (0=side, 1=end)..:    0.000000E+00
-------------------------------------------------------
-------------------------------------------------------
```

```
.......INPUT FILE #2......

 Input Nd:YAG  Side-Pump..MP(20)..GA=20..GL=None..Run=001 03/01/90

..... MIN., MAX. AND INCREMENT OF RADIUS OF ROD     2.500000E-01
  2.500000E-01    2.500000E-01
..... MIN , MAX AND INCR. OF ASPECT RATIO (L/A)          30.400000
     30.400000       50.000000
..... INVERSE OF RADIAL THERMAL DIFFUSIVITY         26.947000
..... THERMAL CONDUCTIVITY    1.030000E-01    1.030000E-01
..... MIN. RADIAL COOLING PARAMETER          20.000000
..... MAX. RADIAL COOLING PARAMETER          20.000000
TYPE OF SCALE 1(LOG) OR 0(LINEAR)                1
  AND INCREMENT (SET TO 1. IF LOG)           1.000000
........ MIN. AND MAX. FRONT COOLING RATIO OR VALUES     6.500000E-04
  6.500000E-04
TYPE OF SCALE 1(LOG) OR 0(LINEAR)                1
  AND INCREMENT (SET TO 1 IF LOG)            1.000000
........ MIN. AND MAX. BACK  COOLING RATIO OR VALUES     6.500000E-04
  6.500000E-04
TYPE OF SCALE 1(LOG) OR 0(LINEAR)                1
  AND INCREMENT (SET TO 1 IF LOG)            1.000000
........ TYPE OF DATA RATIO=0 ACTUAL=1
                     PARAM=2
..............     PROPORTIONAL TO L/A=3             2
....... VARIATION OF END DATA SEPERATE=0
.............................. TOGETHER=1            1
..... MAXIMUM NUMBER OF ROOTS ... RADIAL           17
..... MAXIMUM NUMBER OF ROOTS ... LONGIT           17
      NUMBER OF ORTHOGONAL CHECKS  RADIAL           2
      NUMBER OF ORTHOGONAL CHECKS  LONGIT           3
      BESSEL ROOTS SCHEME ... 1  COMPUTED
                              2  GIVEN
                              3  ALL (GIVEN <21)
                                 (COMPUTED GE 21)
      ROOTS SCHEME IS -             2
RADIAL AND LONG. INTEGRATION DIVISIONS        1000          100
      TYPE OF PUMP BEAM ...........
   RADIAL    EIGENFUNCTION          -ORDER
             SQUARE PULSE           +0
             GAUSSIAN               +1
             PARABOLIC              +2
```

```
    LONGIT     EIGNFUNCTION           -ORDER
               CONSTANT               +0
               CONSTANT & ATTENUATED  +1
               FOCUSED(DEFOCUSED)     +2
               FOCUSED & ATTENUATED   +3
       NOTE  NO DIFFRACTION EFFECTS ALLOWED
             GAUSSIAN ENVELOPE ASSUMED
 PUMP BEAM CODE            0          0
 ....... ATTENUATION DATA..0=ATTEN..1=ATTEN*L          1
 ......OPTICAL DATA        3.000000
 ..... NUMBER OF RADIAL PROFILES ...          11

 ..... NUMBER OF LONGIT PROFILES ...          11
 ........ CONTINUOUS PUMPPING     ... 0
 ........ SINGLE PULSE            ... 1
       OR MULTI-PULSED            ... 2          2
 ..... MIN. REL. TIME OF INTEREST        3.400000
 ..... MAX. REL. TIME OF INTEREST        3.600000
 TYPE OF SCALE 1(LOG) OR 0(LINEAR)           1
   AND INCREMENT (SET TO 1 IF LOG)           1.000000
 ........ MULTIPLE PULSES          ... 2          2
 ........ ONTIME  PER PULSE    1.300000E-04
 ........ OFFTIME PER PULSE    4.987000E-02
 ........ ONTIME  SAMPLING RATE            1
 ........ OFFTIME SAMPLING RATE            1
 ..... ABSORBED ENERGY PER PULSE J/CM3     1574.280000
    .......... DEBUG DESIRED        ... 1
    ............NOT DESIRED         ... 0, NDEBUG=          1
..MIN, MAX, RADIAL CALCULATION RANGE..   0.000000E+00        1.000000
..MIN, MAX LONGITUDINAL CALCULATION RANGE..   0.000000E+00        1.000000
..RADIAL REFERENCE POINTS...          0    0.000000E+00
..AXIAL REFERENCE POINTS...           0    0.000000E+00
 ------------------------------------------
 ROD ASPECT RATIO (L/A) .......... =       30.400000
 ------------------------------------------
 ****************************************
 PARAMETER GA IS         20.000000
 ****************************************
 PARAMETER GL OF FRONT    6.500000E-04
 PARAMETER GL OF BACK     6.500000E-04
 ****************************************
```

BLOCK OF TEMPERATURE PROFILES FROM INPUT FILE #2

TEMPERATURE DISTRIBUTION
RADIAL DIFFUSIVITY .....269470E+02
RADIUS OF ROD .....250000E+00
LENGTH OF ROD .....760000E+01
TIME IN SECONDS .....345000E+01

L/R	.00	.10	.20	.30	.40	.50	.60	.70	.80	.90	1.00
.00	.64626E+00	.64627E+00	.64627E+00	.64627E+00	.64627E+00	.64627E+00	.64627E+00	.64627E+00	.64627E+00	.64627E+00	.64626E+00
.10	.64006E+00	.64006E+00	.64006E+00	.64006E+00	.64006E+00	.64006E+00	.64006E+00	.64006E+00	.64006E+00	.64006E+00	.64006E+00
.20	.62144E+00	.62144E+00	.62144E+00	.62144E+00	.62144E+00	.62144E+00	.62144E+00	.62144E+00	.62144E+00	.62144E+00	.62144E+00
.30	.59040E+00	.59041E+00	.59041E+00	.59041E+00	.59041E+00	.59041E+00	.59041E+00	.59041E+00	.59041E+00	.59041E+00	.59040E+00
.40	.54693E+00	.54694E+00	.54694E+00	.54694E+00	.54694E+00	.54694E+00	.54694E+00	.54694E+00	.54694E+00	.54694E+00	.54693E+00
.50	.49096E+00	.49096E+00	.49096E+00	.49096E+00	.49096E+00	.49096E+00	.49096E+00	.49096E+00	.49096E+00	.49096E+00	.49096E+00
.60	.42244E+00	.42244E+00	.42244E+00	.42244E+00	.42244E+00	.42244E+00	.42244E+00	.42244E+00	.42244E+00	.42244E+00	.42244E+00
.70	.34169E+00	.34169E+00	.34169E+00	.34169E+00	.34169E+00	.34169E+00	.34169E+00	.34169E+00	.34169E+00	.34169E+00	.34169E+00
.80	.25008E+00	.25008E+00	.25008E+00	.25008E+00	.25008E+00	.25008E+00	.25008E+00	.25008E+00	.25008E+00	.25008E+00	.25008E+00
.90	.15093E+00	.15093E+00	.15093E+00	.15093E+00	.15093E+00	.15093E+00	.15093E+00	.15093E+00	.15093E+00	.15093E+00	.15093E+00
1.00	.49856E-01	.49856E-01	.49856E-01	.49856E-01	.49856E-01	.49856E-01	.49856E-01	.49856E-01	.49856E-01	.49856E-01	.49856E-01

THERMAL LENSING PROGRAM OUTPUT DATA

INDEX OF REFRACTION MATRIX

.00	.18250E+01	.18250E+01	.18250E+01	.18250E+01	.18250E+01	.18250E+01	.18250E+01	.18250E+01	.18250E+01	.18250E+01	.18250E+01
.10	.18250E+01	.18250E+01	.18250E+01	.18250E+01	.18250E+01	.18250E+01	.18250E+01	.18250E+01	.18250E+01	.18250E+01	.18250E+01
.20	.18250E+01	.18250E+01	.18250E+01	.18250E+01	.18250E+01	.18250E+01	.18250E+01	.18250E+01	.18250E+01	.18250E+01	.18250E+01
.30	.18250E+01	.18250E+01	.18250E+01	.18250E+01	.18250E+01	.18250E+01	.18250E+01	.18250E+01	.18250E+01	.18250E+01	.18250E+01
.40	.18250E+01	.18250E+01	.18250E+01	.18250E+01	.18250E+01	.18250E+01	.18250E+01	.18250E+01	.18250E+01	.18250E+01	.18250E+01
.50	.18250E+01	.18250E+01	.18250E+01	.18250E+01	.18250E+01	.18250E+01	.18250E+01	.18250E+01	.18250E+01	.18250E+01	.18250E+01
.60	.18250E+01	.18250E+01	.18250E+01	.18250E+01	.18250E+01	.18250E+01	.18250E+01	.18250E+01	.18250E+01	.18250E+01	.18250E+01
.70	.18250E+01	.18250E+01	.18250E+01	.18250E+01	.18250E+01	.18250E+01	.18250E+01	.18250E+01	.18250E+01	.18250E+01	.18250E+01
.80	.18250E+01	.18250E+01	.18250E+01	.18250E+01	.18250E+01	.18250E+01	.18250E+01	.18250E+01	.18250E+01	.18250E+01	.18250E+01
.90	.18250E+01	.18250E+01	.18250E+01	.18250E+01	.18250E+01	.18250E+01	.18250E+01	.18250E+01	.18250E+01	.18250E+01	.18250E+01
1.00	.18250E+01	.18250E+01	.18250E+01	.18250E+01	.18250E+01	.18250E+01	.18250E+01	.18250E+01	.18250E+01	.18250E+01	.18250E+01

THERMAL LENSING CALCUATIONS
WAVELENGTH OF INTEREST(um)..... .115000E+01
TEMPERATURE OF INTEREST(deg C).. .375000E+02
TIME (sec)..... .345000E+01

RAY (no.)	ANGLE OUT (radians)	RADIUS (cm)	FOCAL LENG(cm)	DISTORTION (%)
.00	.0000000E+00	.0000000E+00	.0000000E+00	.0000000E+00
.10	.0000000E+00	.1000000E+00	.0000000E+00	.0000000E+00
.20	.0000000E+00	.2000000E+00	.6898527E+03	.0000000E+00
.30	.0000000E+00	.3000000E+00	.7760843E+03	.1310063E-10
.40	.0000000E+00	.4000000E+00	.7884030E+03	.1007527E-10
.50	.0000000E+00	.5000000E+00	.7839235E+03	.0000000E+00
.60	.0000000E+00	.6000000E+00	.7760843E+03	.0000000E+00
.70	.0000000E+00	.7000000E+00	.7682449E+03	.0000000E+00
.80	.0000000E+00	.8000000E+00	.7612167E+03	.0000000E+00
.90	.0000000E+00	.9000000E+00	.7551089E+03	.0000000E+00
1.00	.0000000E+00	.0000000E+00	.0000000E+00	.0000000E+00

AVERAGE OF THE FOCAL LENGTHS (meters) = .677658E+01
INCREMENTAL DISTORTION (%) RANGES FROM 0.0 TO .131E-10

.. END THERMAL LENSING OUTPUT..

BLOCK OF TEMPERATURE PROFILES FROM INPUT FILE #2

TEMPERATURE DISTRIBUTION

RADIAL DIFFUSIVITY .....269470E+02
RADIUS OF ROD .....250000E+00
LENGTH OF ROD .....760000E+01
TIME IN SECONDS .....345013E+01

L/R	.00	.10	.20	.30	.40	.50	.60	.70	.80	.90	1.00
.00	.72382E+00	.72383E+00	.72383E+00	.72383E+00	.72383E+00	.72383E+00	.72383E+00	.72383E+00	.72383E+00	.72383E+00	.72382E+00
.10	.71330E+00	.71331E+00	.71331E+00	.71331E+00	.71331E+00	.71331E+00	.71331E+00	.71331E+00	.71331E+00	.71331E+00	.71330E+00
.20	.69403E+00	.69404E+00	.69404E+00	.69404E+00	.69404E+00	.69404E+00	.69404E+00	.69404E+00	.69404E+00	.69404E+00	.69403E+00
.30	.66320E+00	.66320E+00	.66320E+00	.66320E+00	.66320E+00	.66320E+00	.66320E+00	.66320E+00	.66320E+00	.66320E+00	.66320E+00
.40	.62046E+00	.62046E+00	.62046E+00	.62046E+00	.62046E+00	.62047E+00	.62046E+00	.62046E+00	.62046E+00	.62046E+00	.62046E+00
.50	.56521E+00	.56522E+00	.56522E+00	.56522E+00	.56522E+00	.56522E+00	.56522E+00	.56522E+00	.56522E+00	.56522E+00	.56521E+00
.60	.49688E+00	.49689E+00	.49689E+00	.49689E+00	.49689E+00	.49689E+00	.49689E+00	.49689E+00	.49689E+00	.49689E+00	.49688E+00
.70	.41552E+00	.41552E+00	.41552E+00	.41552E+00	.41552E+00	.41552E+00	.41552E+00	.41552E+00	.41552E+00	.41552E+00	.41552E+00
.80	.32288E+00	.32288E+00	.32288E+00	.32288E+00	.32288E+00	.32288E+00	.32288E+00	.32288E+00	.32288E+00	.32288E+00	.32288E+00
.90	.22190E+00	.22190E+00	.22190E+00	.22190E+00	.22190E+00	.22190E+00	.22190E+00	.22190E+00	.22190E+00	.22190E+00	.22190E+00
1.00	.10556E+00	.10556E+00	.10556E+00	.10556E+00	.10556E+00	.10556E+00	.10556E+00	.10556E+00	.10556E+00	.10556E+00	.10556E+00

THERMAL LENSING PROGRAM OUTPUT DATA

INDEX OF REFRACTION MATRIX

.00	.18250E+01	.18250E+01	.18250E+01	.18250E+01	.18250E+01	.18250E+01	.18250E+01	.18250E+01	.18250E+01	.18250E+01	.18250E+01
.10	.18250E+01	.18250E+01	.18250E+01	.18250E+01	.18250E+01	.18250E+01	.18250E+01	.18250E+01	.18250E+01	.18250E+01	.18250E+01
.20	.18250E+01	.18250E+01	.18250E+01	.18250E+01	.18250E+01	.18250E+01	.18250E+01	.18250E+01	.18250E+01	.18250E+01	.18250E+01
.30	.18250E+01	.18250E+01	.18250E+01	.18250E+01	.18250E+01	.18250E+01	.18250E+01	.18250E+01	.18250E+01	.18250E+01	.18250E+01
.40	.18250E+01	.18250E+01	.18250E+01	.18250E+01	.18250E+01	.18250E+01	.18250E+01	.18250E+01	.18250E+01	.18250E+01	.18250E+01
.50	.18250E+01	.18250E+01	.18250E+01	.18250E+01	.18250E+01	.18250E+01	.18250E+01	.18250E+01	.18250E+01	.18250E+01	.18250E+01
.60	.18250E+01	.18250E+01	.18250E+01	.18250E+01	.18250E+01	.18250E+01	.18250E+01	.18250E+01	.18250E+01	.18250E+01	.18250E+01
.70	.18250E+01	.18250E+01	.18250E+01	.18250E+01	.18250E+01	.18250E+01	.18250E+01	.18250E+01	.18250E+01	.18250E+01	.18250E+01
.80	.18250E+01	.18250E+01	.18250E+01	.18250E+01	.18250E+01	.18250E+01	.18250E+01	.18250E+01	.18250E+01	.18250E+01	.18250E+01
.90	.18250E+01	.18250E+01	.18250E+01	.18250E+01	.18250E+01	.18250E+01	.18250E+01	.18250E+01	.18250E+01	.18250E+01	.18250E+01
1.00	.18250E+01	.18250E+01	.18250E+01	.18250E+01	.18250E+01	.18250E+01	.18250E+01	.18250E+01	.18250E+01	.18250E+01	.18250E+01

THERMAL LENSING CALCUATIONS

WAVELENGTH OF INTEREST(um)..... .115000E+01
TEMPERATURE OF INTEREST(deg C).. .375000E+02
TIME (sec)..... .345013E+01

RAY (no.)	ANGLE OUT (radians)	RADIUS (cm)	FOCAL LENG(cm)	DISTORTION (%)
.00	.0000000E+00	.0000000E+00	.0000000E+00	.0000000E+00
.10	.0000000E+00	.1000000E+00	.3449263E+03	.5773156E-11
.20	.0000000E+00	.2000000E+00	.6898527E+03	.1398881E-10
.30	.0000000E+00	.3000000E+00	.7760843E+03	.0000000E+00
.40	.0000000E+00	.4000000E+00	.6898527E+03	.1333073E-08
.50	.0000000E+00	.5000000E+00	.7185965E+03	.1547651E-10
.60	.0000000E+00	.6000000E+00	.7304323E+03	.2216745E-10
.70	.0000000E+00	.7000000E+00	.7348430E+03	.0000000E+00
.80	.0000000E+00	.8000000E+00	.7358428E+03	.0000000E+00
.90	.0000000E+00	.9000000E+00	.7551089E+03	.0000000E+00
1.00	.0000000E+00	.1000000E+01	.0000000E+00	.0000000E+00

AVERAGE OF THE FOCAL LENGTHS (meters) = .68617[illegible]E+01
INCREMENTAL DISTORTION (%) RANGES FROM 0.0 TO .133E-08

.. END THERMAL LENSING OUTPUT..

BLOCK OF TEMPERATURE PROFILES FROM INPUT FILE #2

TEMPERATURE DISTRIBUTION

RADIAL DIFFUSIVITY .....269470E+02
RADIUS OF ROD .....250000E+00
LENGTH OF ROD .....760000E+01
TIME IN SECONDS .....350000E+01

L/R	.00	.10	.20	.30	.40	.50	.60	.70	.80	.90	1.00
.00	.64627E+00	.64627E+00	.64627E+00	.64627E+00	.64627E+00	.64627E+00	.64627E+00	.64627E+00	.64627E+00	.64627E+00	.64627E+00
.10	.64006E+00	.64007E+00	.64007E+00	.64007E+00	.64007E+00	.64007E+00	.64007E+00	.64007E+00	.64007E+00	.64007E+00	.64006E+00
.20	.62144E+00	.62145E+00	.62145E+00	.62145E+00	.62145E+00	.62145E+00	.62145E+00	.62145E+00	.62145E+00	.62145E+00	.62144E+00
.30	.59041E+00	.59041E+00	.59041E+00	.59041E+00	.59041E+00	.59041E+00	.59041E+00	.59041E+00	.59041E+00	.59041E+00	.59041E+00
.40	.54693E+00	.54694E+00	.54694E+00	.54694E+00	.54694E+00	.54694E+00	.54694E+00	.54694E+00	.54694E+00	.54694E+00	.54693E+00
.50	.49096E+00	.49096E+00	.49096E+00	.49096E+00	.49096E+00	.49096E+00	.49096E+00	.49096E+00	.49096E+00	.49096E+00	.49096E+00
.60	.42244E+00	.42244E+00	.42244E+00	.42244E+00	.42244E+00	.42244E+00	.42244E+00	.42244E+00	.42244E+00	.42244E+00	.42244E+00
.70	.34169E+00	.34169E+00	.34169E+00	.34169E+00	.34169E+00	.34169E+00	.34169E+00	.34169E+00	.34169E+00	.34169E+00	.34169E+00
.80	.25008E+00	.25008E+00	.25008E+00	.25008E+00	.25008E+00	.25008E+00	.25008E+00	.25008E+00	.25008E+00	.25008E+00	.25008E+00
.90	.15093E+00	.15093E+00	.15093E+00	.15093E+00	.15093E+00	.15093E+00	.15093E+00	.15093E+00	.15093E+00	.15093E+00	.15093E+00
1.00	.49856E-01	.49856E-01	.49856E-01	.49857E-01	.49857E-01	.49857E-01	.49857E-01	.49857E-01	.49856E-01	.49856E-01	.49856E-01

THERMAL LENSING PROGRAM OUTPUT DATA

INDEX OF REFRACTION MATRIX

.00	.18250E+01	.18250E+01	.18250E+01	.18250E+01	.18250E+01	.18250E+01	.18250E+01	.18250E+01	.18250E+01	.18250E+01	.18250E+01
.10	.18250E+01	.18250E+01	.18250E+01	.18250E+01	.18250E+01	.18250E+01	.18250E+01	.18250E+01	.18250E+01	.18250E+01	.18250E+01
.20	.18250E+01	.18250E+01	.18250E+01	.18250E+01	.18250E+01	.18250E+01	.18250E+01	.18250E+01	.18250E+01	.18250E+01	.18250E+01
.30	.18250E+01	.18250E+01	.18250E+01	.18250E+01	.18250E+01	.18250E+01	.18250E+01	.18250E+01	.18250E+01	.18250E+01	.18250E+01
.40	.18250E+01	.18250E+01	.18250E+01	.18250E+01	.18250E+01	.18250E+01	.18250E+01	.18250E+01	.18250E+01	.18250E+01	.18250E+01
.50	.18250E+01	.18250E+01	.18250E+01	.18250E+01	.18250E+01	.18250E+01	.18250E+01	.18250E+01	.18250E+01	.18250E+01	.18250E+01
.60	.18250E+01	.18250E+01	.18250E+01	.18250E+01	.18250E+01	.18250E+01	.18250E+01	.18250E+01	.18250E+01	.18250E+01	.18250E+01
.70	.18250E+01	.18250E+01	.18250E+01	.18250E+01	.18250E+01	.18250E+01	.18250E+01	.18250E+01	.18250E+01	.18250E+01	.18250E+01
.80	.18250E+01	.18250E+01	.18250E+01	.18250E+01	.18250E+01	.18250E+01	.18250E+01	.18250E+01	.18250E+01	.18250E+01	.18250E+01
.90	.18250E+01	.18250E+01	.18250E+01	.18250E+01	.18250E+01	.18250E+01	.18250E+01	.18250E+01	.18250E+01	.18250E+01	.18250E+01
1.00	.18250E+01	.18250E+01	.18250E+01	.18250E+01	.18250E+01	.18250E+01	.18250E+01	.18250E+01	.18250E+01	.18250E+01	.18250E+01

THERMAL LENSING CALCUATIONS

WAVELENGTH OF INTEREST(um)..... .115000E+01
TEMPERATURE OF INTEREST(deg C).. .375000E+02
TIME (sec)..... .350000E+01

RAY (no.)	ANGLE OUT (radians)	RADIUS (cm)	FOCAL LENG(cm)	DISTORTION (%)
.00	.0000000E+00	.0000000E+00	.0000000E+00	.0000000E+00
.10	.0000000E+00	.1000000E+00	.0000000E+00	.4551913E-11
.20	.0000000E+00	.2000000E+00	.6898527E+03	-.1229572E-10
.30	.0000000E+00	.3000000E+00	.7760843E+03	.0000000E+00
.40	.0000000E+00	.4000000E+00	.7884030E+03	.9797715E-11
.50	.0000000E+00	.5000000E+00	.7839235E+03	.0000000E+00
.60	.0000000E+00	.6000000E+00	.7760843E+03	.0000000E+00
.70	.0000000E+00	.7000000E+00	.7682449E+03	.0000000E+00
.80	.0000000E+00	.8000000E+00	.7612167E+03	.0000000E+00
.90	.0000000E+00	.9000000E+00	.7551089E+03	.0000000E+00
1.00	.0000000E+00	.0000000E+00	.0000000E+00	.0000000E+00

AVERAGE OF THE FOCAL LENGTHS (meters) = .677658E+01
INCREMENTAL DISTORTION (%) RANGES FROM 0.0 TO .980E-11

.. END THERMAL LENSING OUTPUT..

BLOCK OF TEMPERATURE PROFILES FROM INPUT FILE #2

TEMPERATURE DISTRIBUTION

RADIAL DIFFUSIVITY .....269470E+02
RADIUS OF ROD .....250000E+00
LENGTH OF ROD .....760000E+01
TIME IN SECONDS .....350013E+01

L/R	.00	.10	.20	.30	.40	.50	.60	.70	.80	.90	1.00
.00	.72382E+00	.72383E+00	.72383E+00	.72383E+00	.72383E+00	.72383E+00	.72383E+00	.72383E+00	.72383E+00	.72383E+00	.72382E+00
.10	.71330E+00	.71331E+00	.71331E+00	.71331E+00	.71331E+00	.71331E+00	.71331E+00	.71331E+00	.71331E+00	.71331E+00	.71330E+00
.20	.69403E+00	.69404E+00	.69404E+00	.69404E+00	.69404E+00	.69404E+00	.69404E+00	.69404E+00	.69404E+00	.69404E+00	.69403E+00
.30	.66320E+00	.66321E+00	.66321E+00	.66321E+00	.66321E+00	.66321E+00	.66321E+00	.66321E+00	.66321E+00	.66321E+00	.66320E+00
.40	.62046E+00	.62047E+00	.62047E+00	.62047E+00	.62047E+00	.62047E+00	.62047E+00	.62047E+00	.62047E+00	.62047E+00	.62046E+00
.50	.56521E+00	.56522E+00	.56522E+00	.56522E+00	.56522E+00	.56522E+00	.56522E+00	.56522E+00	.56522E+00	.56522E+00	.56521E+00
.60	.49688E+00	.49689E+00	.49689E+00	.49689E+00	.49689E+00	.49689E+00	.49689E+00	.49689E+00	.49689E+00	.49689E+00	.49688E+00
.70	.41552E+00	.41552E+00	.41552E+00	.41552E+00	.41552E+00	.41552E+00	.41552E+00	.41552E+00	.41552E+00	.41552E+00	.41552E+00
.80	.32288E+00	.32288E+00	.32288E+00	.32288E+00	.32288E+00	.32288E+00	.32288E+00	.32288E+00	.32288E+00	.32288E+00	.32288E+00
.90	.22190E+00	.22190E+00	.22190E+00	.22190E+00	.22190E+00	.22190E+00	.22190E+00	.22190E+00	.22190E+00	.22190E+00	.22190E+00
1.00	.10556E+00	.10556E+00	.10556E+00	.10556E+00	.10556E+00	.10556E+00	.10556E+00	.10556E+00	.10556E+00	.10556E+00	.10556E+00

THERMAL LENSING PROGRAM OUTPUT DATA

INDEX OF REFRACTION MATRIX

.00	.18250E+01	.18250E+01	.18250E+01	.18250E+01	.18250E+01	.18250E+01	.18250E+01	.18250E+01	.18250E+01	.18250E+01	.18250E+01
.10	.18250E+01	.18250E+01	.18250E+01	.18250E+01	.18250E+01	.18250E+01	.18250E+01	.18250E+01	.18250E+01	.18250E+01	.18250E+01
.20	.18250E+01	.18250E+01	.18250E+01	.18250E+01	.18250E+01	.18250E+01	.18250E+01	.18250E+01	.18250E+01	.18250E+01	.18250E+01
.30	.18250E+01	.18250E+01	.18250E+01	.18250E+01	.18250E+01	.18250E+01	.18250E+01	.18250E+01	.18250E+01	.18250E+01	.18250E+01
.40	.18250E+01	.18250E+01	.18250E+01	.18250E+01	.18250E+01	.18250E+01	.18250E+01	.18250E+01	.18250E+01	.18250E+01	.18250E+01
.50	.18250E+01	.18250E+01	.18250E+01	.18250E+01	.18250E+01	.18250E+01	.18250E+01	.18250E+01	.18250E+01	.18250E+01	.18250E+01
.60	.18250E+01	.18250E+01	.18250E+01	.18250E+01	.18250E+01	.18250E+01	.18250E+01	.18250E+01	.18250E+01	.18250E+01	.18250E+01
.70	.18250E+01	.18250E+01	.18250E+01	.18250E+01	.18250E+01	.18250E+01	.18250E+01	.18250E+01	.18250E+01	.18250E+01	.18250E+01
.80	.18250E+01	.18250E+01	.18250E+01	.18250E+01	.18250E+01	.18250E+01	.18250E+01	.18250E+01	.18250E+01	.18250E+01	.18250E+01
.90	.18250E+01	.18250E+01	.18250E+01	.18250E+01	.18250E+01	.18250E+01	.18250E+01	.18250E+01	.18250E+01	.18250E+01	.18250E+01
1.00	.18250E+01	.18250E+01	.18250E+01	.18250E+01	.18250E+01	.18250E+01	.18250E+01	.18250E+01	.18250E+01	.18250E+01	.18250E+01

THERMAL LENSING CALCUATIONS

WAVELENGTH OF INTEREST(um)..... .115000E+01
TEMPERATURE OF INTEREST(deg C).. .375000E+02
TIME (sec)..... .350013E+01

RAY (no.)	ANGLE OUT (radians)	RADIUS (cm)	FOCAL LENG(cm)	DISTORTION (%)
.00	.0000000E+00	.0000000E+00	.0000000E+00	.0000000E+00
.10	.0000000E+00	.1000000E+00	.3449263E+03	.5773156E-11
.20	.0000000E+00	.2000000E+00	.6898527E+03	-.4718448E-11
.30	.0000000E+00	.3000000E+00	.7760843E+03	.3552712E-11
.40	.0000000E+00	.4000000E+00	.6898527E+03	.9936493E-11
.50	.0000000E+00	.5000000E+00	.7185965E+03	-.6661338E-12
.60	.0000000E+00	.6000000E+00	.7304323E+03	.2216745E-10
.70	.0000000E+00	.7000000E+00	.7348430E+03	.0000000E+00
.80	.0000000E+00	.8000000E+00	.7358428E+03	.0000000E+00
.90	.0000000E+00	.9000000E+00	.7551089E+03	.0000000E+00
1.00	.0000000E+00	.0000000E+00	.0000000E+00	.0000000E+00

AVERAGE OF THE FOCAL LENGTHS (meters) = .686171E+01
INCREMENTAL DISTORTION (%) RANGES FROM 0.0 TO .222E-10

.. END THERMAL LENSING OUTPUT..

BLOCK OF TEMPERATURE PROFILES FROM INPUT FILE #2

TEMPERATURE DISTRIBUTION

RADIAL DIFFUSIVITY .....269470E+02
RADIUS OF ROD .....250000E+00
LENGTH OF ROD .....760000E+01
TIME IN SECONDS .....355000E+01

L/R	.00	.10	.20	.30	.40	.50	.60	.70	.80	.90	1.00
.00	.64627E+00	.64627E+00	.64627E+00	.64627E+00	.64628E+00	.64628E+00	.64628E+00	.64627E+00	.64627E+00	.64627E+00	.64627E+00
.10	.64006E+00	.64007E+00	.64007E+00	.64007E+00	.64007E+00	.64007E+00	.64007E+00	.64007E+00	.64007E+00	.64007E+00	.64006E+00
.20	.62144E+00	.62145E+00	.62145E+00	.62145E+00	.62145E+00	.62145E+00	.62145E+00	.62145E+00	.62145E+00	.62145E+00	.62144E+00
.30	.59041E+00	.59041E+00	.59041E+00	.59041E+00	.59042E+00	.59042E+00	.59042E+00	.59041E+00	.59041E+00	.59041E+00	.59041E+00
.40	.54694E+00	.54694E+00	.54694E+00	.54694E+00	.54694E+00	.54694E+00	.54694E+00	.54694E+00	.54694E+00	.54694E+00	.54694E+00
.50	.49096E+00	.49097E+00	.49097E+00	.49097E+00	.49097E+00	.49097E+00	.49097E+00	.49097E+00	.49097E+00	.49097E+00	.49096E+00
.60	.42244E+00	.42244E+00	.42244E+00	.42244E+00	.42244E+00	.42244E+00	.42244E+00	.42244E+00	.42244E+00	.42244E+00	.42244E+00
.70	.34169E+00	.34169E+00	.34169E+00	.34169E+00	.34169E+00	.34169E+00	.34169E+00	.34169E+00	.34169E+00	.34169E+00	.34169E+00
.80	.25008E+00	.25008E+00	.25008E+00	.25008E+00	.25008E+00	.25008E+00	.25008E+00	.25008E+00	.25008E+00	.25008E+00	.25008E+00
.90	.15093E+00	.15093E+00	.15093E+00	.15093E+00	.15093E+00	.15093E+00	.15093E+00	.15093E+00	.15093E+00	.15093E+00	.15093E+00
1.00	.49856E-01	.49857E-01	.49857E-01	.49857E-01	.49857E-01	.49857E-01	.49857E-01	.49857E-01	.49857E-01	.49857E-01	.49856E-01

THERMAL LENSING FROGRAM OUTPUT DATA

INDEX OF REFRACTION MATRIX

.00	.18250E+01	.18250E+01	.18250E+01	.18250E+01	.18250E+01	.18250E+01	.18250E+01	.18250E+01	.18250E+01	.18250E+01	.18250E+01
.10	.18250E+01	.18250E+01	.18250E+01	.18250E+01	.18250E+01	.18250E+01	.18250E+01	.18250E+01	.18250E+01	.18250E+01	.18250E+01
.20	.18250E+01	.18250E+01	.18250E+01	.18250E+01	.18250E+01	.18250E+01	.18250E+01	.18250E+01	.18250E+01	.18250E+01	.18250E+01
.30	.18250E+01	.18250E+01	.18250E+01	.18250E+01	.18250E+01	.18250E+01	.18250E+01	.18250E+01	.18250E+01	.18250E+01	.18250E+01
.40	.18250E+01	.18250E+01	.18250E+01	.18250E+01	.18250E+01	.18250E+01	.18250E+01	.18250E+01	.18250E+01	.18250E+01	.18250E+01
.50	.18250E+01	.18250E+01	.18250E+01	.18250E+01	.18250E+01	.18250E+01	.18250E+01	.18250E+01	.18250E+01	.18250E+01	.18250E+01
.60	.18250E+01	.18250E+01	.18250E+01	.18250E+01	.18250E+01	.18250E+01	.18250E+01	.18250E+01	.18250E+01	.18250E+01	.18250E+01
.70	.18250E+01	.18250E+01	.18250E+01	.18250E+01	.18250E+01	.18250E+01	.18250E+01	.18250E+01	.18250E+01	.18250E+01	.18250E+01
.80	.18250E+01	.18250E+01	.18250E+01	.18250E+01	.18250E+01	.18250E+01	.18250E+01	.18250E+01	.18250E+01	.18250E+01	.18250E+01
.90	.18250E+01	.18250E+01	.18250E+01	.18250E+01	.18250E+01	.18250E+01	.18250E+01	.18250E+01	.18250E+01	.18250E+01	.18250E+01
1.00	.18250E+01	.18250E+01	.18250E+01	.18250E+01	.18250E+01	.18250E+01	.18250E+01	.18250E+01	.18250E+01	.18250E+01	.18250E+01

THERMAL LENSING CALCUATIONS

WAVELENGTH OF INTEREST(um)..... .115000E+01
TEMPERATURE OF INTEREST(deg C).. .375000E+02
TIME (sec)..... .355000E+01

RAY (no.)	ANGLE OUT (radians)	RADIUS (cm)	FOCAL LENG(cm)	DISTORTION (%)
.00	.0000000E+00	.0000000E+00	.0000000E+00	.0000000E+00
.10	.0000000E+00	.1000000E+00	.0000000E+00	.4551913E-11
.20	.0000000E+00	.2000000E+00	.6898527E+03	-.1229572E-10
.30	.0000000E+00	.3000000E+00	.7760843E+03	.9963511E-09
.40	.0000000E+00	.4000000E+00	.7884030E+03	.0000000E+00
.50	.0000000E+00	.5000000E+00	.7839235E+03	-.1709743E-11
.60	.0000000E+00	.6000000E+00	.7760843E+03	.0000000E+00
.70	.0000000E+00	.7000000E+00	.7682449E+03	.0000000E+00
.80	.0000000E+00	.8000000E+00	.7612167E+03	.0000000E+00
.90	.0000000E+00	.9000000E+00	.7551089E+03	.0000000E+00
1.00	.0000000E+00	.0000000E+00	.0000000E+00	.0000000E+00

AVERAGE OF THE FOCAL LENGTHS (meters) = .677658E+01
INCREMENTAL DISTORTION (%) RANGES FROM 0.0 TO .996E-09

.. END THERMAL LENSING OUTPUT..

C-2

BLOCK OF TEMPERATURE PROFILES FROM INPUT FILE #2

TEMPERATURE DISTRIBUTION

RADIAL DIFFUSIVITY .....269470E+02
RADIUS OF ROD .....250000E+00
LENGTH OF ROD .....760000E+01
TIME IN SECONDS .....355013E+01

L/R	.00	.10	.20	.30	.40	.50	.60	.70	.80	.90	1.00
.00	.72382E+00	.72383E+00	.72383E+00	.72383E+00	.72383E+00	.72383E+00	.72383E+00	.72383E+00	.72383E+00	.72383E+00	.72382E+00
.10	.71331E+00	.71331E+00	.71331E+00	.71331E+00	.71331E+00	.71331E+00	.71331E+00	.71331E+00	.71331E+00	.71331E+00	.71331E+00
.20	.69403E+00	.69404E+00	.69404E+00	.69404E+00	.69404E+00	.69404E+00	.69404E+00	.69404E+00	.69404E+00	.69404E+00	.69403E+00
.30	.66320E+00	.66321E+00	.66321E+00	.66321E+00	.66321E+00	.66321E+00	.66321E+00	.66321E+00	.66321E+00	.66321E+00	.66320E+00
.40	.62046E+00	.62047E+00	.62047E+00	.62047E+00	.62047E+00	.62047E+00	.62047E+00	.62047E+00	.62047E+00	.62047E+00	.62046E+00
.50	.56521E+00	.56522E+00	.56522E+00	.56522E+00	.56522E+00	.56522E+00	.56522E+00	.56522E+00	.56522E+00	.56522E+00	.56521E+00
.60	.49688E+00	.49689E+00	.49689E+00	.49689E+00	.49689E+00	.49689E+00	.49689E+00	.49689E+00	.49689E+00	.49689E+00	.49689E+00
.70	.41552E+00	.41552E+00	.41552E+00	.41552E+00	.41552E+00	.41552E+00	.41552E+00	.41552E+00	.41552E+00	.41552E+00	.41552E+00
.80	.32288E+00	.32288E+00	.32288E+00	.32288E+00	.32288E+00	.32288E+00	.32288E+00	.32288E+00	.32288E+00	.32288E+00	.32288E+00
.90	.22190E+00	.22190E+00	.22190E+00	.22190E+00	.22190E+00	.22190E+00	.22190E+00	.22190E+00	.22190E+00	.22190E+00	.22190E+00
1.00	.10556E+00	.10556E+00	.10556E+00	.10556E+00	.10556E+00	.10556E+00	.10556E+00	.10556E+00	.10556E+00	.10556E+00	.10556E+00

THERMAL LENSING PROGRAM OUTPUT DATA

INDEX OF REFRACTION MATRIX

.00	.18250E+01	.18250E+01	.18250E+01	.18250E+01	.18250E+01	.18250E+01	.18250E+01	.18250E+01	.18250E+01	.18250E+01	.18250E+01
.10	.18250E+01	.18250E+01	.18250E+01	.18250E+01	.18250E+01	.18250E+01	.18250E+01	.18250E+01	.18250E+01	.18250E+01	.18250E+01
.20	.18250E+01	.18250E+01	.18250E+01	.18250E+01	.18250E+01	.18250E+01	.18250E+01	.18250E+01	.18250E+01	.18250E+01	.18250E+01
.30	.18250E+01	.18250E+01	.18250E+01	.18250E+01	.18250E+01	.18250E+01	.18250E+01	.18250E+01	.18250E+01	.18250E+01	.18250E+01
.40	.18250E+01	.18250E+01	.18250E+01	.18250E+01	.18250E+01	.18250E+01	.18250E+01	.18250E+01	.18250E+01	.18250E+01	.18250E+01
.50	.18250E+01	.18250E+01	.18250E+01	.18250E+01	.18250E+01	.18250E+01	.18250E+01	.18250E+01	.18250E+01	.18250E+01	.18250E+01
.60	.18250E+01	.18250E+01	.18250E+01	.18250E+01	.18250E+01	.18250E+01	.18250E+01	.18250E+01	.18250E+01	.18250E+01	.18250E+01
.70	.18250E+01	.18250E+01	.18250E+01	.18250E+01	.18250E+01	.18250E+01	.18250E+01	.18250E+01	.18250E+01	.18250E+01	.18250E+01
.80	.18250E+01	.18250E+01	.18250E+01	.18250E+01	.18250E+01	.18250E+01	.18250E+01	.18250E+01	.18250E+01	.18250E+01	.18250E+01
.90	.18250E+01	.18250E+01	.18250E+01	.18250E+01	.18250E+01	.18250E+01	.18250E+01	.18250E+01	.18250E+01	.18250E+01	.18250E+01
1.00	.18250E+01	.18250E+01	.18250E+01	.18250E+01	.18250E+01	.18250E+01	.18250E+01	.18250E+01	.18250E+01	.18250E+01	.18250E+01

THERMAL LENSING CALCUATIONS

WAVELENGTH OF INTEREST(um)..... .115000E+01
TEMPERATURE OF INTEREST(deg C).. .375000E+02
TIME (sec)..... .355013E+01

RAY (no.)	ANGLE OUT (radians)	RADIUS (cm)	FOCAL LENG(cm)	DISTORTION (%)
.00	.0000000E+00	.0000000E+00	.0000000E+00	.0000000E+00
.10	.0000000E+00	.1000000E+00	.3449263E+03	.0000000E+00
.20	.0000000E+00	.2000000E+00	.6898527E+03	.2553516E-11
.30	.0000000E+00	.3000000E+00	.7760843E+03	.3552712E-11
.40	.0000000E+00	.4000000E+00	.6898527E+03	.9936493E-11
.50	.0000000E+00	.5000000E+00	.7185965E+03	-.6661338E-12
.60	.0000000E+00	.6000000E+00	.7304323E+03	.2216745E-10
.70	.0000000E+00	.7000000E+00	.7348430E+03	.0000000E+00
.80	.0000000E+00	.8000000E+00	.7358428E+03	.0000000E+00
.90	.0000000E+00	.9000000E+00	.7551089E+03	.0000000E+00
1.00	.0000000E+00	.0000000E+00	.0000000E+00	.0000000E+00

AVERAGE OF THE FOCAL LENGTHS (meters) = .686171E+01
INCREMENTAL DISTORTION (%) RANGES FROM 0.0 TO .222E-10

.. END THERMAL LENSING OUTPUT..

.....

References

1. Farrukh, U. O., Buoncristiani, A. M., and Byvik, C. E., An Analysis of the Temperature Distribution in Finite Solid-State Laser Rods, IEEE Journal of Quantum Electronics, Vol. 24, No. 11, November 1988.

2. Koechner, Walter., Solid State Laser Engineering, Springer-Verlag: Berlin, Heidalburg, New York, 1988.

3. Farrukh, U. O., Buoncristiani, A. M., and Byvik, C. E., Time Dependent Temperature Distribution in Pulsed Ti: Sapphire Lasers, Proceedings of SPIE-The International Society for Optical Engineering, Vol. 892, 1988.

4. Bendow, B. and Gianino, P. D., Thermal Lensing of Laser Beams in Optically Transmitting Materials - I. General Formulation, Journal of Applied Physics, Vol. 2, pp. 1-10, 1973.

5. Koechner, W., Transient Thermal Profiles in Optically Pumped Laser Rods, Journal of Applied Physics, Vol. 44, No. 7, pp. 3162-3170, 1973.

6. Antipenko, B. M., Cross-Relaxation Schemes for Pumping Laser Rods, Soviet Physics, Technical Physics, Vol. 29, No. 2, pp. 228-230, 1984.

7. Farrukh, U., Brackett, V., and Brockman, P., Steady-State Temperature in End-Pumped Repetitively Pulsed Laser Rods, Technical Digest, Paper presented at the Optical Society of America, 1989 Annual Meeting, 15-20 October 1989.

8. Foster, J. D. and Osterink, L. M., Thermal Effects in Nd:YAG Lasers, Journal of Applied Physics, Vol. 41, No. 9, pp. 3656-3663, 1970.

9. Koechner, W., Thermal Lensing in Nd:YAG Laser Rod, Journal of Applied Optics, Vol. 9, No. 11, pp. 2548-2553, Nov. 1970.

10. Sparks, M., Optical Distortion by Heated Windows in High Power Laser Systems, Journal of Applied Physics, Vol. 42, No. 12, pp. 5029-5046, 1971.

11. Jasperse, J. R. and Gianino, P. D., Thermal Lensing in Infrared Laser Window Materials, Journal of Applied Physics, Vol. 43, No. 4, pp. 1686-1693, 1972.

References (cont.)

12. Bendow, B. and Gianino, P. D., Thermal Lensing of Laser Beams in Optically Transmitting Materials - II. Numerical Computations, Journal of Applied Physics, Vol. 2, pp. 71-90, 1973.

13. Carslaro, H. S. and Jaeger, J. C., Conduction of Heat in Solids, Oxford University Press: London, 1948.

14. Kogelnik, H., Imaging of Optical Modes - Resonators with Internal Lenses, Bell Systems Technical Journal, Vol. 44, pp. 455-494, 1965.

15. Timoshenko, S. and Goodier, J. N., Theory of Elasticity, McGraw-Hill: New York, 1951.

16. Born, M. and Wolf, E., Principles of Optics, Pergamon Press: London, 1965.

17. Koechner, W. and Rice, D. K., Effect of Birefringence on the Performance of Linearly Polarized YAG: Nd Lasers, IEEE Journal of Quantum Electronics, Vol. QE6, No. 9, pp. 557-566, September 1970.

18. Koechner, W., Absorbed Pump Power, Thermal Profiles and Stresses in a CW Pumped Nd:YAG Crystal, Journal of Applied Optics, Vol. 9, No. 6, pp. 1429-1434, June 1970.

19. Yariv, A. and Yeh, P., Optical Waves in Crystals, John Wiley & Sons: New York, 1984.

20. Williams-Burg, J. A. and Barnes, N. P., Laser Performance, Thermal Focusing and Depolarization Effects in Nd:Cr:CSGG and Nd:YAG, Presented at SPIE Conference in Los Angeles, Ca., January 1990.

NASA National Aeronautics and Space Administration

Report Documentation Page

1. Report No.	2. Government Accession No.	3. Recipient's Catalog No.
NASA CR-4300		

4. Title and Subtitle	5. Report Date
Modeling of Thermal Lensing in Side and End-Pumped Finite Solid-State Laser Rods	June 1990
	6. Performing Organization Code

7. Author(s)	8. Performing Organization Report No.
Vincent G. Brackett	
	10. Work Unit No. 590-31-31

9. Performing Organization Name and Address	11. Contract or Grant No.
Hampton University Physics Department Hampton, VA 23668	NAG1-666
	13. Type of Report and Period Covered
12. Sponsoring Agency Name and Address	Contractor Report
NASA Langley Research Center Hampton, VA 23665-5225	14. Sponsoring Agency Code

15. Supplementary Notes

Langley Technical Monitor: Philip Brockman
Thesis presented to The Graduate College, Hampton University, in partial fulfillment of the requirements for the Degree of Master of Science.

16. Abstract

An analytical expression for approximating the time-dependent thermal focal length in finite solid-state laser rods has been derived. The analysis is based on the temperature variation of the material refractive index caused by optical pumping of these rods. Several quantities were found to be relevant to this analysis. These quantities were the specific thermal profiles of the rods, type of optical pumping employed, type of cooling scheme employed (side and end-cooling parameters), and the specific material characteristics of the rods. The Thermal Lensing Model was formulated using the geometric ray tracing approach. The focal lengths are then approximated, by calculating the phase shift in the index of refraction, as the different rays of an incident plane wave are tracked through a lens-like crystal medium. The approach also applies in the case of Gaussian or parabolic pump beams. It is shown that the prediction of thermal focal length is in good quantitative agreement with experimentally obtained data.

17. Key Words (Suggested by Author(s))	18. Distribution Statement
optical pumping, solid-state lasers, optical properties, rods, temperature effects, pulsed lasers	Unclassified - Unlimited Subject Category 36

19. Security Classif. (of this report)	20. Security Classif. (of this page)	21. No. of pages	22. Price
Unclassified	Unclassified	104	A06

NASA-Langley, 1990